Catalog of Earthquake Hypocenters at Alaskan Volcanoes: January 1 through December 31, 2004

By James P. Dixon,[1] Scott D. Stihler,[2] John A. Power,[3] Guy Tytgat,[2] Steve Estes,[2] Stephanie Prejean,[3] John J. Sánchez,[2] Rebecca Sanches,[2] Stephen R. McNutt,[2] and John Paskievitch[3]

Open-File Report 2005-1312

2005

U.S. DEPARTMENT OF THE INTERIOR
U.S. GEOLOGICAL SURVEY

[1] U. S. Geological Survey - Alaska Science Center, 903 Koyukuk Drive, Fairbanks, AK 99775-7320
[2] University of Alaska Fairbanks - Geophysical Institute, 903 Koyukuk Drive, Fairbanks, AK 99775-7320
[3] U. S. Geological Survey - Alaska Science Center, 4200 University Drive, Anchorage, AK 99508-4667

CONTENTS

Introduction

The Alaska Volcano Observatory (AVO), a cooperative program of the U.S. Geological Survey, the Geophysical Institute of the University of Alaska Fairbanks, and the Alaska Division of Geological and Geophysical Surveys, has maintained seismic monitoring networks at historically active volcanoes in Alaska since 1988 (Power and others, 1993; Jolly and others, 1996; Jolly and others, 2001; Dixon and others, 2002; Dixon and others, 2003, Dixon and others, 2004). The primary objectives of the seismic program are the real-time seismic monitoring of active, potentially hazardous, Alaskan volcanoes and the investigation of seismic processes associated with active volcanism. This catalog presents the calculated earthquake hypocenter and phase arrival data, and changes in the seismic monitoring program for the period January 1 through December 31, 2004.

The AVO seismograph network was used to monitor the seismic activity at twenty-eight volcanoes within Alaska in 2004 (Figure 1). These include Mount Wrangell, Mount Spurr, Redoubt Volcano, Iliamna Volcano, Augustine Volcano, Katmai volcanic cluster (Snowy Mountain, Mount Griggs, Mount Katmai, Novarupta, Trident Volcano, Mount Mageik, Mount Martin), Mount Peulik, Aniakchak Crater, Mount Veniaminof, Pavlof Volcano, Mount Dutton, Isanotski Peaks, Shishaldin Volcano, Fisher Caldera, Westdahl Peak, Akutan Peak, Makushin Volcano, Okmok Caldera, Great Sitkin Volcano, Kanaga Volcano, Tanaga Volcano, and Mount Gareloi. Over the past year, formal monitoring of Okmok, Tanaga and Gareloi were announced following an extended period of monitoring to determine the background seismicity at each volcanic center. The seismicity at Mount Peulik was still being studied at the end of 2004 and has yet to be added to the list of monitored volcanoes in the AVO weekly update. AVO located 6928 earthquakes in 2004 (Table 1).

Monitoring highlights in 2004 include: (1) an earthquake swarm at Westdahl Peak in January; (2) an increase in seismicity at Mount Spurr starting in February continuing through the end of the year into 2005; (4) low-level tremor, and low-frequency events related to intermittent ash and steam emissions at Mount Veniaminof between April and October; (4) low-level tremor at Shishaldin Volcano between April and October; (5) an earthquake swarm at Akutan in July; and (6) low-level tremor at Okmok Caldera

throughout the year (Table 2). Instrumentation and data acquisition highlights in 2004 were the installation of subnetworks on Mount Peulik and Korovin Volcano and the installation of broadband stations to augment the Katmai and Spurr subnetworks.

This catalog includes: (1) a description of instruments deployed in the field and their locations; (2) a description of earthquake detection, recording, analysis, and data archival systems; (3) a description of velocity models used for earthquake locations; (4) a summary of earthquakes located in 2004; and (5) an accompanying UNIX tar-file with a summary of earthquake origin times, hypocenters, magnitudes, phase arrival times, and location quality statistics; daily station usage statistics; and all HYPOELLIPSE files used to determine the earthquake locations in 2004.

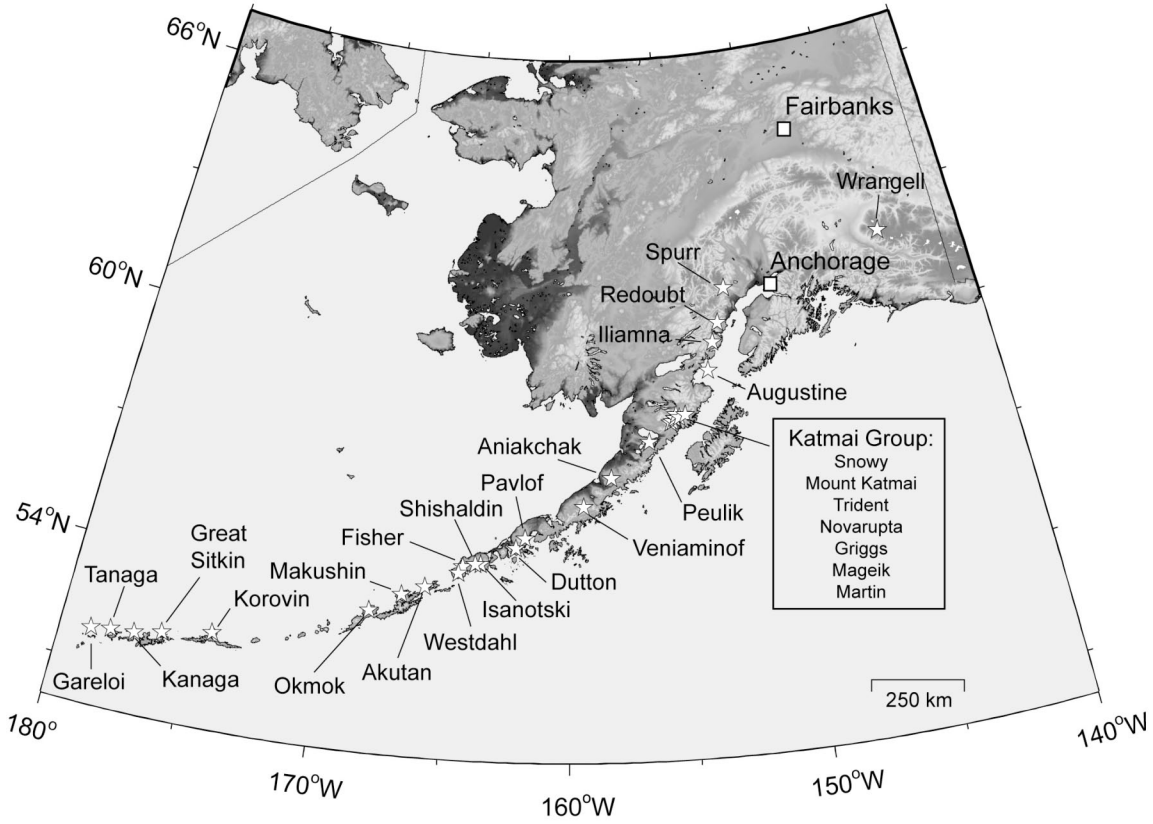

Figure 1. Stars show the location of Alaskan volcanoes seismically instrumented by AVO in 2004. Squares show the location of Anchorage and Fairbanks.

Table 1: Number of earthquakes located per year by AVO for the last nine years.

Year	Earthquakes located per year	Volcanoes with seismograph networks
1996	6466	15
1997	2930	17
1998	2873	19
1999	2769	21
2000	1551	21
2001	1427	23
2002	7242	24
2003	3911	27
2004	6928	28

Table 2: Highlights of Alaskan volcanic seismicity in 2004.

Dates	Volcano	Event
January 2004	Westdahl	Earthquake Swarm
February-December 2004	Spurr	Increased seismicity
April-October 2004	Veniaminof	Low-level tremor and low-frequency events
April-October 2004	Shishaldin	Low-level tremor
July 2004	Akutan	Earthquake Swarm
January-December 2004	Okmok	Low-level tremor

Instrumentation

In 2004, the AVO seismograph network was expanded from 160 to 182 permanent seismograph stations (Appendix B, C). The AVO seismograph network is composed of 21 subnetworks with 4-18 seismograph stations per subnetwork, and 14 regional seismograph stations. In August, two broadband seismograph stations were installed to augment the existing Katmai subnetwork. In response to increased activity at Mount Spurr, three broadband and two single-component short-period stations were installed in late August and early September. One broadband station was added to the Okmok subnetwork in September. Two new subnetworks were installed to monitor Mount Peulik and Korovin Volcano. The telemetry for the Peulik subnetwork was

completed in August and the Korovin subnetwork was completed until March 2005. The 182 permanent seismograph stations have a total of 254 components.

Of the 182 permanent seismograph stations operated by AVO, 148 were short-period vertical-component seismograph stations. All these stations had either Mark Products L4 or Teledyne-Geotech S-13 seismometers with a one-second natural period. AVO also operated 20 three-component, short-period instruments during the catalog period. The instruments used at sites with three component sensors were Mark Products L22 seismometers with a 0.5-second period, Mark Products L4 seismometers with a one-second period and Teledyne-Geotech S-13 seismometers with a one-second natural period. A total of 15 broadband stations were operated with either Guralp CMG-40T seismometers (frequency range: 0.102Hz to 50 Hz) or Guralp CMG-6TD seismometers (frequency range: 0.033Hz to 50 Hz). Short-period stations are digitized at 100 samples/second and broadband stations are digitized at 50 samples/second. Typical calibration curves for seismometers used in the AVO seismograph network are shown in Figures 2-6.

Data from short-period seismograph stations were telemetered using voltage-controlled oscillators (VCOs) to transform the ground motion signals from the seismometers to frequency-modulated signals suitable for transmission over a radio link or telephone circuit. AVO used both the A1VCO (Rogers and others, 1980) and McVCO (McChesney, 1999) to modulate signals in the field. The vast majority of seismograph stations used the McVCO since all A1VCO's are currently being phased out. These signals were transmitted via UHF and VHF radio to communication hubs located in Adak, Akutan, Anchorage, Cold Bay, Dutch Harbor, Homer, Kasilof, King Cove, King Salmon, Port Heiden, Sourdough, Sterling, and Tolsona. At the Adak, Dutch Harbor, Homer and King Salmon communication hubs, the data were digitized at the hub and then directed to AVO offices via high speed digital circuits. From all other hubs, signals were relayed via leased telephone circuits to AVO offices in Anchorage and Fairbanks where the signals were digitized. Data from broadband seismograph stations were digitized at the seismograph station site and transmitted digitally using spread-spectrum radios to communication hubs in Akutan, Anchorage, Dutch Harbor, Homer, and King

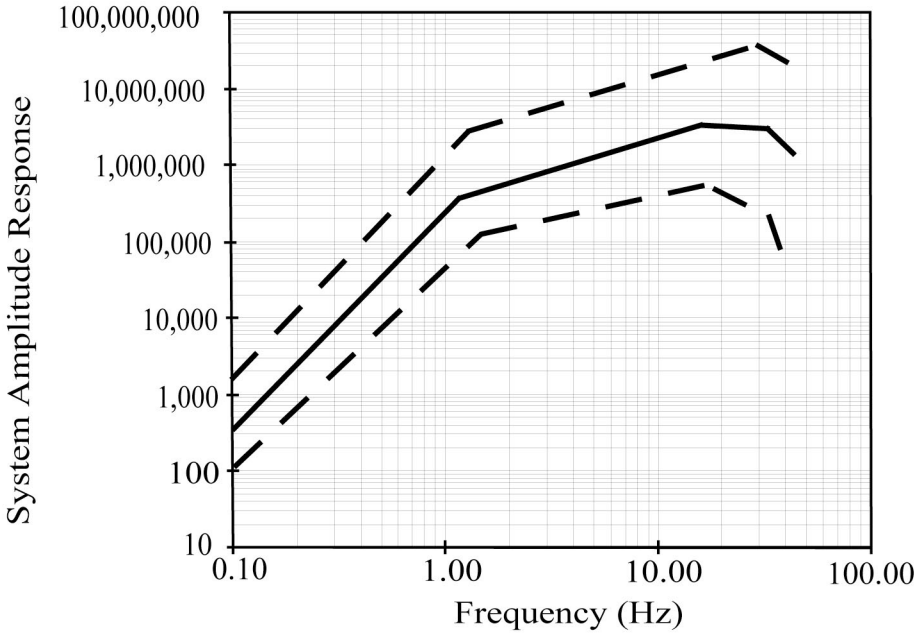

Figure 2. Representative displacement response curves for the 136 stations using a Mark Products L4 seismometer. The solid line illustrates the typical calibration curve and the dashed lines show the range of calibration curves for all AVO stations using an L4 seismometer.

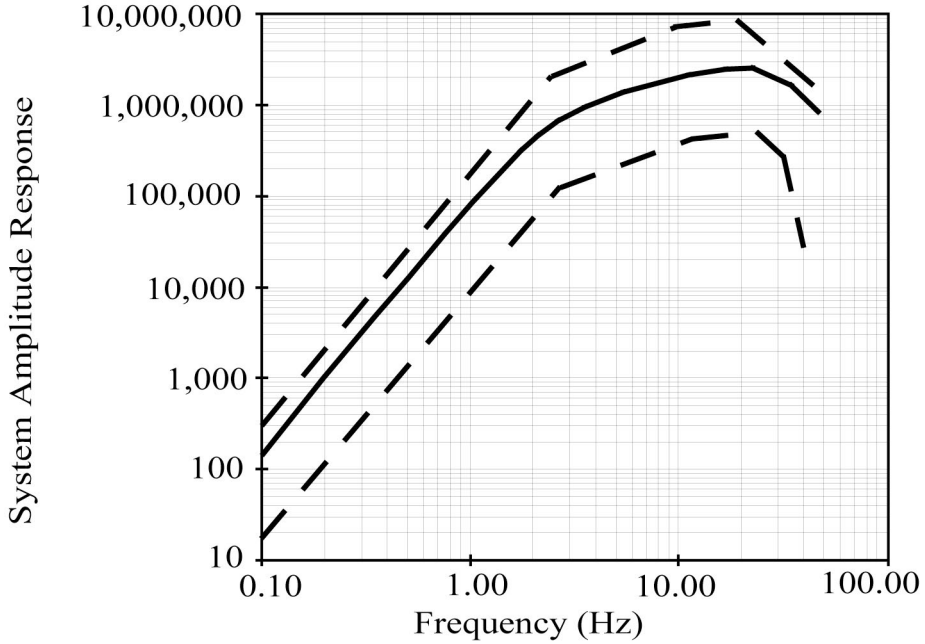

Figure 3. Representative displacement response curves for the 16 stations using a Mark Products L22 seismometer. The solid line illustrates the typical calibration curve and the dashed lines show the range of calibration curves for all AVO stations using an L22 seismometer.

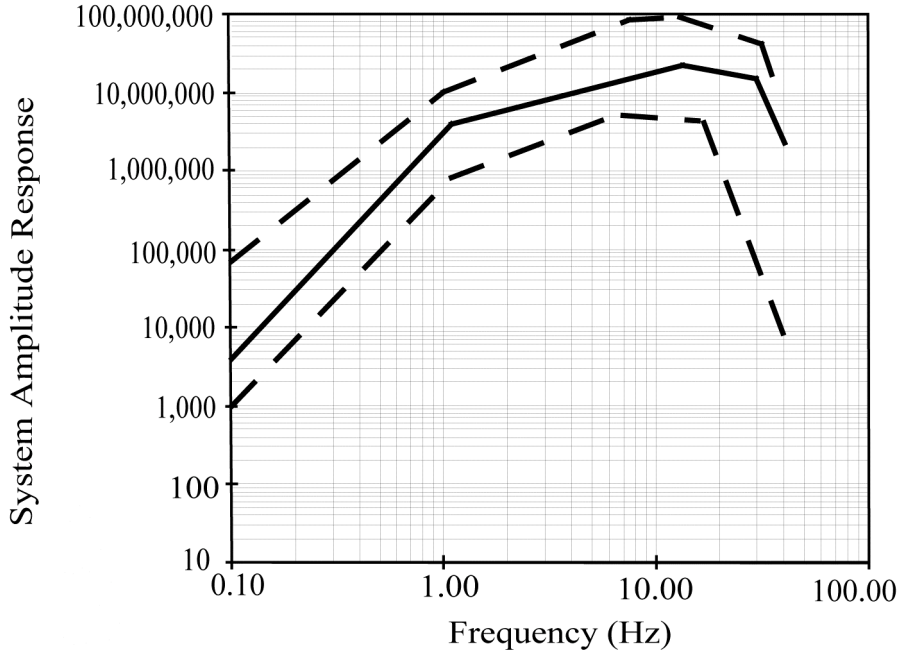

Figure 4. Representative displacement response curves for the 17 stations using a Teledyne-Geotech S-13 seismometer. The solid line illustrates the typical calibration curve and the dashed lines show the range of calibration curves for all AVO stations using an S-13 seismometer.

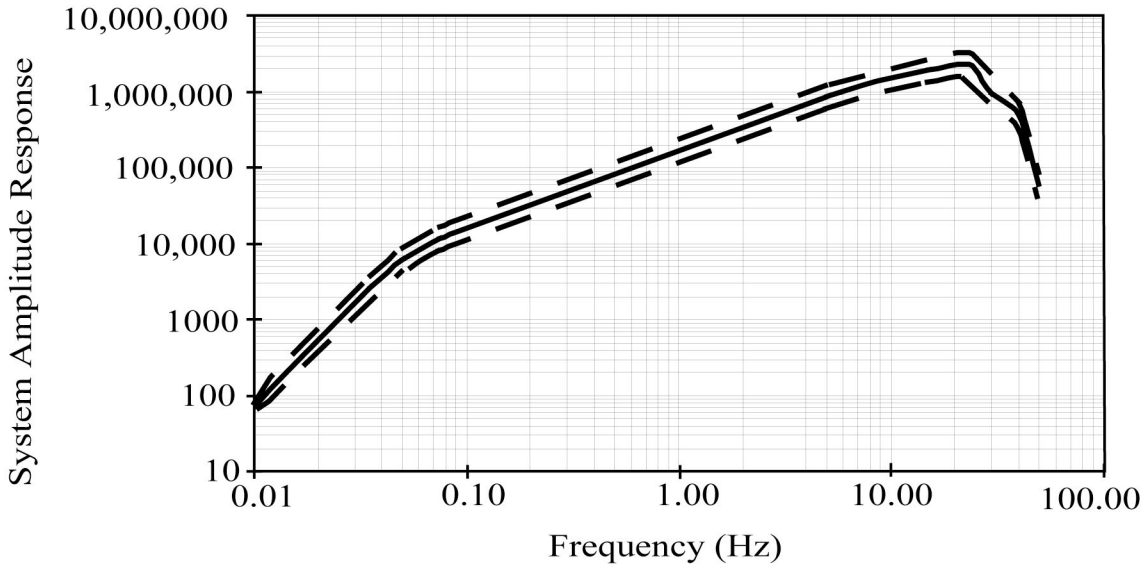

Figure 5. Representative displacement response curves for the two stations using a Guralp CMG-40T seismometer. The solid line illustrates the typical calibration curve and the dashed lines show the range of calibration curves for all AVO stations using a Guralp CMG-40T seismometer.

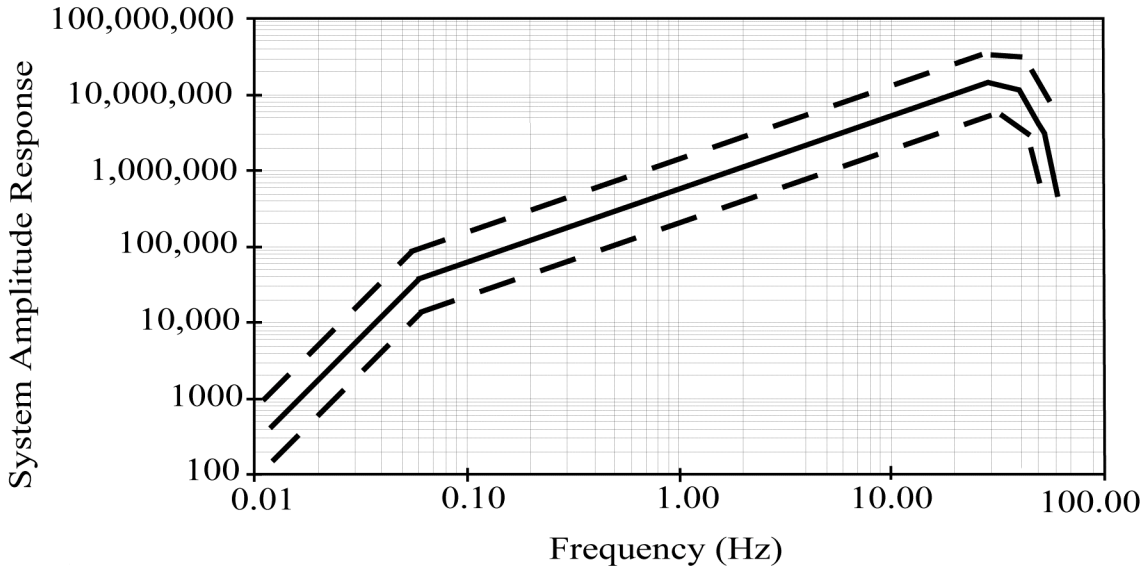

Figure 6. Representative displacement response curves for the 13 stations using a Guralp CMG-6TD seismometer. The solid line illustrates the typical calibration curve and the dashed lines show the range of calibration curves for all AVO stations using a Guralp CMG-6TD seismometer.

Salmon. The data were forwarded to AVO offices in Fairbanks and Anchorage via leased telephone circuits.

Locations and descriptions for all AVO stations operated during 2004 are contained in Appendix B. Maps showing the locations of stations with respect to individual volcanoes are contained in Appendix C. Estimates of each station's operational status for the catalog period are shown in Appendix D. Other station information, such as calibration information contained in the file CALDATA.PRM, is available within the associated compressed UNIX tar-file.

Data Acquisition and Reduction

Data acquisition for the AVO seismograph network was accomplished with duplicate EARTHWORM systems (Johnson, 1995) located at AVO offices in Anchorage and Fairbanks, providing a backup in case of failure at either location. Data were recorded in continuous and event detected modes. Event detected data were collected using the EARTHWORM modules, Carlstatrig and Carlsubtrig. The Carlstatrig

parameters were set as follows: LTA time = 8 seconds, Ratio = 2.3, and Quiet = 4. Carlsubtrig was modified such that a two-letter code was appended to the filename of each trigger to identify which subnetwork triggered or if the event was a regional trigger. If four or more subnetworks triggered on the same event, all data were saved in a single trigger. These network codes are summarized in Table 3. All data are saved in SAC format.

Table 3: Volcano Subnetwork Designators

Volcano Subnetwork	**Network Code**
Akutan Peak	ak
Aniakchak Crater	an
Augustine Volcano	au
Mount Dutton	dt
Iliamna Volcano	il
Mount Gareloi	ga
Great Sitkin Volcano	gs
Kanaga Volcano	ki
Katmai Volcanic Cluster	ka
Korovin Volcano	ko
Makushin Volcano	ma
Okmok Caldera	ok
Pavlof Volcano	pv
Mount Peulik	pl
Redoubt Volcano	rd
Regional event	rg
Shishaldin Volcano	sh
Mount Spurr	sp
Tanaga Volcano	ta
Mount Veniaminof	vn
Westdahl Peak	we
Mount Wrangell	wa

Event triggers were processed daily using the interactive seismic data analysis program XPICK (Robinson, 1990), and the earthquake location program HYPOELLIPSE (Lahr, 1999). Each event trigger was visually inspected and false triggers were deleted. Each subsequent event was identified by a classification code (Table 4) stored in the event location pick file. This classification system was modeled after that described by

Lahr and others (1994). Earthquakes with a P-wave and S-wave separation of greater than five seconds on the closest station were assumed to come from non-volcanic sources and were typically discarded. The quality of each hypocenter was checked using a computer algorithm that identified events without magnitude, with fewer than three P-phases, with less than two S-phases, and with standard hypocentral errors greater than 15 km. Events not meeting these requirements after further evaluation were removed from the final catalog listing. For all the 2004 earthquakes in the AVO catalog, the average root-mean-square travel-time error was 0.128 seconds.

Table 4: Classification codes

Event Classification	Classification Code
Volcano-Tectonic (VT)	a
Low-Frequency (LF)	b
Hybrid	h
Regional-Tectonic	E
Teleseismic	T
Shore-Ice	i
Calibrations	C
Other non-seismic	o
Cause unknown	x

Velocity Models

During 2004, AVO employed eight local velocity models and one regional seismic velocity model (Appendix E) to locate earthquakes at monitored volcanoes in 2004. All velocity models were one-dimensional models utilizing horizontal layers to approximate the local seismic velocity structures. Each model, with one exception, assumed a series of constant velocity layers. The single exception was the Akutan velocity model (Power and others, 1996), which had a velocity gradient in the top layer overlying a half-space of constant velocity.

One or more vertical cylinders were used to model the volcanic source zones on all volcanoes where a local volcano-specific velocity model was used. Earthquakes within these cylindrical volumes were located with a local model and earthquakes outside of the cylindrical volumes were located with the regional model. All cylindrical volumes

had a radius of 20 km with the exception of the cylinder centered on Shishaldin Volcano. The cylinder centered on Shishaldin Volcano had a radius of 30 km in order to encompass Isanotski Peaks. The top of each cylinder is set at three km above sea level and the bottom is set at a depth of 50 km with respect to sea level.

The Akutan, Augustine (Power, 1988), and Iliamna (Roman and others, 2001) velocity models were used to locate hypocenters that fell within cylindrical volumes described above, centered on each respective volcano. The Cold Bay velocity model (McNutt and Jacob, 1986) was used to locate earthquakes that fell within single cylindrical volumes centered on Mount Dutton and Pavlof Volcano. Earthquakes on Fisher Caldera, Isanotski Peaks, Shishaldin Volcano, and Westdahl Peak that fell within the cylindrical regions centered on Shishaldin Volcano and Westdahl Peak were also located with the Cold Bay velocity model. Five overlapping cylinders defined the area in which the Spurr velocity model (Jolly and others, 1994) was used, four overlapping cylinders defined the area in which the Redoubt velocity model (Lahr and others, 1994) was used, and four overlapping cylinders defined the area in which the Katmai model (Searcy, 2003) was used. The Andreanof velocity model (Toth and Kisslinger, 1984) was used to locate earthquakes within a volume defined by three cylinders centered on Kanaga Volcano, Mount Moffet, and Great Sitkin Volcano. Specific velocity models for Aniakchak Crater, Mount Gareloi, Korovin Volcano, Makushin Volcano, Okmok Volcano, Mount Peulik, Tanaga Volcano, Mount Veniaminof, and Mount Wrangell were not available in 2004 and the regional velocity model (Fogleman and others, 1993) was used to locate earthquakes surrounding these volcanoes. The cylindrical model parameters, regional velocity model, and volcano-specific models used to locate earthquakes in this report are summarized in Appendix E. Figures showing the volcanic source zones modeled by cylinders in map view are shown in Appendix F.

Seismicity

The 6928 earthquakes located in 2004 represent the third highest annual total determined by AVO in a single calendar year since recording began in 1989 and an increase from the 3911 earthquakes located in 2003. Of the earthquakes located in 2004, 5326 were classified as volcano-tectonic earthquakes, 1411 are classified as low-

frequency earthquakes and 191 are classified in other categories listed in Table 4. Of the earthquakes located in 2003 and 2004, a total of 3264 earthquakes in 2003 and 6105 earthquakes in 2004 were located within 20 km of an active volcanic center. The number of located events in the last two years, by seismograph subnetwork, is shown in Table 5.

Using the 2004 earthquake catalog, the magnitude of completeness (Mc) for each subnetwork was calculated (Table 6). The Mc, calculated using ZMAP (Weimer, 2001), is the lowest magnitude at which we are reasonably certain that all events of greater magnitude were detected. The Mc was determined automatically using a maximum likelihood estimate of the inflection point in the frequency magnitude distribution. Earthquakes from previous years were included to calculate the Mc for the Aniakchak.

Table 5: Number of earthquakes located for each seismograph subnetwork in 2003 and 2004 within 20 km of the volcanic centers in each subnetwork. The totals for 2004 are broken into three event types: volcanic-tectonic (VT), low-frequency (LF) and other (all possible event types are shown in Table 3).

Volcano Subnetwork	Earthquakes located in 2003	Earthquakes located in 2004	2004 VT	2004 LF	2004 Other
Akutan Peak	66	120	108	12	0
Aniakchak Crater	11	5	2	3	0
Augustine Volcano	107	241	236	0	5
Mount Dutton	37	40	38	2	0
Mount Gareloi	9	376	69	307	0
Great Sitkin Volcano	84	65	65	0	0
Iliamna Volcano	587	805	306	498	1
Kanaga Volcano	22	32	30	2	0
Katmai Vol. Cluster	1065	976	956	19	1
Makushin Volcano	59	233	226	7	0
Okmok Caldera	34	44	43	1	0
Pavlof Volcano	80	58	22	36	0
Mount Peulik	n/a	5	5	0	0
Redoubt Volcano	62	94	90	4	0
Shishaldin Volcano	285	98	20	78	0
Mount Spurr	549	2616	2312	301	3
Tanaga Volcano	3	11	11	0	0
Mount Veniaminof	38	21	20	1	0
Westdahl Peak	75	166	145	21	0
Mount Wrangell	91	99	11	88	0
Totals	3264	6105	4715	1380	10

Table 6: Magnitude of completeness (Mc) for AVO seismograph subnetworks using the 2004 Catalog. The Peulik subnetwork was not included because there were too few earthquakes to calculate a Mc.

Volcano Subnetwork	Magnitude of Completeness
Akutan Peak	0.2
Aniakchak Crater	1.7
Augustine Volcano	0.0
Mount Dutton	0.5
Mount Gareloi	1.1
Great Sitkin Volcano	0.7
Iliamna Volcano	-0.4
Kanaga Volcano	1.2
Katmai Volcanic Cluster	0.6
Makushin Volcano	0.7
Okmok Caldera	1.5
Pavlof Volcano	0.7
Redoubt Volcano	0.2
Shishaldin Volcano	1.0
Mount Spurr	0.2
Tanaga Volcano	0.7
Mount Veniaminof	1.1
Westdahl Peak	0.6
Mount Wrangell	0.8

and Tanaga subnetworks because the sample size in 2004 was not sufficiently large to allow one to compute a Mc for these subnetworks.

The increase in the number of earthquakes located in 2004 compared to those in 2003 at the Augustine and Iliamna subnetworks were a direct result of station maintenance which corrected several station outages in the summer of 2004. The earthquake rates in 2002 at both Augustine and Iliamna Volcanoes were comparable to the earthquakes rates in 2004. The July earthquake swarm at Akutan Volcano accounts for only half of the increase in detected seismicity. The additional increase in detected seismicity seen at Akutan Volcano was a likely result of the installation of four broadband seismometers in 2003 as the magnitude of completeness improved from 1.2 (Dixon and others, 2005) to 0.2. The networks for Gareloi and Tanaga were installed last year so a comparison between earthquakes located in 2003 and 2004 was not possible.

The increase in seismicity at Westdahl Peak was a result of an earthquake swarm in January 2004. The Mount Spurr seismicity in 2004 was dominated by the volcanic unrest first noted in July 2004 (Power, 2004). The Mount Spurr seismicity slowly increased in February and peaked in July. From July through the end of the year, the Mount Spurr seismicity continued well above historical levels.

On Mount Veniaminof, the seismic activity was dominated by non-locatable tremor and low-frequency events. Some of these low-frequency events have been correlated to small ash and steam emissions (Sánchez, 2005). For this reason the seismicity was not adequately described by the number of located earthquakes. Long episodes of tremor also masked the ability of the data acquisition system in detecting individual earthquakes. The seismic activity at Shishaldin Volcano has continued to decline from the 2620 earthquakes located in 2002. Between April and October 2004, there were periods in which numerous low-frequency events were detected at Shishaldin Volcano but were unable to be located. The magnitude of completeness for the Shishaldin subnetwork in 2004 increased to 1.0 from a value of 0.5 (Dixon and others, 2005) although all methods of estimating rates of seismicity at the AVO indicated a decrease in activity in 2004 compared to that in 2003.

The decreases in seismicity at Pavlof and Makushin Volcanoes were related to tectonic earthquakes that occurred within 20 km of each volcanic center. The number of earthquakes that were located within a five km radius circle centered on Makushin Volcano was 27 in 2003 and 31 in 2004. The vast majority of the seismicity increase seen in Table 5 occurred greater than 10 km from the summit of Makushin Volcano. A similar trend was seen for Pavlof Volcano in which 10 earthquakes were located within five km of Pavlof Volcano during 2004, a decrease of a single earthquake from the eleven earthquakes located in 2003.

Seismicity at the Katmai Volcanic Cluster and Great Sitkin Volcano declined compared to that in 2003 but the seismicity is not significantly different than the overall seismicity since 2002. Seismicity rates at the remaining subnetworks in 2004, Wrangell, Redoubt, Aniakchak, Dutton, Okmok, and Kanaga subnetworks, were similar to those in 2003.

Summary

Between January 1, 2004, and December 31, 2004, AVO located 6928 earthquakes that occurred at or near volcanoes in Alaska. Monitoring highlights in 2004 include: earthquake swarms at Westdahl Peak and Akutan Volcano, elevated seismicity and low level tremor at Mount Veniaminof, Shishaldin Volcano, and Okmok Volcano, and an increase in seismicity at Mount Spurr related to an episode of volcanic unrest. New seismic subnetworks were installed on Mount Peulik and Korovin Volcano and broadband stations were installed to augment the subnetworks on Spurr, Katmai and Okmok volcanic centers.

Available for download with this report is a compressed Unix tar-file containing a summary listing of earthquake hypocenters and all the necessary HYPOELLIPSE input files to recalculate the hypocenters including station locations and calibrations, velocity models, and phase information. The reader should refer to Lahr (1999) for information on file formats and instructions for configuring and running the location program HYPOELLIPSE. Archives of waveform data are maintained on CD-ROM at AVO offices in Fairbanks and Anchorage.

Acknowledgements

The contents of this report reflect a great deal of hard work by a large number of people including AVO, AEIC, and USGS personnel and various students, interns and volunteers. We thank Peter Cervelli, Silvio DeAngelis and Mike West for formal reviews of the text and figures.

References

Dixon, J.P, Stihler, S.D., Power J.A., Tytgat, G., Estes, S., Moran, S.C., Paskievitch, J., McNutt, S.R., 2002, Catalog of Earthquake Hypocenters at Alaska Volcanoes: January 1, 2000 – December 31, 2001: U.S. Geological Survey Open-file Report 02-342, 56p.

Dixon, J.P., Stihler, S.D., Power J.A., Tytgat, G., Moran, S.C., Sánchez, J., Estes, S., McNutt, S.R., Paskievitch, J., 2003, Catalog of Earthquake Hypocenters at Alaska Volcanoes: January 1 – December 31, 2002: U.S. Geological Survey Open-file Report 03-267, 58p.

Dixon, J.P., Stihler, S.D., Power J.A., Tytgat, G., Moran, S.C., Sánchez, J., Estes, S., McNutt, S.R., Paskievitch, J., 2004, Catalog of Earthquake Hypocenters at Alaska Volcanoes: January 1 – December 31, 2003: U.S. Geological Survey Open-file Report 2004-1234, 59p.

Dixon, J.P., Power, J.A., Stihler, S.D., 2005, A Comparison of Seismic Event Detection with IASPEI and Earthworm Acquisition Systems at Alaskan Volcanoes, Seismological Research Letters, v. 2, p. 168-176.

Fogleman, K.A., Lahr, J.C., Stephens, C.D., and Page, R.A., 1993, Earthquake locations determined by the southern Alaska seismograph network for October 1971 through May 1989: U.S. Geological Survey Open-file Report 93-309, 54p.

Johnson, C.E., Bittenbinder, A., Bogaert, B., Dietz, L., Kohler, W., 1995, EARTHWORM: A Flexible Approach to Seismograph network Processing, Incorporated Research Institutions for Seismology Newsletter, v. 14, no. 2, p. 1-4.

Jolly, A.D., Page, R.A., and Power, J.A., 1994, Seismicity and stress in the vicinity of Mt. Spurr volcano, south-central Alaska: Journal of Geophysical Research, v. 99, p. 15305-15318.

Jolly, A.D, Power, J.A., Stihler, S.D., Rao, L.N., Davidson, G., Paskievitch, J., Estes, S., Lahr, J.C., 1996, Catalog of earthquake hypocenters for Augustine, Redoubt, Iliamna, and Mount Spurr Volcanoes, Alaska: January 1, 1991 – December 31, 1993: U.S. Geological Survey Open-file Report 96-70, 90p.

Jolly, A.D., Stihler, S.D., Power, J.A., Lahr, J.C., Paskievitch, J., Tytgat, G., Estes, S., Lockhart, A.B., Moran, S.C., McNutt, S.R., Hammond, W.R., 2001, Catalog of earthquake hypocenters at Alaskan Volcanoes: January 1, 1994 – December 31, 1999: U.S. Geological Survey Open-file Report 01-189, 202p.

Lahr, J.C, Chouet, B.A., Stephens, C.D., Power, J.A., Page, R.A., 1994, Earthquake classification, location, and error analysis in a volcanic environment: Implications for the magmatic system of the 1989-90 eruptions at Redoubt Volcano, Alaska: Journal of Volcanology and Geothermal Research, v. 62, p. 137–152.

Lahr, J.C., 1999, HYPOELLIPSE: A Computer Program for Determining Local Earthquake Hypocentral Parameters, Magnitude, and First Motion Pattern: U.S. Geological Survey Open File Report 99-23, 116p.

McChesney, P.J., 1999, McVCO Handbook 1999: U.S. Geological Survey, Open-File Report 99-361, 48p.

McNutt, S.R., and Jacob, K.H., 1986, Determination of large-scale velocity structure of the crust and upper mantle in the vicinity of Pavlof volcano, Alaska: Journal of Geophysical Research, v. 91, p. 5013-5022.

Power, J.A., 1988, Seismicity associated with the 1986 eruption of Augustine Volcano, Alaska: University of Alaska Fairbanks, Masters thesis, 149p.

Power, J.A., Paskievitch, J.F., Richter, D.H., McGimsey, R.G., Stelling, P., Jolly, A.D., Fletcher, H.J., 1996, 1996 seismicity and ground deformation at Akutan Volcano, Alaska: EOS Transactions of the American Geophysical Union, v. 77, p. F514.

Power, J.A., 2004, Renewed unrest at Mount Spurr Volcano, Alaska, EOS, v. 85, p. 434.

Power, J.A., March, G.D., Lahr, J.C., Jolly, A.D., Cruse, G.R., 1993, Catalog of earthquake hypocenters at Redoubt Volcano and Mount Spurr, Alaska: October 12, 1989-December 31, 1990: U.S. Geological Survey Open-File Report, 93-685-A, 57p.

Robinson, M., 1990, XPICK users manual, version 2.7: Seismology Lab, Geophysical Institute, University of Alaska Fairbanks, 93p.

Rogers, J.A., Maslak, S., and Lahr, J.C., 1980, A seismic electronic system with automatic calibration and crystal reference: U.S. Geological Survey Open-file Report 80-324, 130p.

Roman, D.C., Power, J.A., Moran, S.C., Cashman, K.V., Stihler, S.D., 2001, Unrest at Iliamna Volcano, Alaska in 1996, Evidence for a magmatic intrusion: EOS Transactions of the American Geophysical Union, v. 82, p. F1329.

Sánchez, J.J, 2005, Volcano Seismology from around the World: Case Studies from Mount Pinatubo (Philippines), Galeras (Columbia), Mount Wrangell and Mount Veniaminof (Alaska): University of Alaska Fairbanks Phd Dissertation, 208p.

Searcy, C.K., 2003, Station Corrections for the Katmai Region Seismograph network: U.S. Geological Survey Open-file Report 03-403, 16p.

Toth, T., and Kisslinger, C., 1984, Revised focal depths and velocity model for local earthquakes in the Adak seismic zone: Bulletin of the Seismological Society of America, v. 74, p. 1349-1360.

Wiemer, S., 2001, A software package to analyze seismicity: ZMAP, Seismological Research Letters 72, 373-382.

Appendix A: Maps showing the locations of the earthquakes located in 2004.

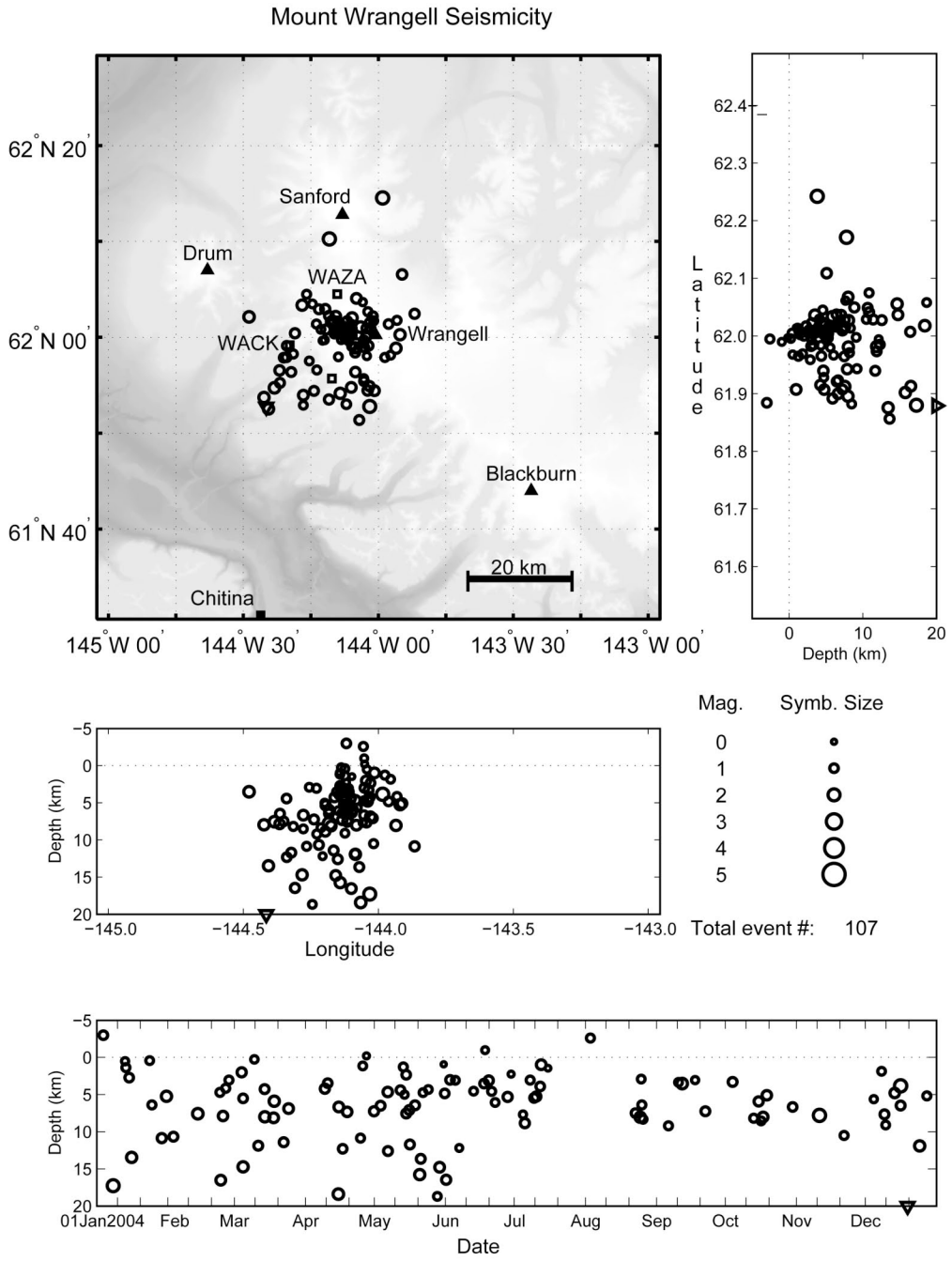

Figure A1. Summary plots of 107 earthquakes located near Mount Wrangell in 2004. Open circles show hypocenter locations shallower than 20 km and open triangles show hypocenters with depths of 20 km and deeper. Hypocenter symbols are scaled with magnitude. Seismograph stations are shown by open squares and labeled by station code. (See Appendix B for station information). Solid triangles are used to show volcanic centers and closed squares are used to show other points of interest.

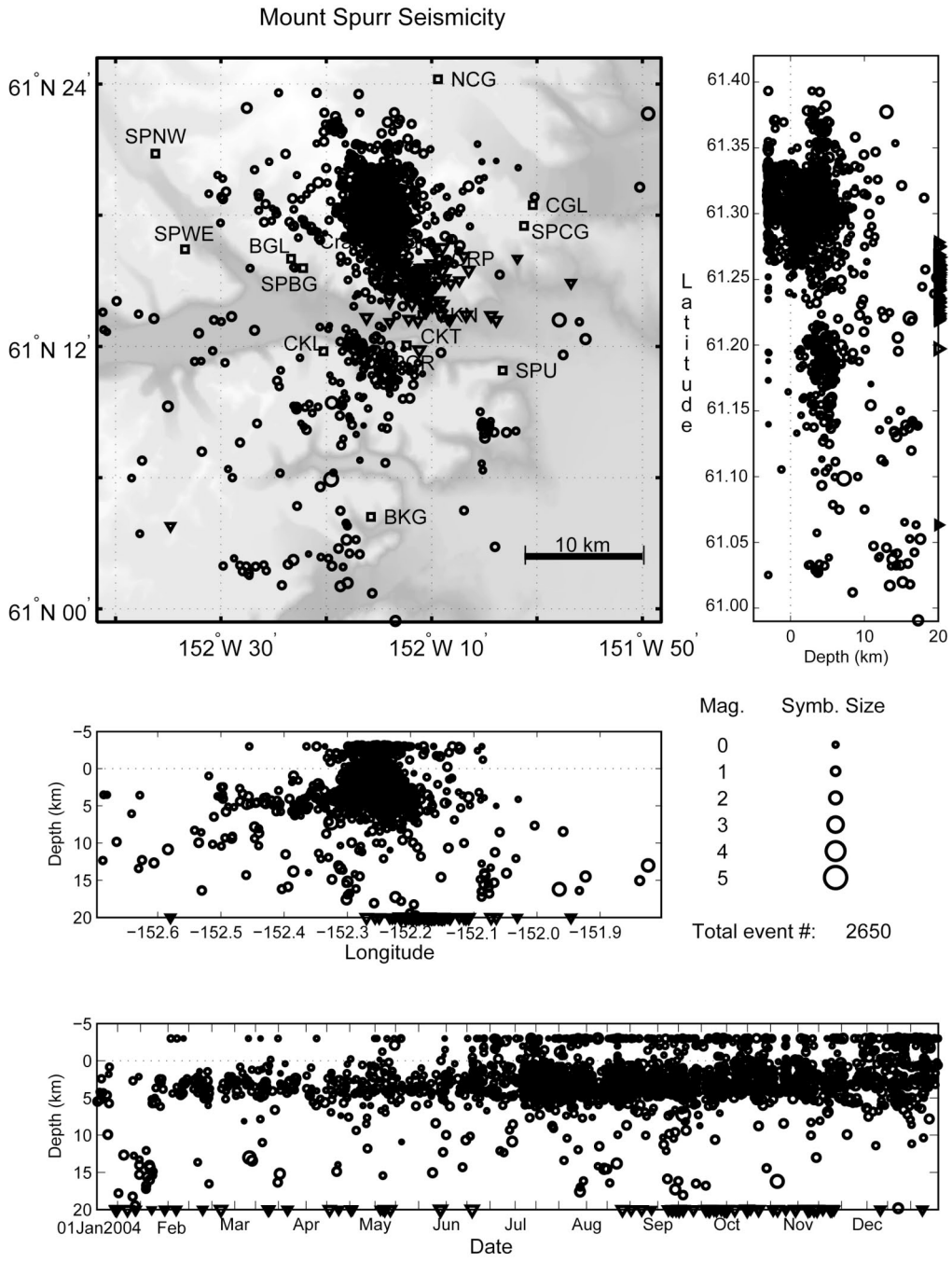

Figure A2. Summary plots of 2650 earthquakes located near Mount Spurr in 2004. Open circles show hypocenter locations shallower than 20 km and open triangles show hypocenters with depths of 20 km and deeper. Hypocenter symbols are scaled with magnitude. Seismograph stations are shown by open squares and labeled by station code. (See Appendix B for station information). Solid triangles are used to show volcanic centers and closed squares are used to show other points of interest.

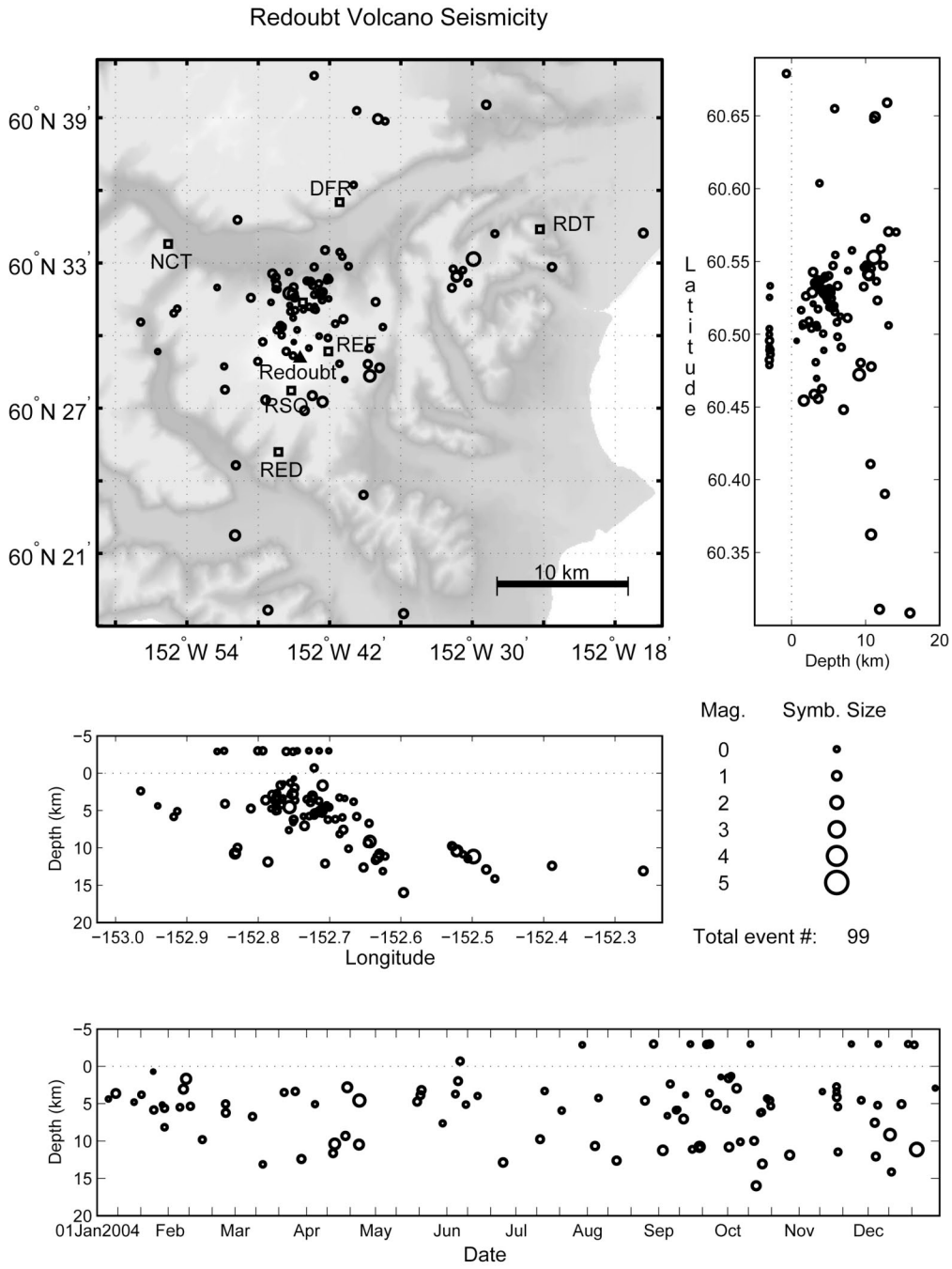

Figure A3. Summary plots of 99 earthquakes located near Redoubt Volcano in 2004. Open circles scaled with magnitude show hypocenter locations. Seismograph stations are shown by open squares and labeled by station code. (See Appendix B for station information). Solid triangles are used to show volcanic centers and closed squares are used to show other points of interest.

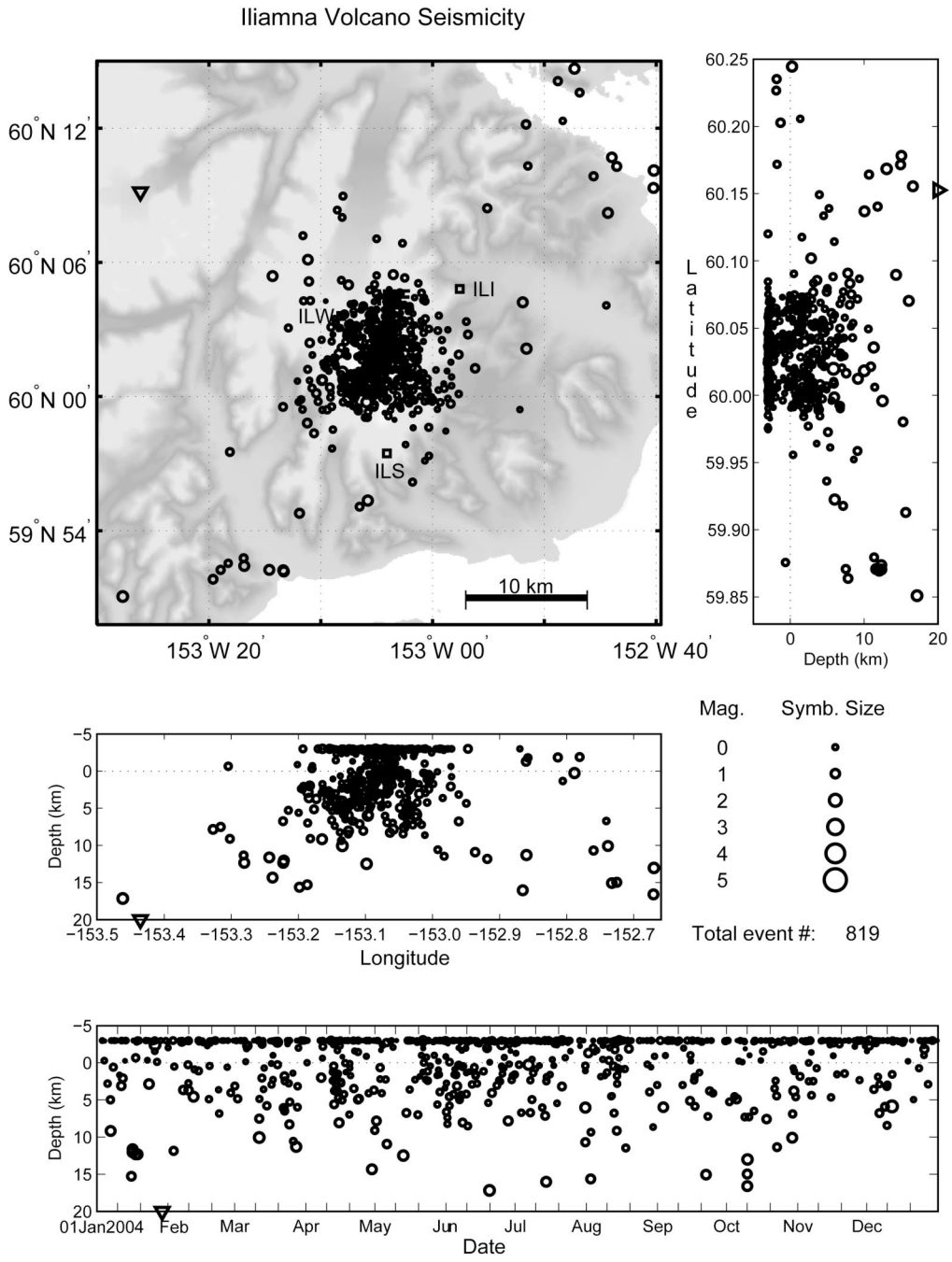

Figure A4. Summary plots of 819 earthquakes located near Iliamna Volcano in 2004. Open circles show hypocenter locations shallower than 20 km and open triangles show hypocenters with depths of 20 km and deeper. Hypocenter symbols are scaled with magnitude. Seismograph stations are shown by open squares and labeled by station code. (See Appendix B for station information). Solid triangles are used to show volcanic centers and closed squares are used to show other points of interest.

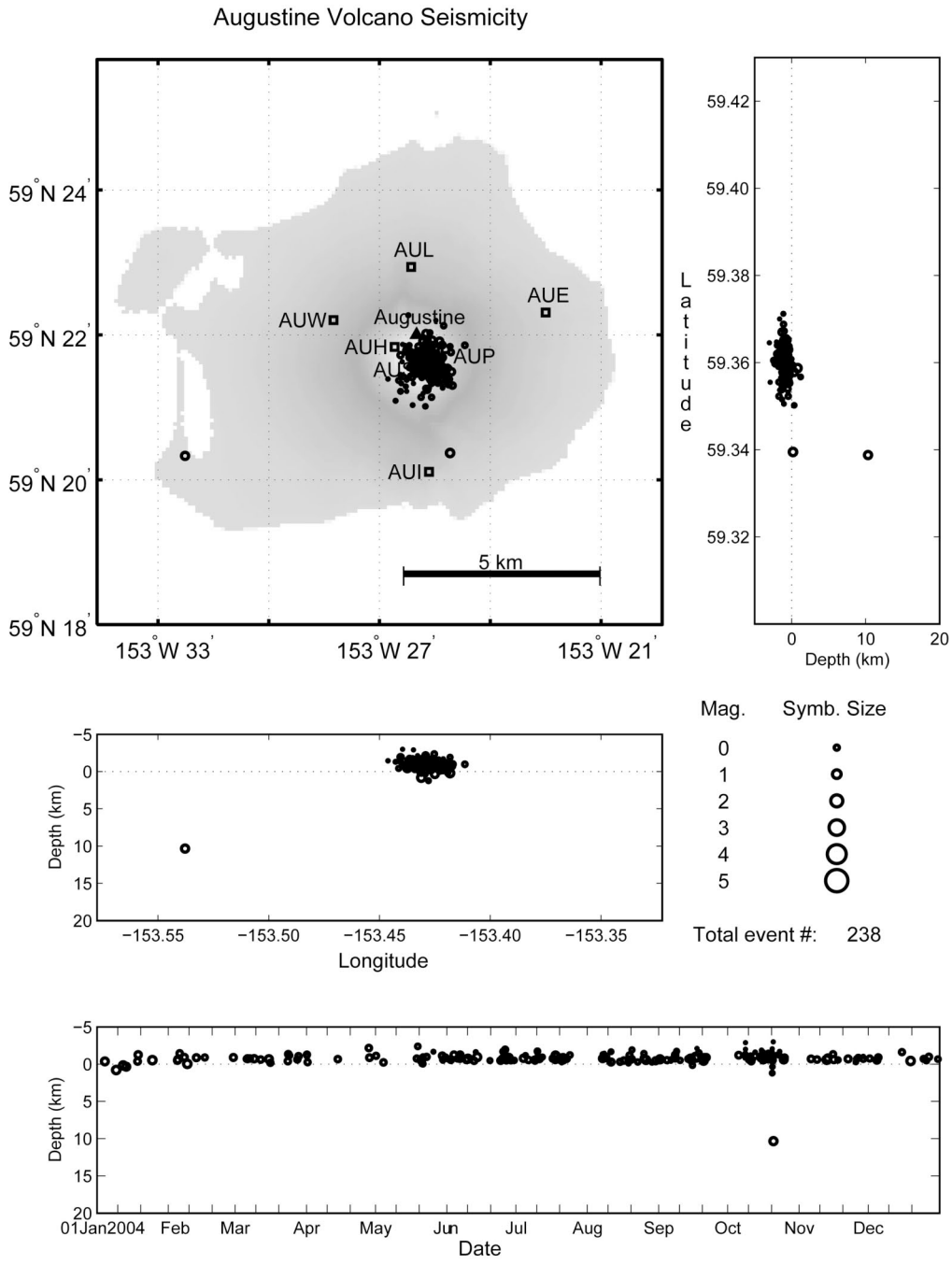

Figure A5. Summary plots of 238 earthquakes located near Augustine Volcano in 2004. Open circles scaled with magnitude show hypocenter locations. Seismograph stations are shown by open squares and labeled by station code. (See Appendix B for station information). Solid triangles are used to show volcanic centers and closed squares are used to show other points of interest.

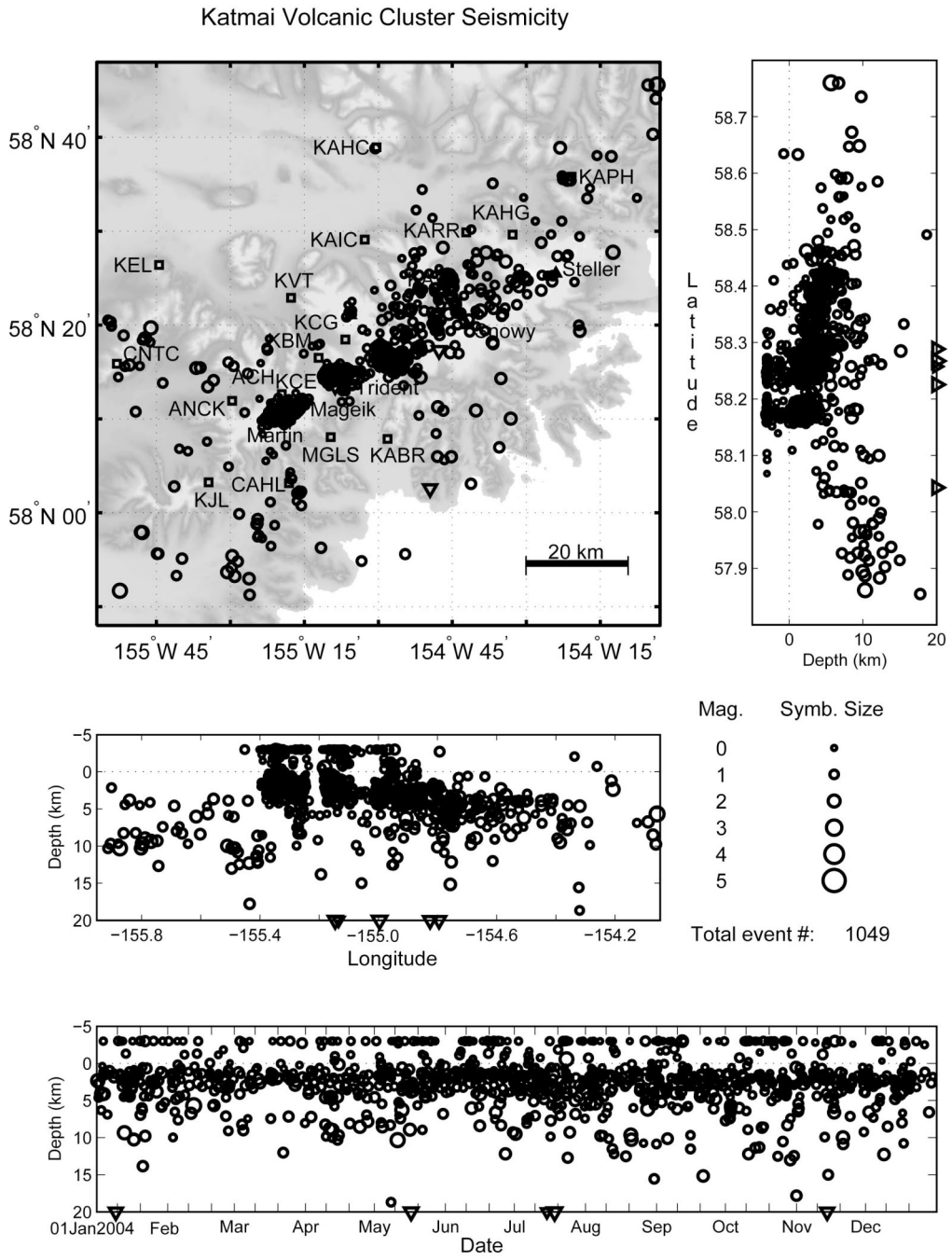

Figure A6. Summary plots of 1049 earthquakes located near the Katmai volcanic cluster in 2004. Open circles show hypocenter locations shallower than 20 km and open triangles show hypocenters with depths of 20 km and deeper. Hypocenter symbols are scaled with magnitude. Seismograph stations are shown by open squares and labeled by station code. (See Appendix B for station information). Solid triangles are used to show volcanic centers and closed squares are used to show other points of interest.

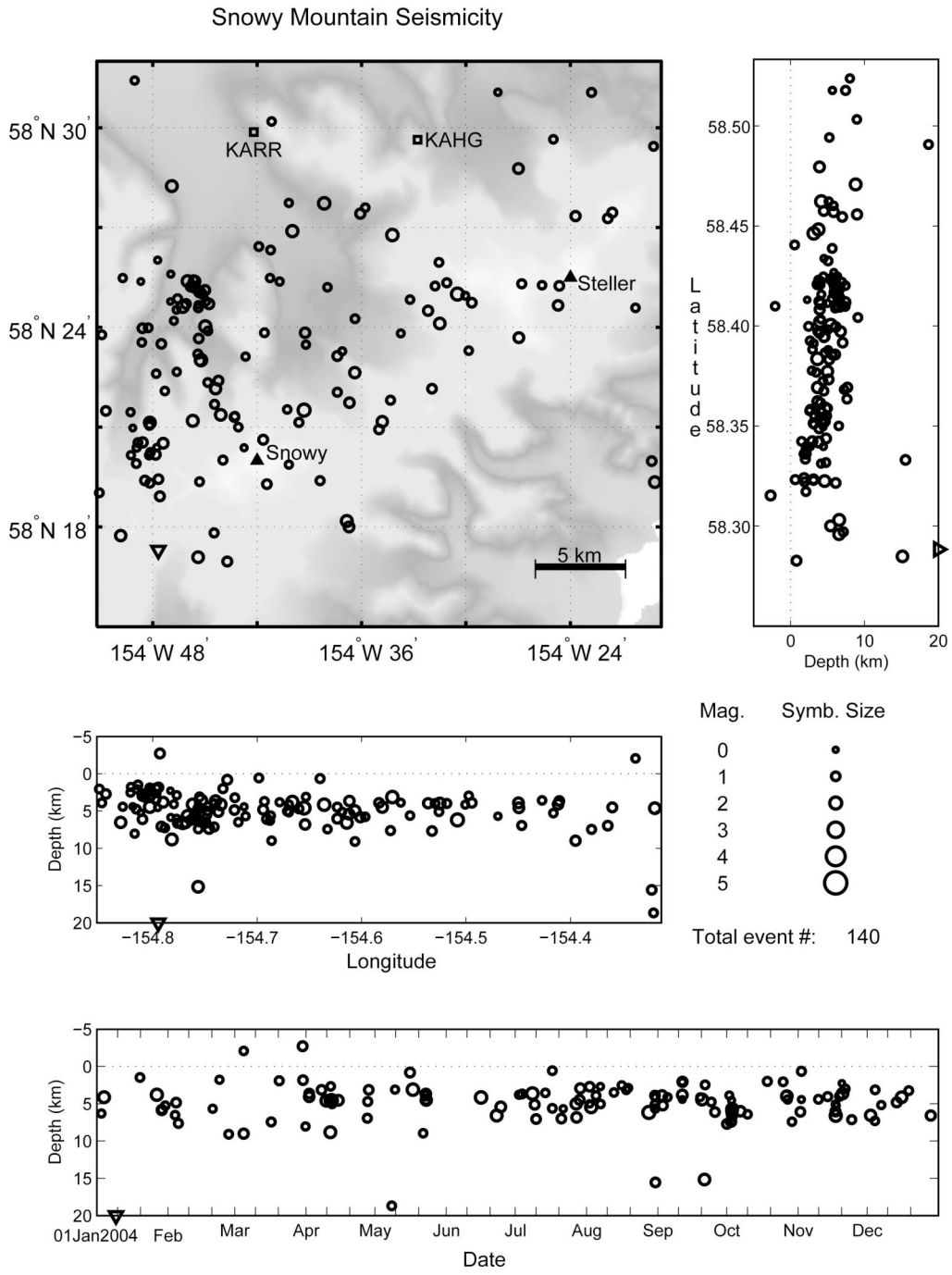

Figure A7. Summary plots of 140 earthquakes located near Snowy Mountain in the Katmai volcanic cluster in 2004. Open circles show hypocenter locations shallower than 20 km and open triangles show hypocenters with depths of 20 km and deeper. Hypocenter symbols are scaled with magnitude. Seismograph stations are shown by open squares and labeled by station code. (See Appendix B for station information). Solid triangles are used to show volcanic centers and closed squares are used to show other points of interest.

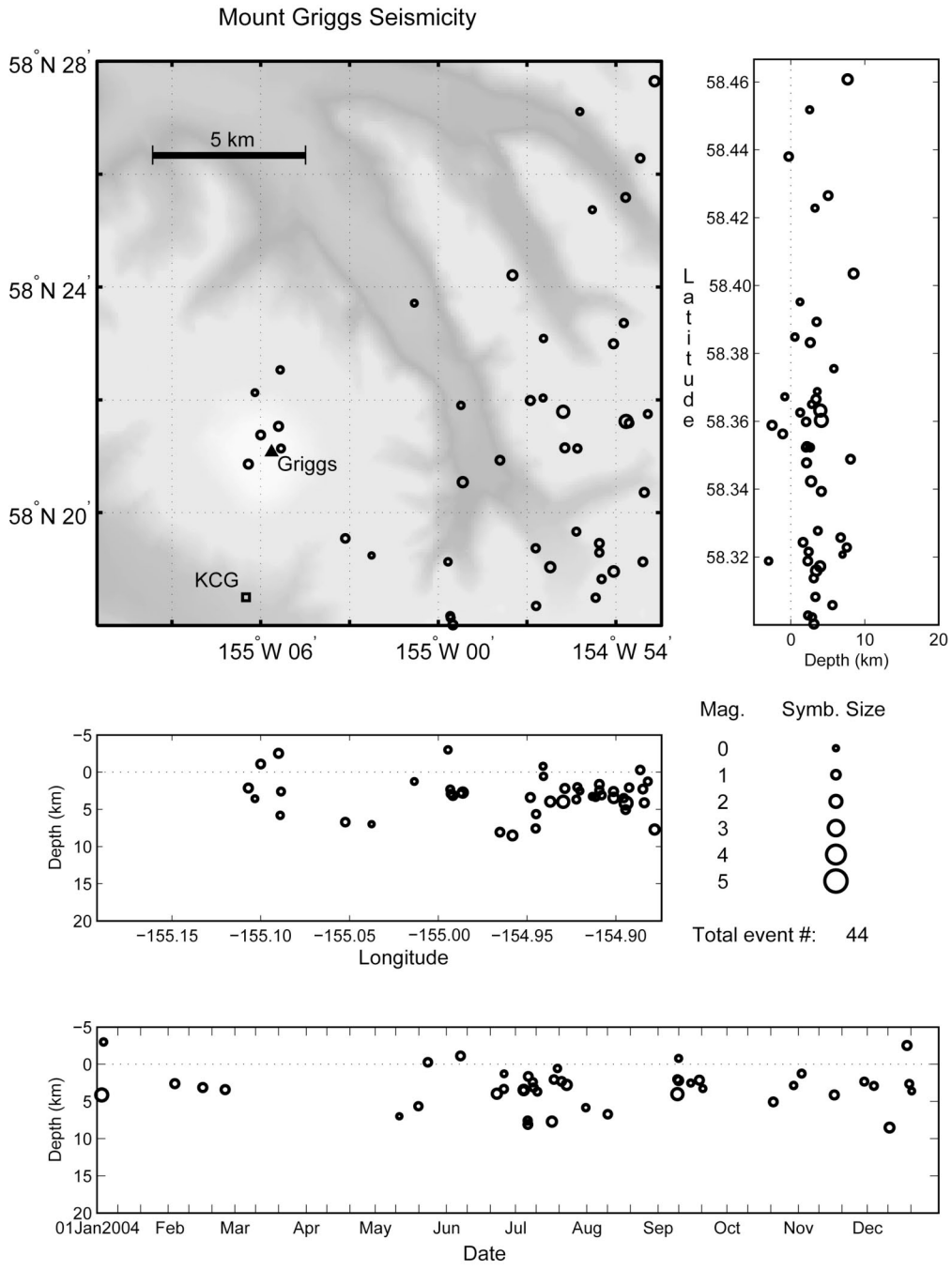

Figure A8. Summary plots of 44 earthquakes located near Mount Griggs in the Katmai volcanic cluster in 2004. Open circles scaled with magnitude show hypocenter locations. Seismograph stations are shown by open squares and labeled by station code. (See Appendix B for station information). Solid triangles are used to show volcanic centers and closed squares are used to show other points of interest. Several earthquakes that appear on this figure appear on other figures.

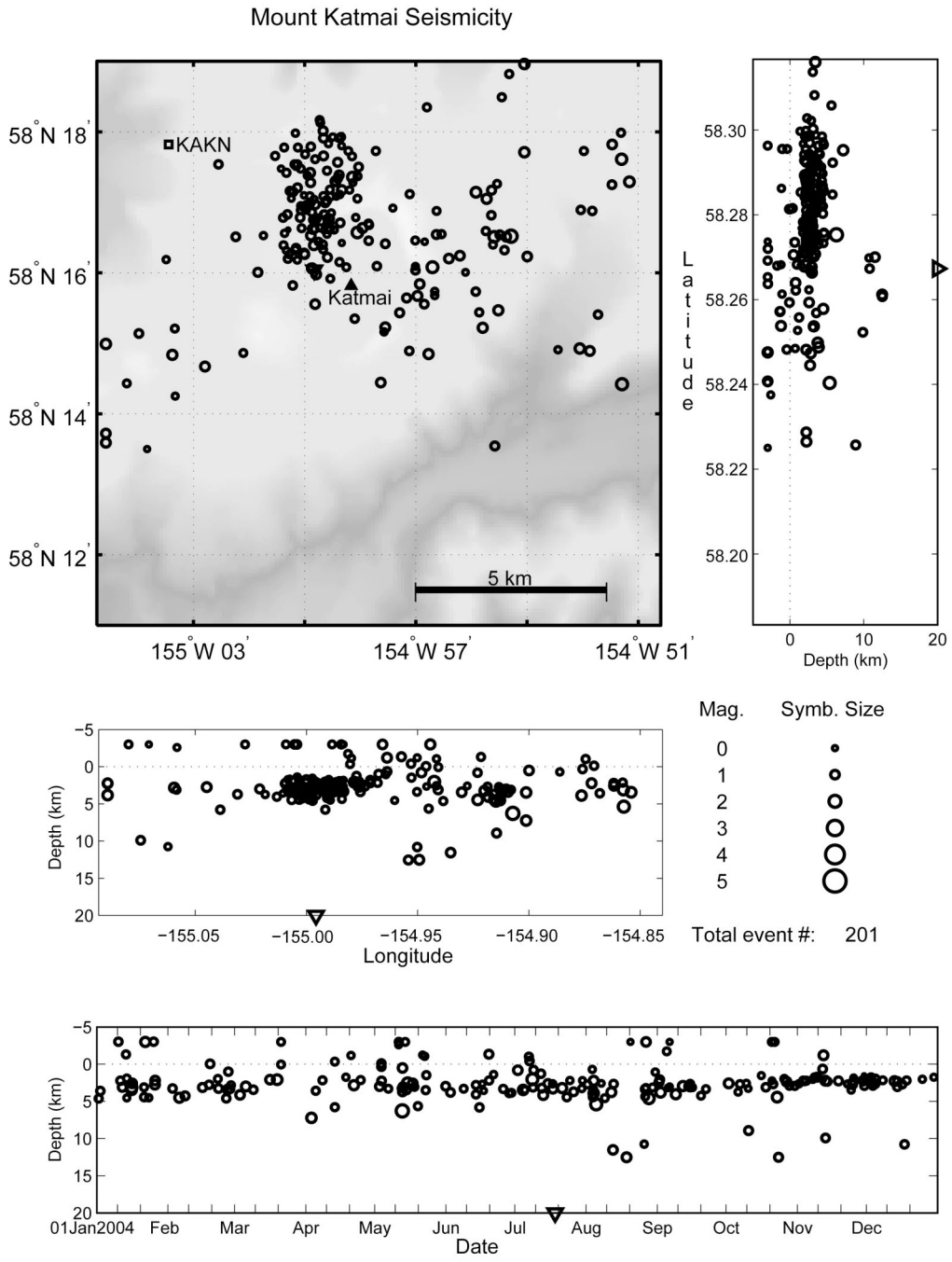

Figure A9. Summary plots of 201 earthquakes located near Mount Katmai in the Katmai volcanic cluster in 2004. Open circles show hypocenter locations shallower than 20 km and open triangles show hypocenters with depths of 20 km and deeper. Hypocenter symbols are scaled with magnitude. Seismograph stations are shown by open squares and labeled by station code. (See Appendix B for station information). Solid triangles are used to show volcanic centers and closed squares are used to show other points of interest. Several earthquakes that appear on this figure appear on other figures.

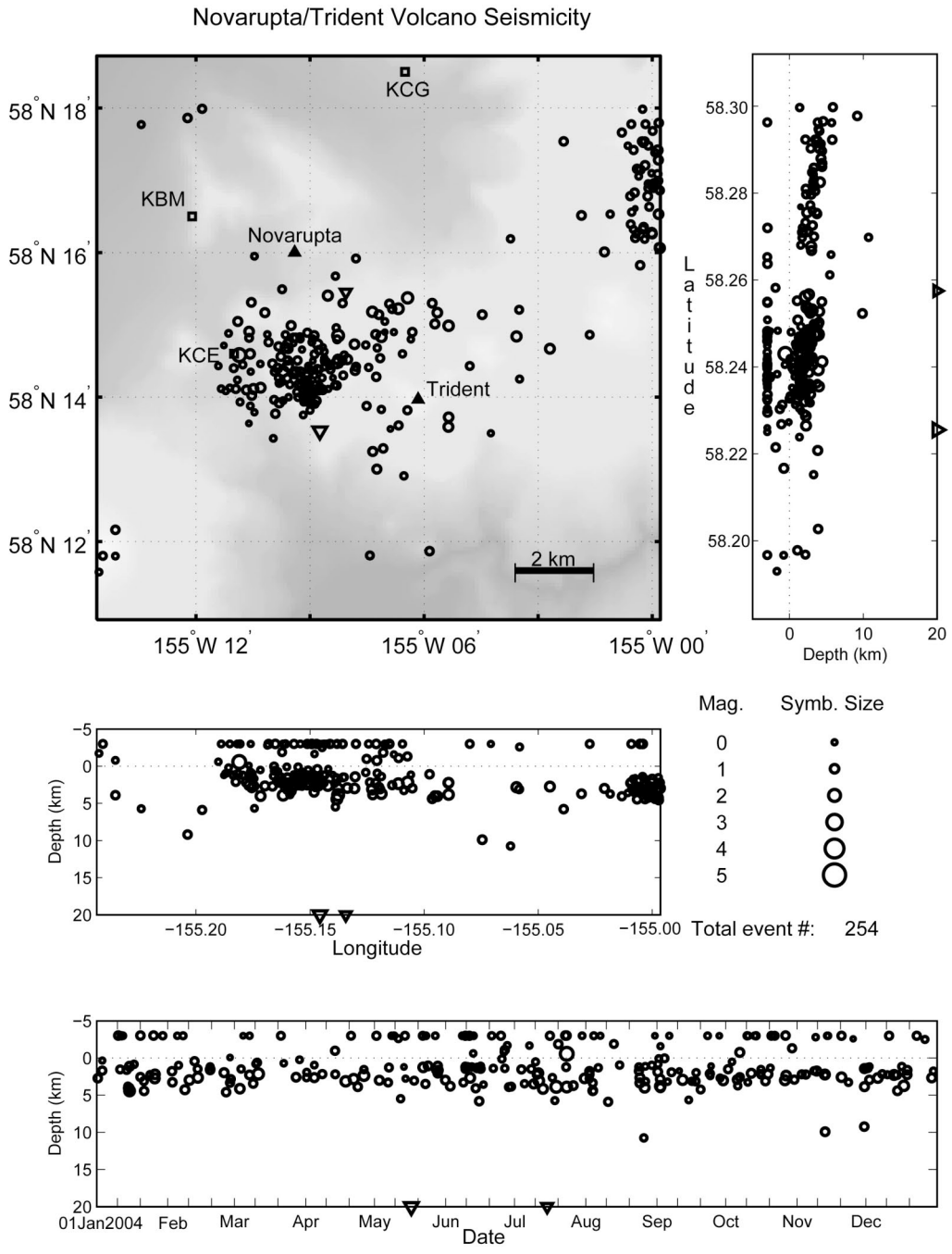

Figure A10. Summary plots of 254 earthquakes located near Novarupta and Trident Volcano in the Katmai volcanic cluster in 2004. Open circles show hypocenter locations shallower than 20 km and open triangles show hypocenters with depths of 20 km and deeper. Hypocenter symbols are scaled with magnitude. Seismograph stations are shown by open squares and labeled by station code. (See Appendix B for station information). Solid triangles are used to show volcanic centers and closed squares are used to show other points of interest. Several earthquakes that appear on this figure appear on other figures.

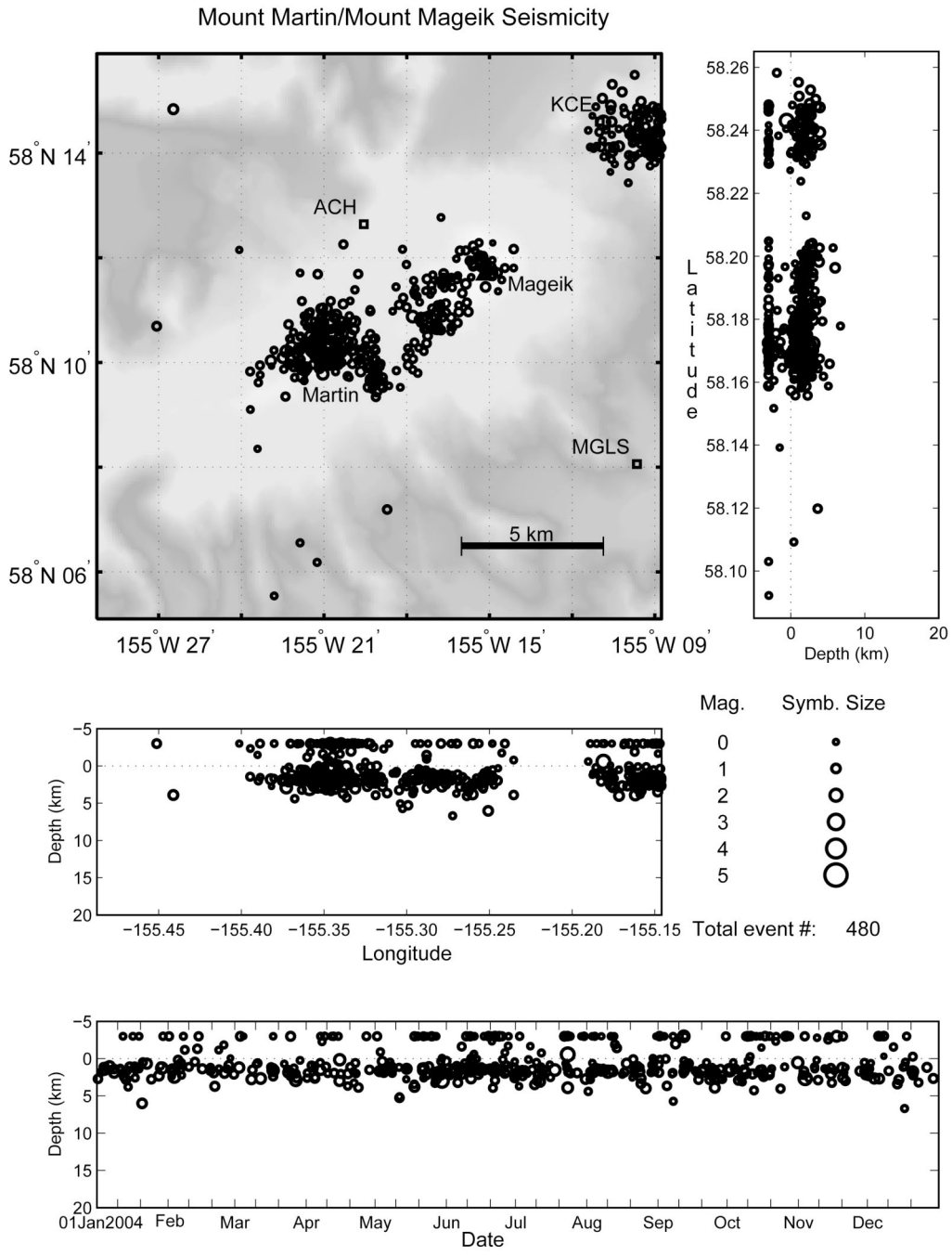

Figure A11. Summary plots of 480 earthquakes located near Mount Mageik and Mount Martin in the Katmai volcanic cluster in 2004. Open circles scaled with magnitude show hypocenter locations. Seismograph stations are shown by open squares and labeled by station code. (See Appendix B for station information). Solid triangles are used to show volcanic centers and closed squares are used to show other points of interest. Several earthquakes that appear on this figure appear on other figures.

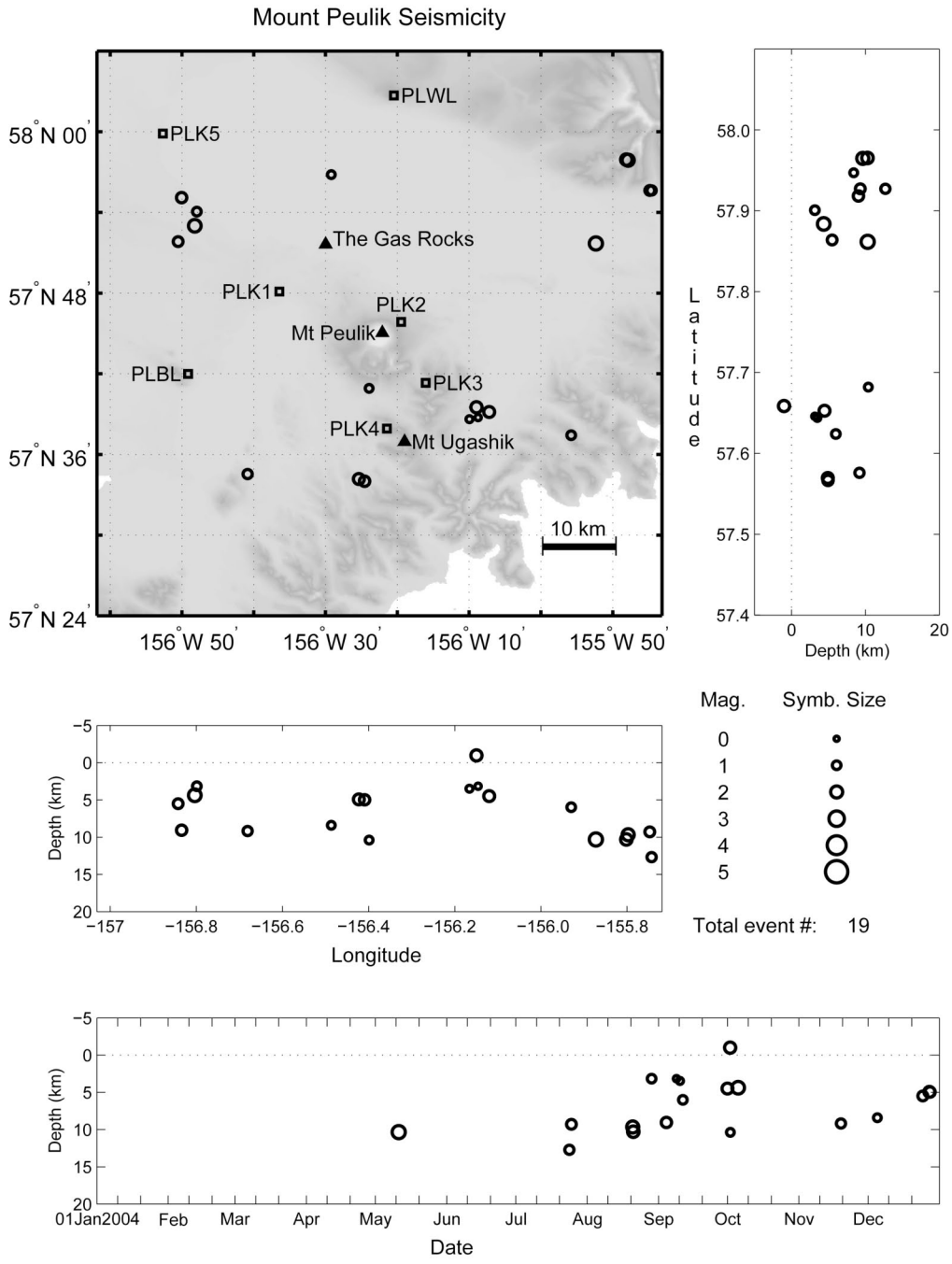

Figure A12. Summary plots of 19 earthquakes located near Mount Peulik in 2004. Open circles scaled with magnitude show hypocenter locations. Seismograph stations are shown by open squares and labeled by station code. (See Appendix B for station information). Solid triangles are used to show volcanic centers and closed squares are used to show other points of interest. The Peulik Subnetwork was installed in August 2004 and the three events located before August were located with only Katmai and/or Aniakchak seismic stations.

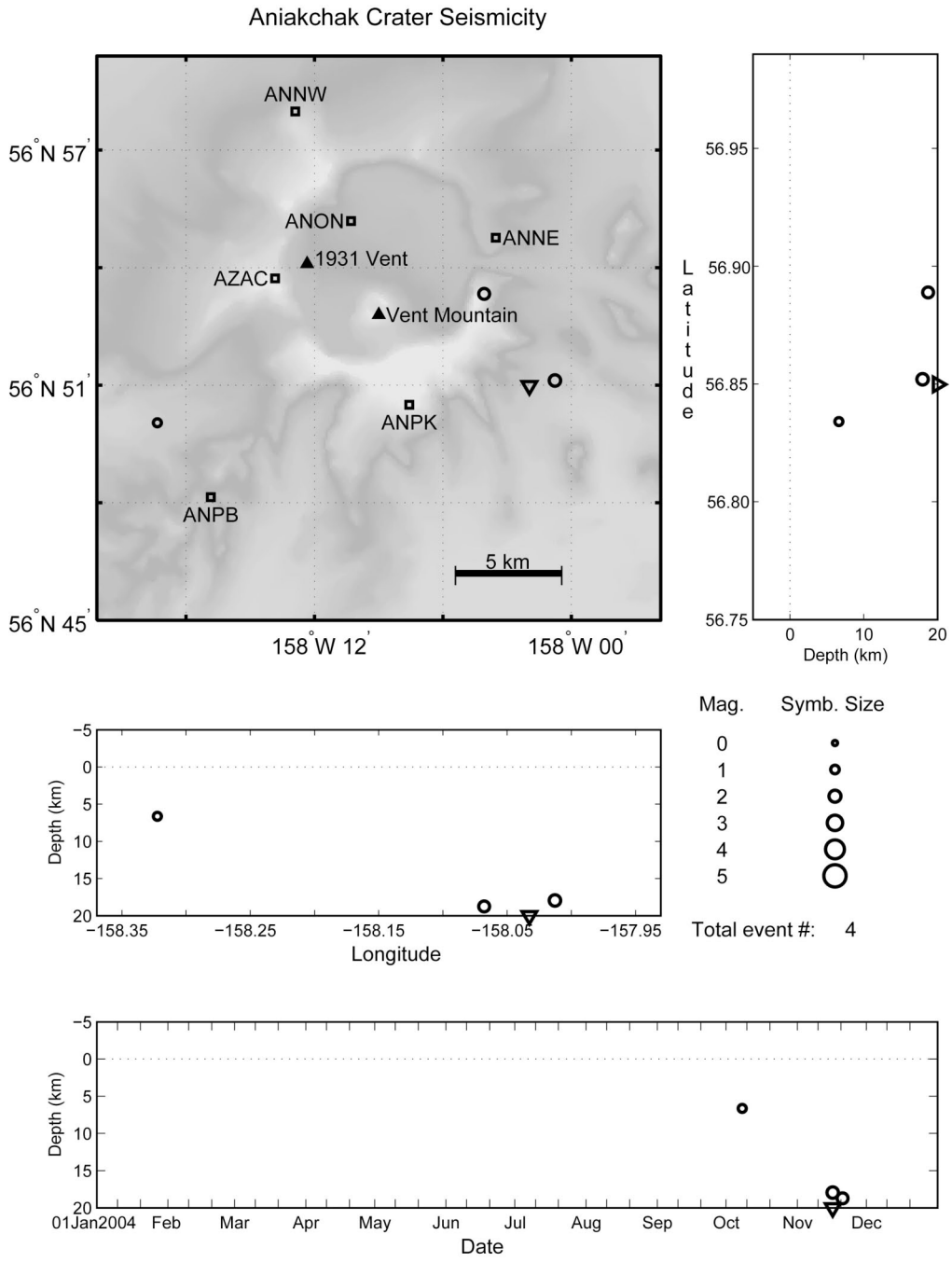

Figure A13. Summary plots of four earthquakes located near Aniakchak Crater in 2004. Open circles show hypocenter locations shallower than 20 km and open triangles show hypocenters with depths of 20 km and deeper. Hypocenter symbols are scaled with magnitude. Seismograph stations are shown by open squares and labeled by station code. (See Appendix B for station information). Solid triangles are used to show volcanic centers and closed squares are used to show other points of interest.

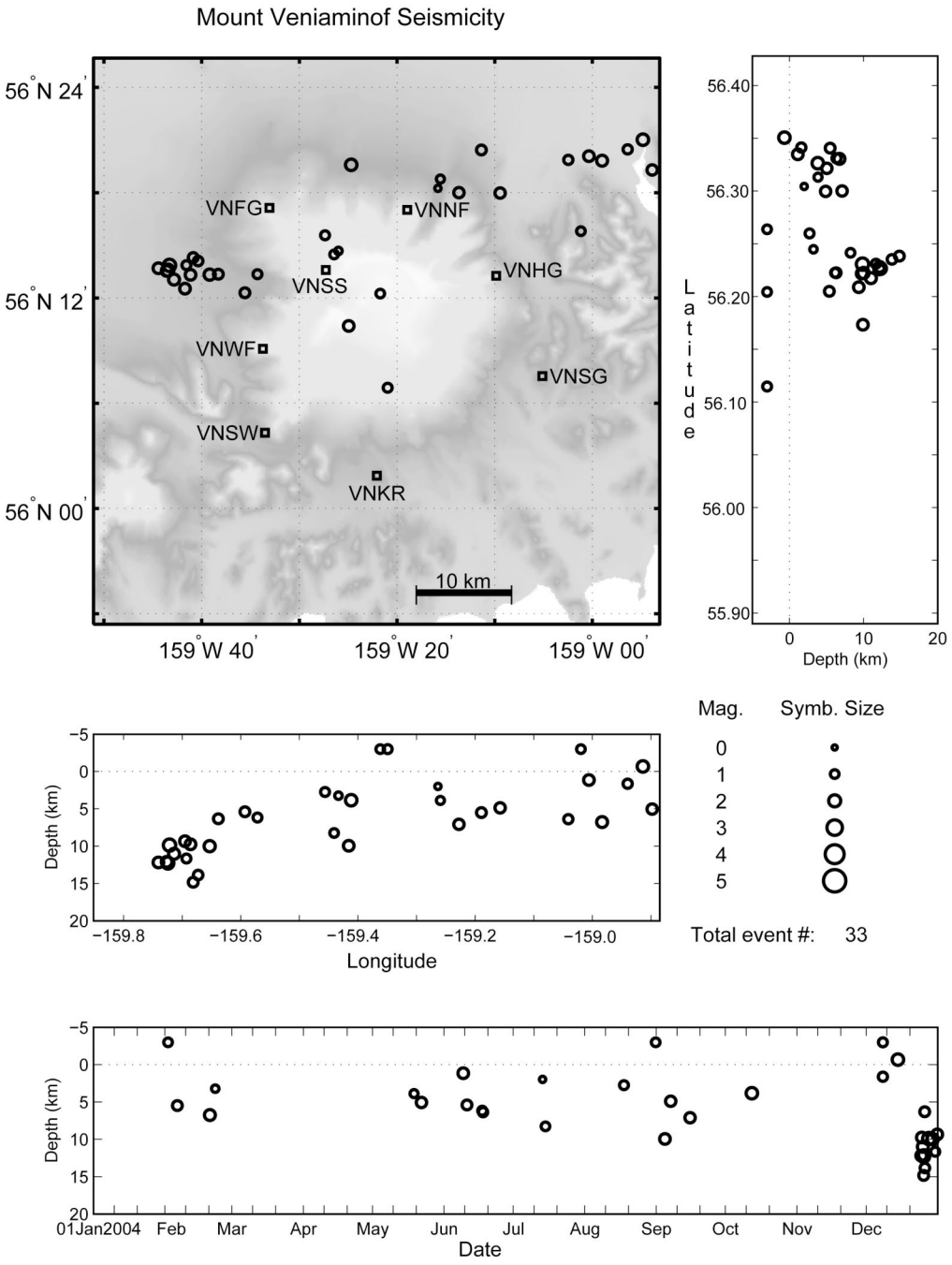

Figure A14. Summary plots of 33 earthquakes located near Mount Veniaminof in 2004. Open circles scaled with magnitude show hypocenter locations. Seismograph stations are shown by open squares and labeled by station code. (See Appendix B for station information). Solid triangles are used to show volcanic centers and closed squares are used to show other points of interest.

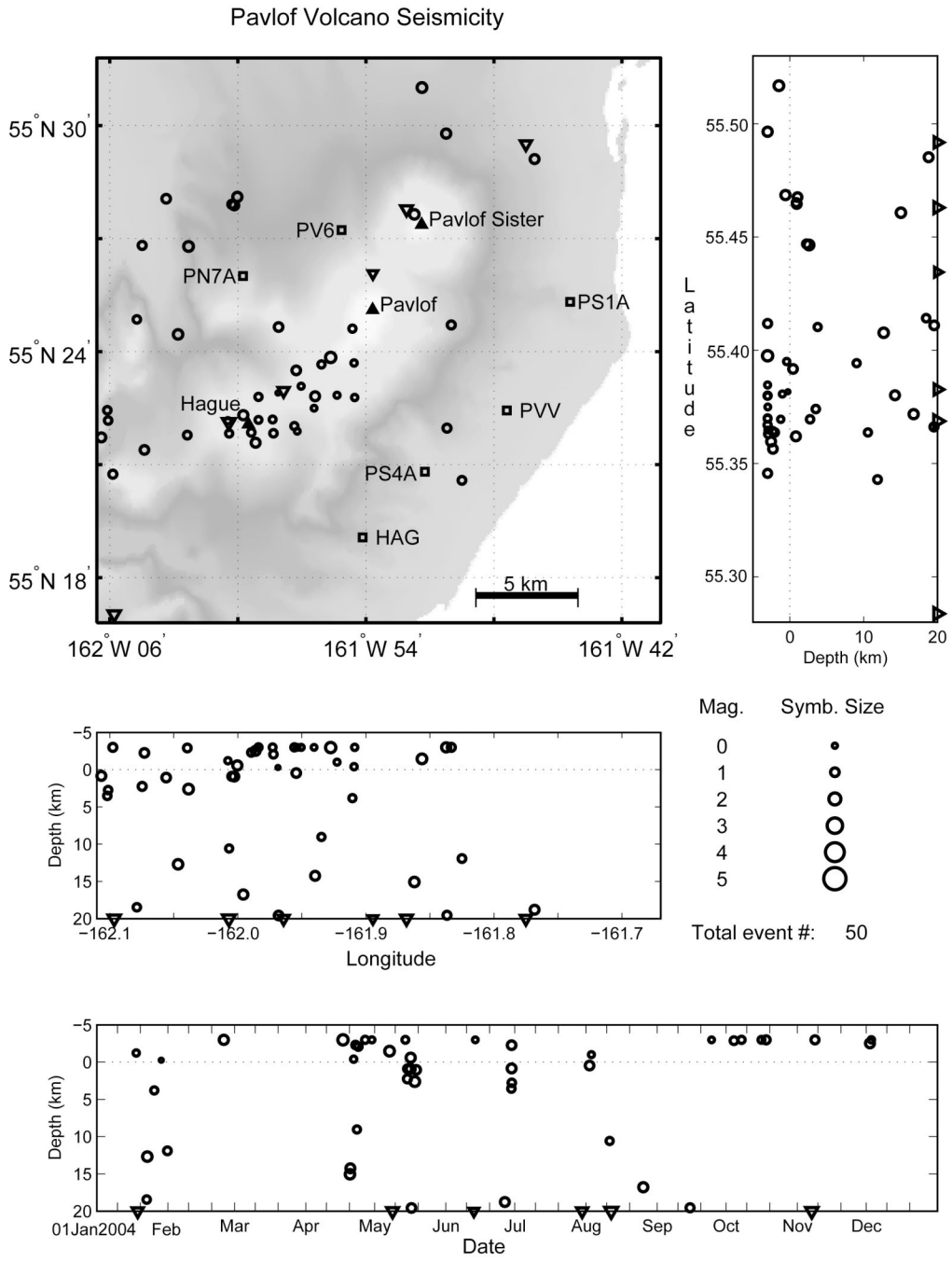

Figure A15. Summary plots of 50 earthquakes located near Pavlof Volcano in 2004. Open circles show hypocenter locations shallower than 20 km and open triangles show hypocenters with depths of 20 km and deeper. Hypocenter symbols are scaled with magnitude. Seismograph stations are shown by open squares and labeled by station code. (See Appendix B for station information). Solid triangles are used to show volcanic centers and closed squares are used to show other points of interest.

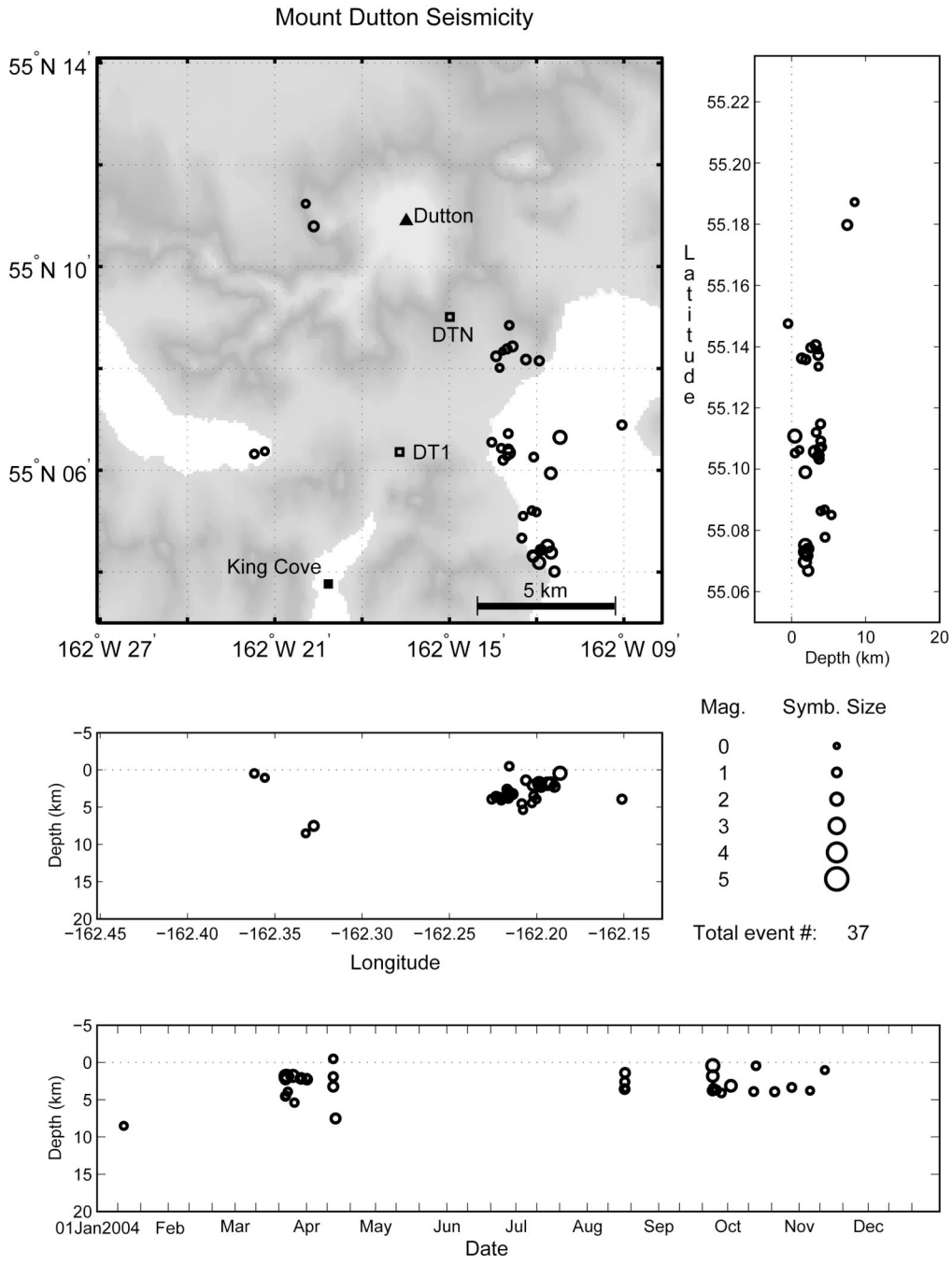

Figure A16. This summary plot shows 37 earthquakes located near Mount Dutton in 2004. Open circles scaled with magnitude show hypocenter locations. Seismograph stations are shown by open squares and labeled by station code. (See Appendix B for station information). Solid triangles are used to show volcanic centers and closed squares are used to show other points of interest.

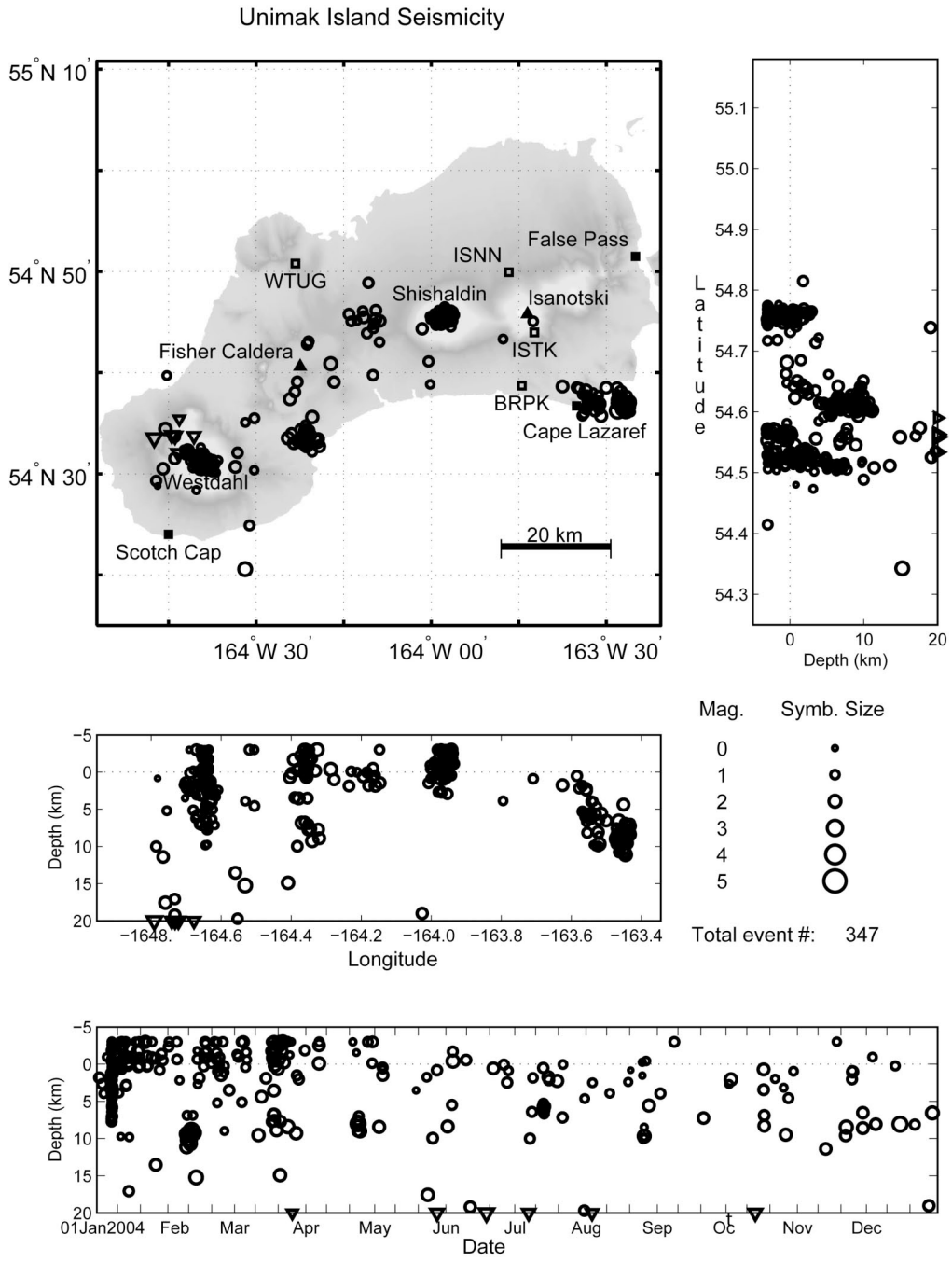

Figure A17. Summary plots of 347 earthquakes located near Unimak Island in 2004. Open circles show hypocenter locations shallower than 20 km and open triangles show hypocenters with depths of 20 km and deeper. Hypocenter symbols are scaled with magnitude. Seismograph stations are shown by open squares and labeled by station code. (See Appendix B for station information). Solid triangles are used to show volcanic centers and closed squares are used to show other points of interest.

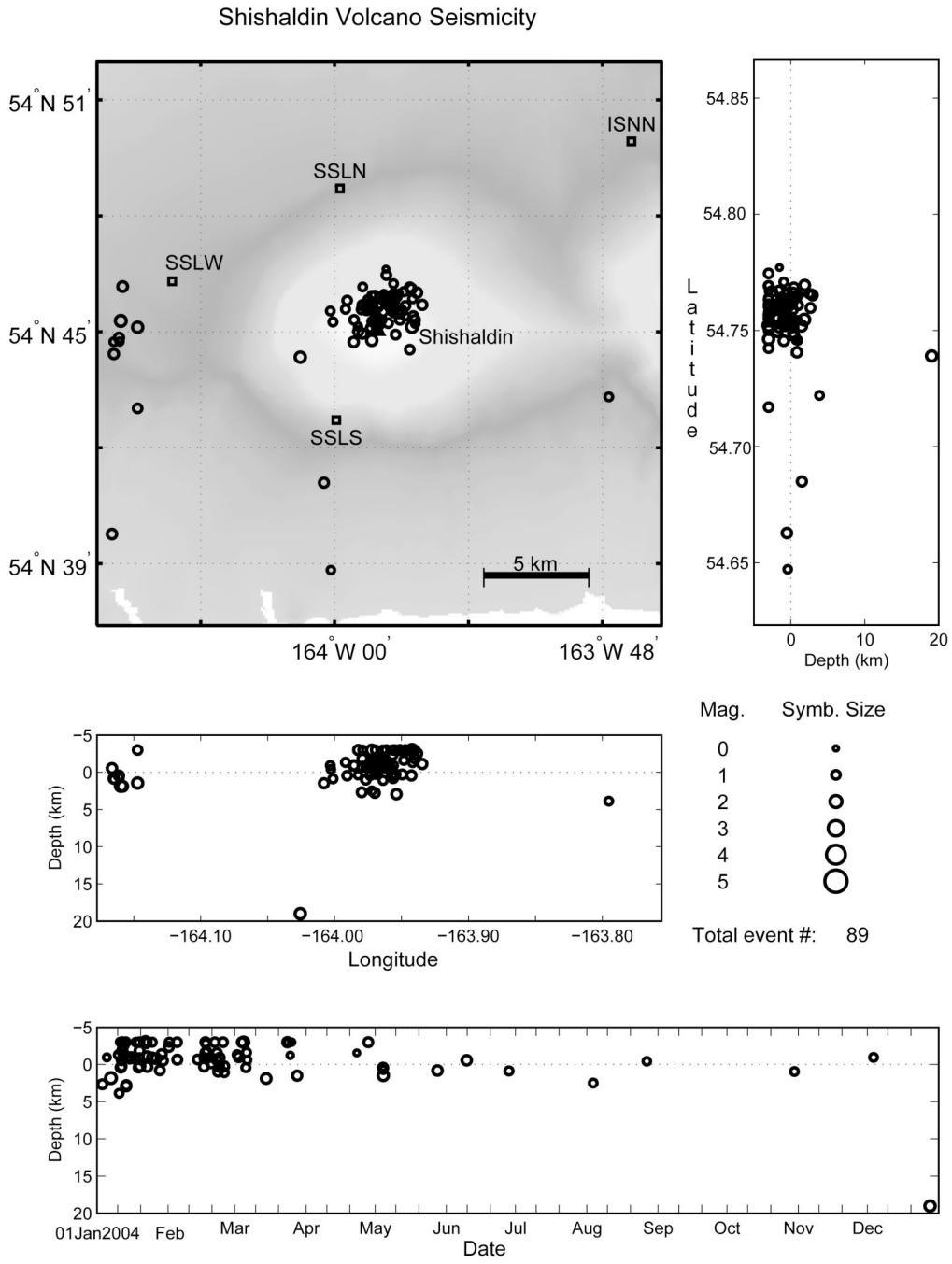

Figure A18. Summary plots of 89 earthquakes located near Shishaldin Volcano in 2004. Open circles scaled with magnitude show hypocenter locations. Seismograph stations are shown by open squares and labeled by station code. (See Appendix B for station information). Solid triangles are used to show volcanic centers and closed squares are used to show other points of interest.

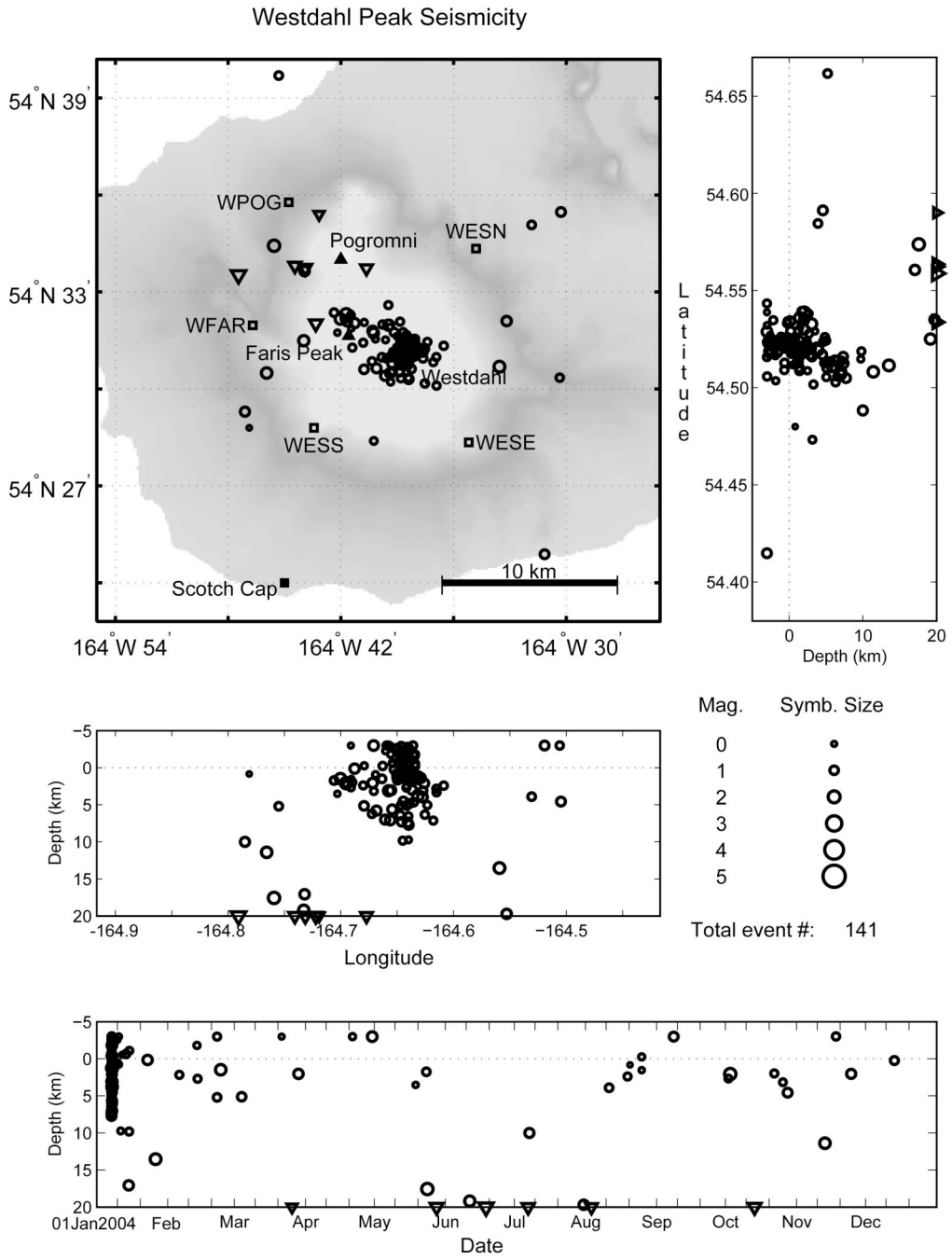

Figure A19. Summary plots of 141 earthquakes located near Westdahl Peak in 2004. Open circles show hypocenter locations shallower than 20 km and open triangles show hypocenters with depths of 20 km and deeper. Hypocenter symbols are scaled with magnitude. Seismograph stations are shown by open squares and labeled by station code. (See Appendix B for station information). Solid triangles are used to show volcanic centers and closed squares are used to show other points of interest.

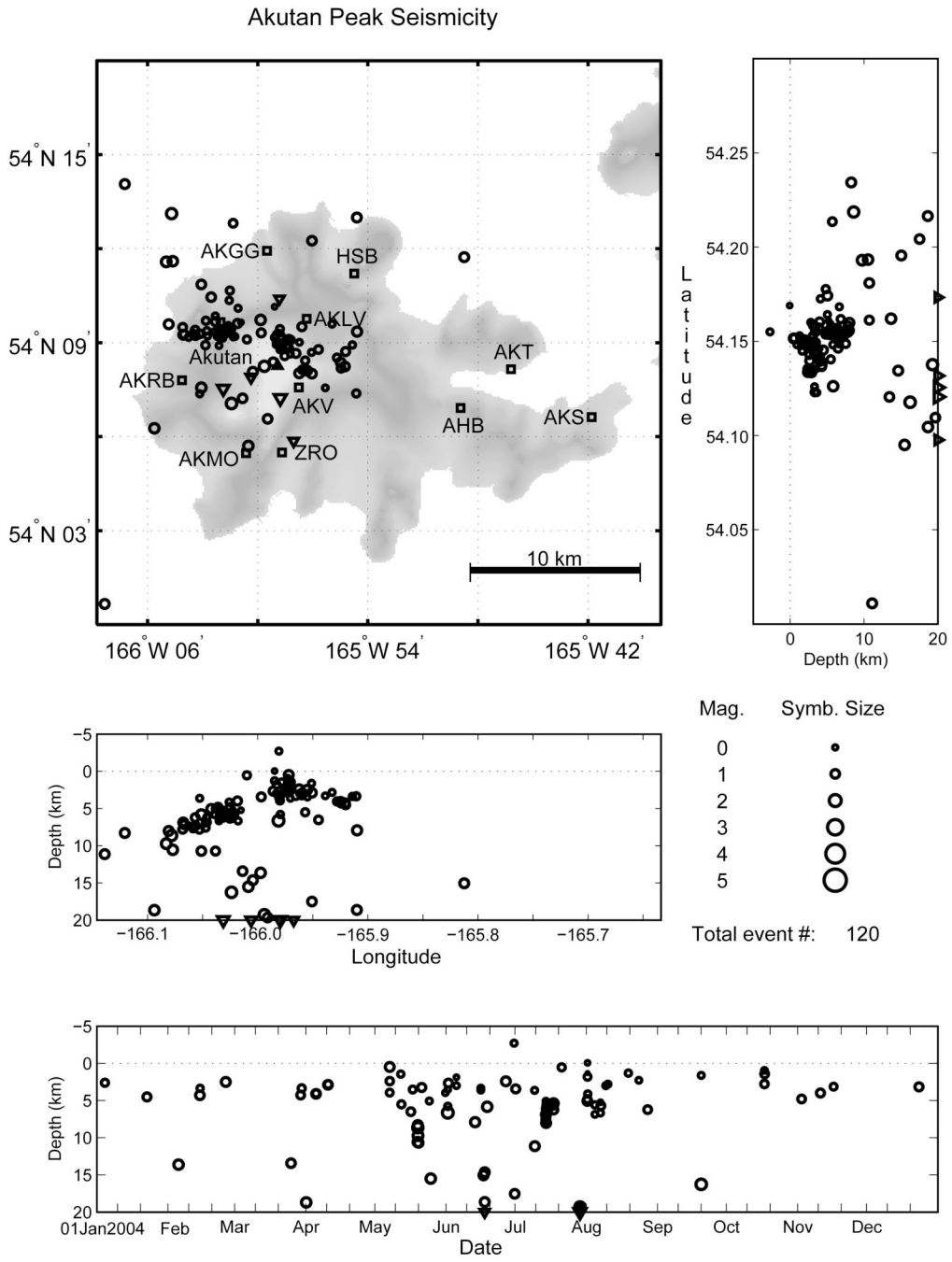

Figure A20. Summary plots of 120 earthquakes located near Akutan Peak in 2004. Open circles show hypocenter locations shallower than 20 km and open triangles show hypocenters with depths of 20 km and deeper. Hypocenter symbols are scaled with magnitude. Seismograph stations are shown by open squares and labeled by station code. (See Appendix B for station information). Solid triangles are used to show volcanic centers and closed squares are used to show other points of interest.

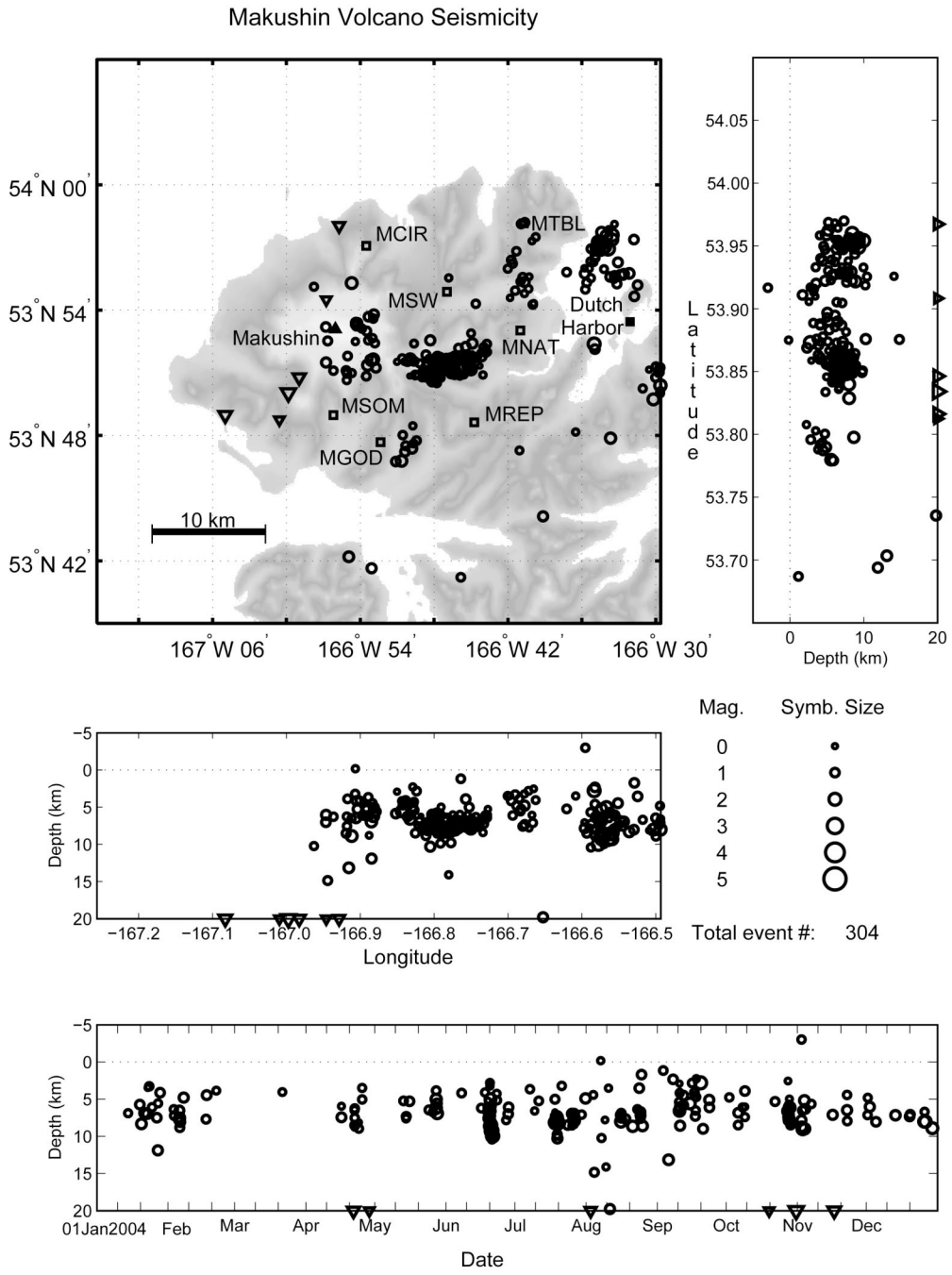

Figure A21. Summary plots of 304 earthquakes located near Makushin Volcano in 2004. Open circles show hypocenter locations shallower than 20 km and open triangles show hypocenters with depths of 20 km and deeper. Hypocenter symbols are scaled with magnitude. Seismograph stations are shown by open squares and labeled by station code. (See Appendix B for station information). Solid triangles are used to show volcanic centers and closed squares are used to show other points of interest.

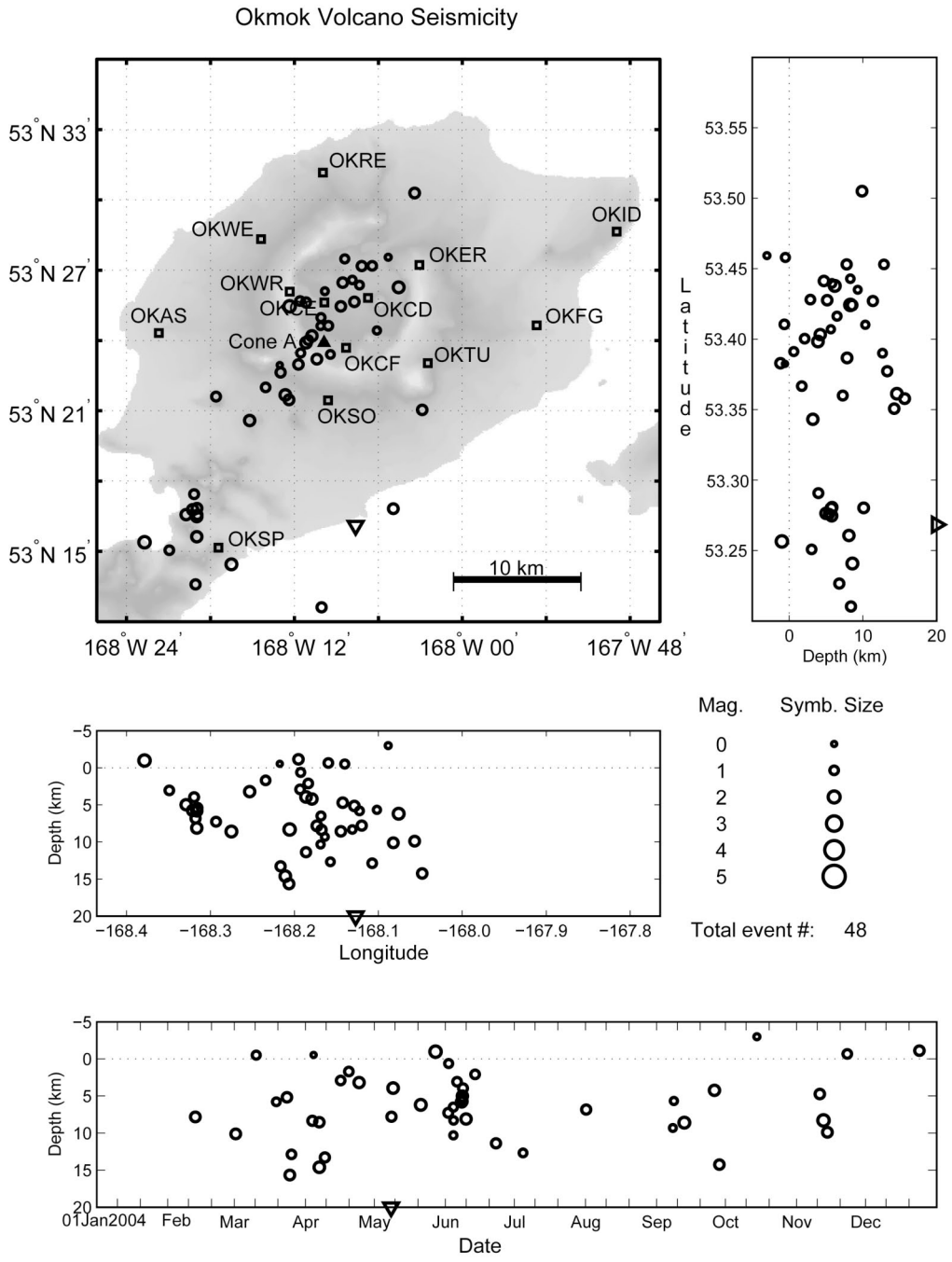

Figure A22. Summary plots of 48 earthquakes located near Okmok Caldera in 2004. Open circles show hypocenter locations shallower than 20 km and open triangles show hypocenters with depths of 20 km and deeper. Hypocenter symbols are scaled with magnitude. Seismograph stations are shown by open squares and labeled by station code. (See Appendix B for station information). Solid triangles are used to show volcanic centers and closed squares are used to show other points of interest.

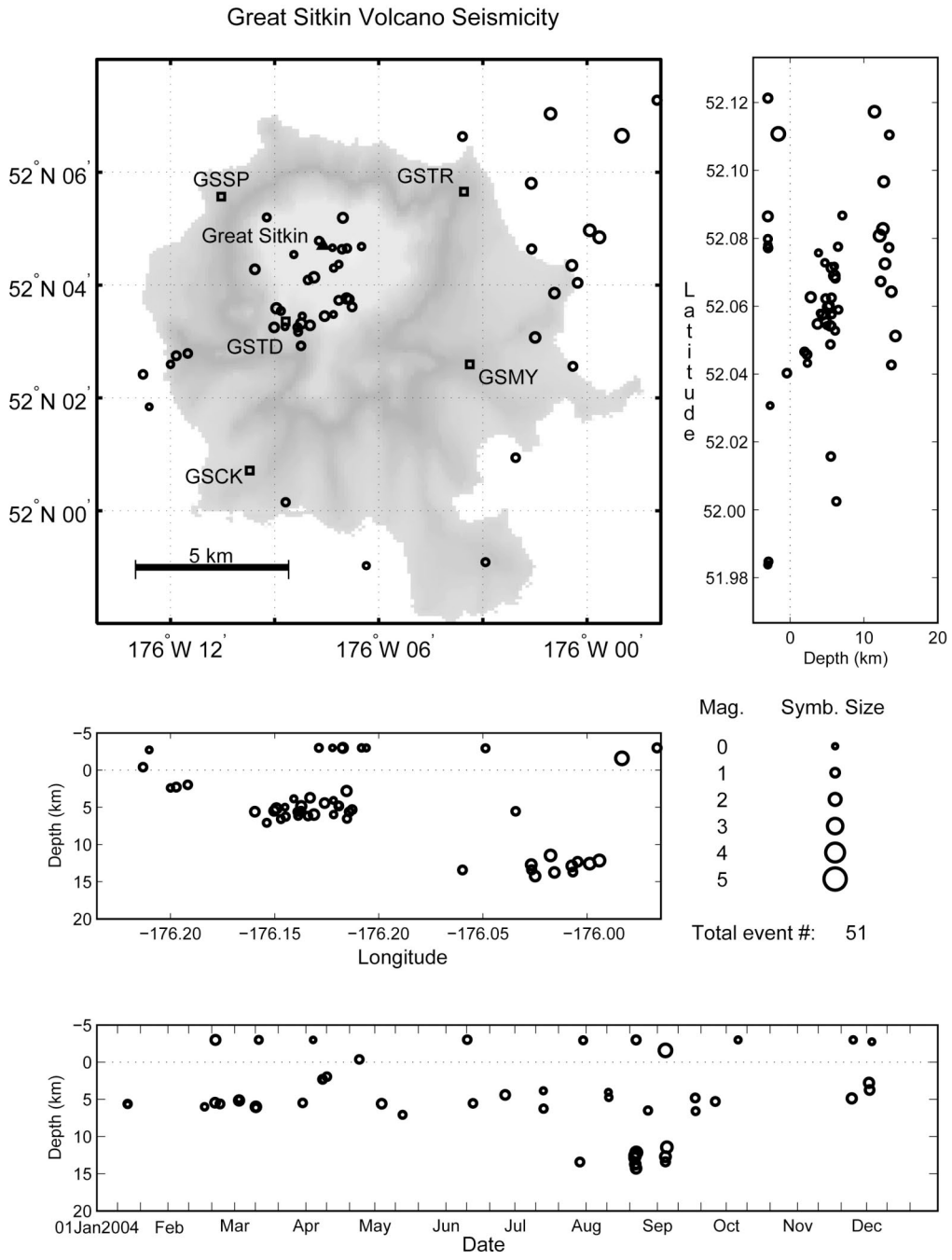

Figure A23. Summary plots of 51 earthquakes located near Great Sitkin Volcano in 2004. Open circles scaled with magnitude show hypocenter locations. Seismograph stations are shown by open squares and labeled by station code. (See Appendix B for station information). Solid triangles are used to show volcanic centers and closed squares are used to show other points of interest.

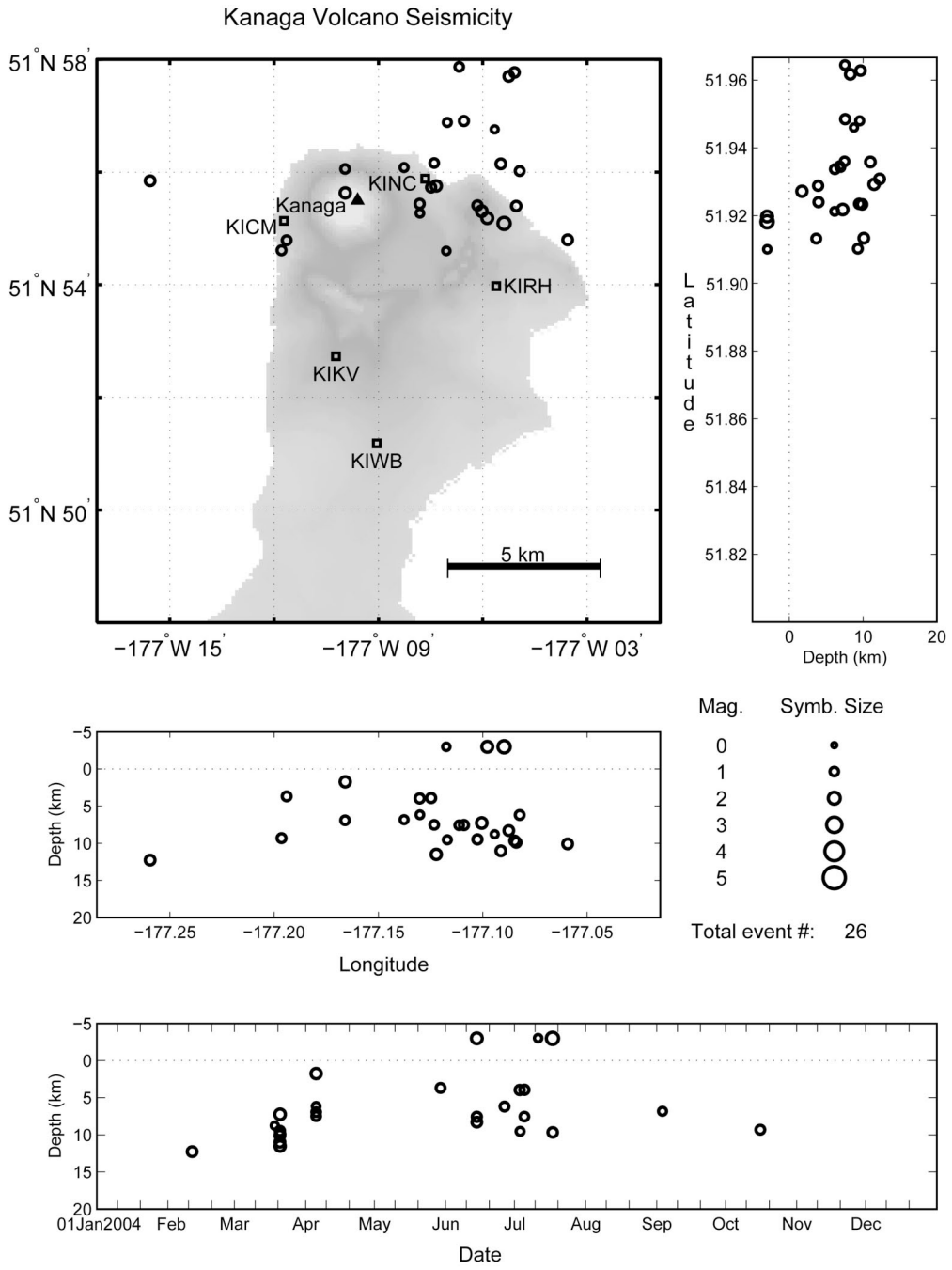

Figure A24. Summary plots of 26 earthquakes located near Kanaga Volcano in 2004. Open circles scaled with magnitude show hypocenter locations. Seismograph stations are shown by open squares and labeled by station code. (See Appendix B for station information). Solid triangles are used to show volcanic centers and closed squares are used to show other points of interest.

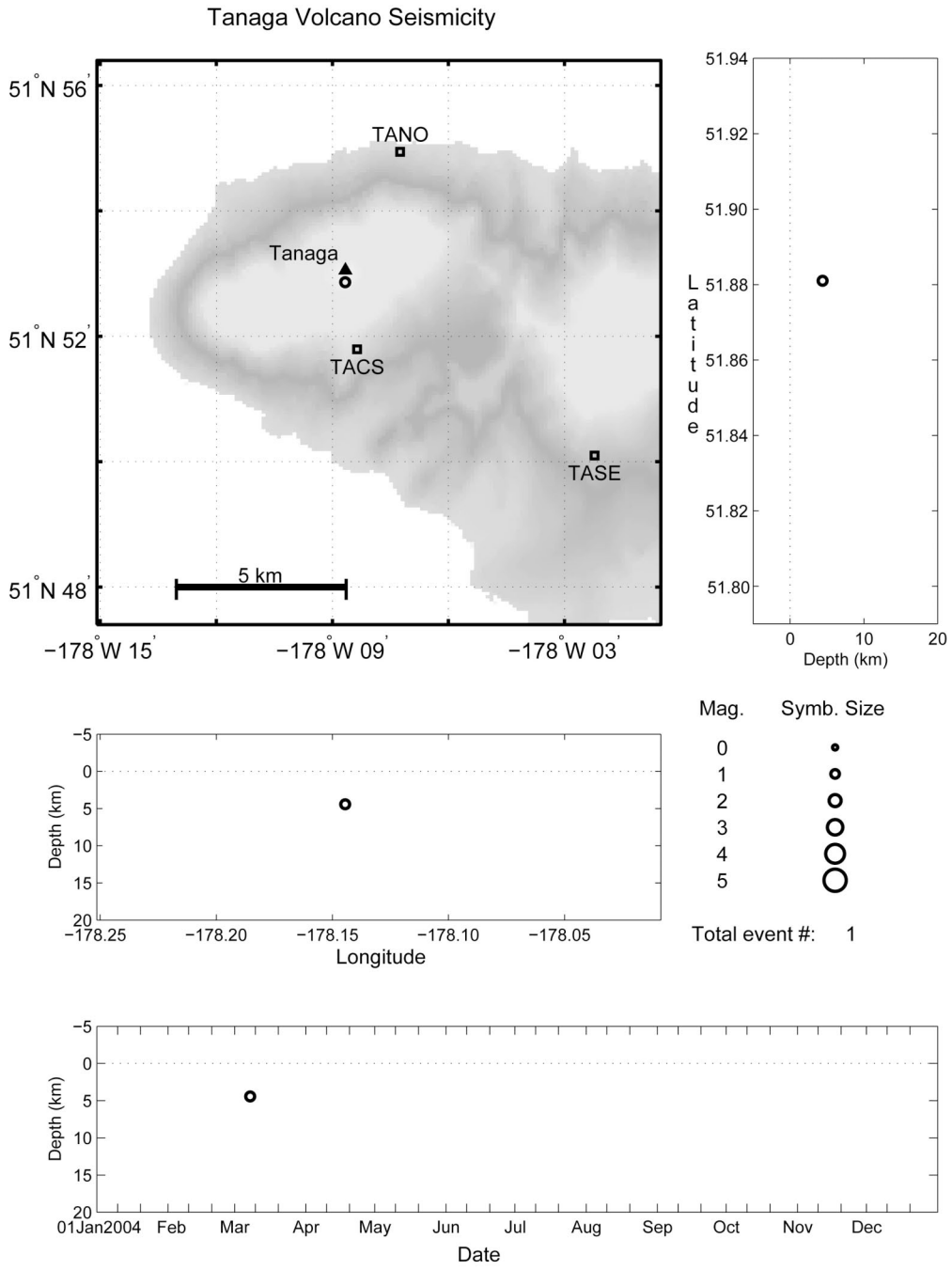

Figure A25. Summary plots of one earthquake located near Tanaga Volcano in 2004. Open circles scaled with magnitude show hypocenter locations. Seismograph stations are shown by open squares and labeled by station code. (See Appendix B for station information). Solid triangles are used to show volcanic centers and closed squares are used to show other points of interest.

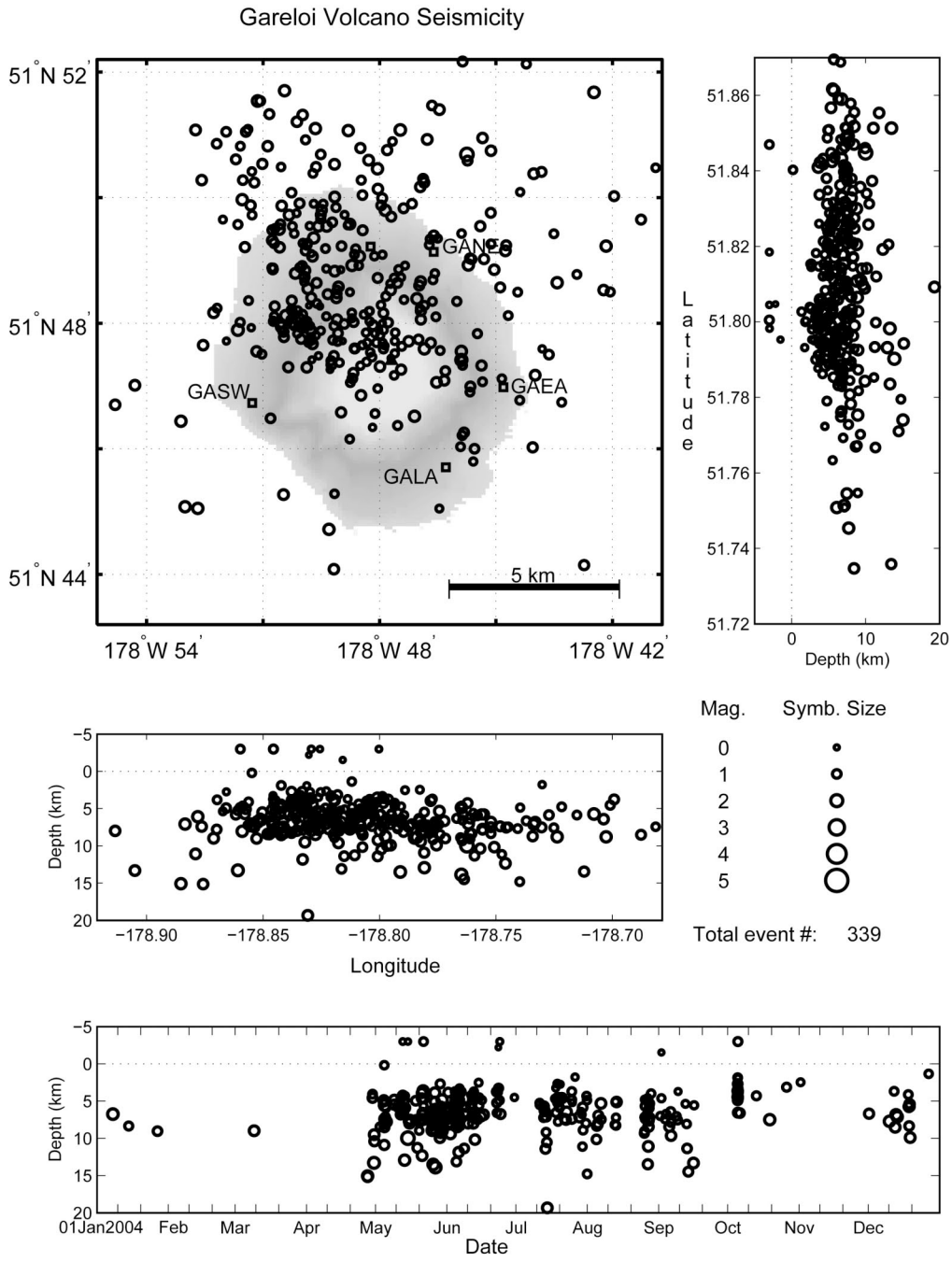

Figure A26. Summary plots of 339 earthquakes located near Mount Gareloi in 2004. Open circles scaled with magnitude show hypocenter locations. Seismograph stations are shown by open squares and labeled by station code. (See Appendix B for station information). Solid triangles are used to show volcanic centers and closed squares are used to show other points of interest.

Appendix B: Parameters for AVO seismograph stations (datum NAD27)

Station	Latitude (N)	Longitude (W)	Elevation (m)	Seismometer	Station open date
Akutan Peak subnet (11 stations - 23 components)					
AHB	54 06.916	165 48.943	447	L-4	1996/07/24
AKGG[B]	54 11.930	165 59.495	326	CMG-6TD	2003/06/27
AKLV[B]	54 09.762	165 57.336	551	CMG-6TD	2003/07/02
AKMO[B]	54 05.471	166 00.634	277	CMG-6TD	2003/06/25
AKRB[B]	54 07.803	166 04.125	334	CMG-6TD	2003/06/29
AKS[3]	54 06.624	165 41.803	213	L-22	1996/07/24
AKT[B]	54 08.15	165 46.2	12	CMG-40T	1996/03/18
AKV	54 07.571	165 57.763	863	L-4	1996/07/24
HSB	54 11.205	165 54.743	497	L-4	1996/07/24
LVA	54 09.655	166 02.025	457	L-4	1996/07/24
ZRO	54 05.494	165 58.678	446	L-4	1996/07/24
Aniakchak Crater subnet (6 stations - 8 components)					
ANNE	56 54.763	158 03.534	705	L-4	1997/07/18
ANNW	56 57.986	158 12.895	816	L-4	1997/07/18
ANON[3]	56 55.188	158 10.293	445	L-22	2000/07/10
ANPB	56 48.141	158 16.847	658	L-4	1997/07/18
ANPK	56 50.499	158 07.572	972	L-4	1997/07/18
AZAC	56 53.727	158 13.841	1057	L-4	2003/07/12
Augustine Volcano subnet (8 stations - 13 components)					
AUE	59 22.308	153 22.504	168	S-13	1980/10/29
AUH	59 21.833	153 26.591	890	S-13	1978/12/01
AUI[3]	59 20.11	153 25.66	293	S-13	1978/04/06
AUL[BS]	59 22.937	153 26.142	360	S-13,CMG-40T	1978/08/27
AUP	59 21.805	153 25.210	1033	S-13	1977/09/22
AUR	59 21.766	153 25.876	1225	L-4	1995/11/01
AUS	59 21.599	153 25.840	1226	L-4	1990/09/01
AUW	59 22.205	153 28.249	276	S-13	1976/10/17
Mount Dutton subnet (5 stations - 5 components)					
BLDY	55 11.670	162 47.018	259	L-4	1996/07/11
DOL	55 08.960	161 51.683	442	L-4	1996/07/11
DRR3	54 58.014	162 15.665	457	L-4	1996/07/11
DT1	55 06.427	162 16.859	198	L-4	1991/06/21
DTN	55 08.744	162 15.419	396	S-13	1988/07/16
Gareloi Volcano subnet (6 stations - 8 components)					
GAEA	51 46.980	178 44.810	326	L-4	2003/08/30
GAKI	51 33.267	178 48.725	99	L-4	2003/09/01
GALA	51 45.704	178 46.292	315	L-4	2003/08/30
GANE	51 49.135	178 46.603	325	L-4	2003/09/02
GANO	51 49.220	178 48.230	451	L-4	2003/09/02
GASW[3]	51 46.731	178 51.276	248	L-22	2003/08/30

AVO Stations-continued.

Station	Latitude (N)	Longitude (W)	Elevation (m)	Seismometer	Station open date
Great Sitkin Volcano subnet (6 stations - 8 components)					
GSCK	52 00.712	176 09.718	384	L-4	1999/09/15
GSIG	51 59.181	175 55.502	407	L-4	1999/09/03
GSMY	52 02.594	176 03.376	418	L-4	1999/09/03
GSSP	52 05.566	176 10.541	295	L-4	1999/09/15
GSTD[3]	52 03.356	176 08.685	873	L-22	1999/09/03
GSTR	52 05.655	176 03.546	536	L-4	1999/09/03
Iliamna Volcano subnet (6 stations - 8 components)					
ILI	60 04.877	152 57.502	771	L-4	1987/09/15
ILS	59 57.454	153 04.083	1125	S-13	1996/08/28
ILW	60 03.585	153 08.222	1646	S-13	1994/09/09
INE	60 03.65	153 03.75	1585	S-13	1990/08/29
IVE[3]	60 01.014	153 00.981	1173	S-13,L-22	1996/09/19
IVS	60 00.55	153 04.85	2332	L-4	1990/08/29
Kanaga Volcano subnet (6 stations - 6 components)					
KICM	51 55.136	177 11.718	183	L-4	1999/09/15
KIKV	51 52.730	177 10.223	411	L-4	1999/09/15
KIMD	51 45.697	177 14.093	183	L-4	1999/09/15
KINC	51 55.884	177 07.657	198	L-4	1999/09/15
KIRH	51 53.976	177 05.611	309	L-4	1999/09/03
KIWB	51 51.183	177 09.049	244	L-4	1999/09/03
Katmai Volcanic Cluster subnet (18 stations - 24 components)					
ACH[3]	58 12.64	155 19.56	960	L-22	1996/07/25
ANCK	58 11.93	155 29.64	869	L-4	1996/07/25
CAHL	58 03.15	155 18.09	807	L-4	1996/07/25
CNTC	58 15.87	155 53.02	1158	L-4	1996/07/25
KABR	58 07.87	154 58.15	884	L-4	1998/08/12
KABU[B]	58 16.225	155 16.934	1065	CMT-6TD	2004/08/01
KAHC	58 38.94	155 00.36	1250	L-4	1998/10/12
KAHG	58 29.64	154 32.78	923	L-4	1998/10/12
KAIC	58 29.10	155 02.75	734	L-4	1998/10/12
KAKN[B]	58 17.819	155 03.668	1049	CMG-6TD	2004/08/01
KAPH[3]	58 35.81	154 20.81	907	L-22	1998/10/12
KARR	58 29.87	154 42.20	610	L-4	1998/10/12
KAWH	58 23.02	154 47.95	777	L-4	1998/10/12
KBM	58 16.50	155 12.10	732	L-4	1991/07/22
KCE	58 14.60	155 11.00	777	L-4	1991/07/22
KCG[3]	58 18.457	155 06.684	762	L-22	1988/08/01
KEL	58 26.401	155 44.442	975	L-4	1988/08/01
KJL	58 03.24	155 34.39	792	L-4	1996/07/25
KVT	58 22.90	155 17.70	457	L-4	1988/08/01
MGLS	58 08.06	155 09.65	472	L-4	1996/07/25

AVO Stations-continued.

Station	Latitude (N)	Longitude (W)	Elevation (m)	Seismometer	Station open date
Korovin Volcano subnet (7 stations - 9 components)					
KOFP	53 57.08	166 53.51	662	L-4	2004/07/02
KOKL	53 47.68	166 52.35	758	L-4	2004/07/05
KOKV[3]	53 53.03	166 41.00	776	L-22	2004/07/05
KONE	53 48.629	166 44.736	253	L-4	2004/07/10
KONW	53 48.978	166 56.187	334	L-4	2004/07/04
KOSE	53 54.88	166 46.96	625	L-4	2004/07/07
KOWE	53 58.16	166 40.71	527	L-4	2004/07/06
Makushin Volcano subnet (7 stations - 9 components)					
MCIR	53 57.086	166 53.529	800	L-4	1996/07/25
MGOD	53 47.683	166 52.561	650	L-4	1996/07/25
MNAT	53 53.028	166 41.016	397	L-4	1996/07/25
MREP	53 48.629	166 44.736	785	L-4	2002/01/01
MSOM	53 48.978	166 56.187	146	L-4	1996/07/25
MSW[3]	53 54.929	166 47.186	418	L-22	1996/07/25
MTBL	53 58.136	166 40.760	810	L-4	1996/07/25
Okmok Volcano subnet (12 stations - 18 components)					
OKAS	53 24.319	168 21.686	270	L-4	2003/01/09
OKCD[B]	53 25.818	168 06.737	459	CMG-6TD	2003/01/09
OKCE[B]	53 25.622	168 09.858	515	CMG-6TD	2003/01/09
OKCF	53 23.749	168 08.175	685	L-4	2003/01/09
OKER	53 27.278	168 02.960	956	L-4	2003/01/09
OKFG[B]	53 24.702	167 54.568	201	CMG-6TD	2003/01/09
OKID	53 28.645	167 48.972	437	L-4	2003/01/09
OKRE	53 31.215	168 09.846	422	L-4	2003/01/09
OKSO[B]	53 21.447	168 09.591	460	CMG-6TD	2004/09/01
OKSP	53 15.156	168 17.431	608	L-4	2003/01/09
OKTU	53 23.035	168 02.466	646	L-4	2003/01/09
OKWE	53 28.328	168 14.388	445	L-4	2003/01/09
OKWR	53 26.084	168 12.333	1017	L-4	2003/01/09
Pavlof Volcano subnet (7 stations - 9 components)					
BLHA	55 42.227	162 03.907	411	L-4	1996/07/11
HAG	55 19.068	161 54.150	503	L-4	1996/07/11
PN7A	55 26.020	161 59.713	838	L-4	1996/07/11
PS1A	55 25.321	161 44.425	293	L-4	1996/07/11
PS4A	55 20.811	161 51.233	322	L-4	1996/07/11
PV6[3]	55 27.217	161 55.112	747	L-22	1996/07/11
PVV	55 22.438	161 47.396	161	L-4	1996/07/11
Mount Peulik subnet (7 stations - 9 components)					
PLBL	57 41.990	156 49.131	461	L-4	2004/08/01
PLK1	57 48.114	156 36.433	78	L-4	2004/08/01
PLK2	57 45.852	156 19.458	401	L-4	2004/08/01
PLK3[3]	57 41.320	156 16.044	494	L-22	2004/08/01
PLK4	57 37.928	156 21.464	1031	L-4	2004/08/01
PLK5	57 59.864	156 52.662	49	L-4	2004/08/01
PLWL	58 02.696	156 20.479	585	L-4	2004/08/01

AVO Stations-continued.

Station	Latitude (N)	Longitude (W)	Elevation (m)	Seismometer	Station open date
Redoubt Volcano subnet (7 stations - 12 components)					
DFR	60 35.514	152 41.160	1090	L-4	1988/08/15
NCT	60 33.789	152 55.568	1079	L-4	1988/08/14
RDN	60 31.377	152 44.273	1400	L-4	1988/08/13
RDT	60 34.394	152 24.315	930	L-4	1971/08/09
RED[3]	60 25.192	152 46.308	1064	L-4	1990/08/30
REF[3*]	60 29.35	152 42.10	1801	L-22	1992/07/27
RSO	60 27.73	152 45.23	1921	L-4	1990/03/01
Shishaldin Volcano subnet (6 stations - 8 components)					
BRPK	54 38.730	163 44.449	393	L-4	1997/07/27
ISNN	54 49.937	163 46.706	466	L-4	1997/07/27
ISTK	54 43.929	163 42.376	704	L-4	1997/07/27
SSLN	54 48.709	163 59.756	637	L-4	1997/07/27
SSLS[3]	54 42.718	163 59.926	817	L-22	1997/07/27
SSLW	54 46.307	164 07.282	628	L-4	1997/07/27
Mount Spurr subnet (15 stations - 23 components)					
BGL	61 16.012	152 23.340	1127	L-4	1989/08/13
BKG	61 04.21	152 15.76	1009	L-4	1991/07/01
CGL	61 18.46	152 00.40	1082	L-4	1981/09/22
CKL	61 11.782	152 20.268	1281	L-4	1989/08/05
CKN	61 13.44	152 10.89	735	L-4	1991/08/19
CKT	61 12.05	152 12.37	975	L-4	1992/09/16
CP2	61 15.85	152 14.51	1981	L-4	1992/10/23
CRP[3]	61 16.02	152 09.33	1622	L-4	1981/08/26
NCG	61 24.22	152 09.40	1244	L-4	1989/08/06
SPBG[B]	61 15.583	152 22.194	1087	CMG-6TD	2004/09/09
SPCG[B]	61 17.512	152 01.228	1329	CMG-6TD	2004/09/08
SPCR[B]	61 12.051	152 12.409	984	CMG-6TD	2004/09/08
SPNW	61 20.826	152 36.236	1040	L-4	2004/08/17
SPU	61 10.90	152 03.26	800	L-4	1971/08/10
SPWE	61 16.441	152 33.410	1233	L-4	2004/08/18
Tanaga Volcano subnet (6 stations - 8 components)					
TACS	51 51.792	178 08.363	918	L-4	2003/08/28
TAFL	51 45.396	177 53.867	186	L-4	2003/08/28
TAFP[3]	51 54.003	177 58.997	440	L-22	2003/08/27
TANO	51 54.942	178 07.249	269	L-4	2003/08/24
TAPA	51 48.932	177 48.770	640	L-4	2003/08/27
TASE	51 50.099	178 02.222	682	L-4	2003/08/24
Mount Veniaminof subnet (9 stations - 9 components)					
BPBC	56 35.383	158 27.153	584	L-4	2002/10/03
VNFG	56 17.140	159 33.066	1068	L-4	2002/02/06
VNHG	56 13.267	159 09.853	966	L-4	2002/02/06
VNKR	56 01.871	159 22.068	620	L-4	2002/02/06
VNNF	56 17.022	159 18.961	1153	L-4	2002/06/20
VNSG	56 07.549	159 05.121	761	L-4	2002/02/06
VNSS	56 13.600	159 27.290	1733	L-4	2002/02/06
VNSW	56 04.317	159 33.508	716	L-4	2002/06/20
VNWF	56 09.104	159 33.733	1095	L-4	2002/02/06

AVO Stations-continued.

Station	Latitude (N)	Longitude (W)	Elevation (m)	Seismometer	Station open date
Westdahl Peak subnet (6 stations - 8 components)					
WESE	54 28.389	164 35.038	953	L-4	1998/08/28
WESN	54 34.600	164 34.703	549	L-4	1998/10/17
WESS[3]	54 28.828	164 43.333	908	L-22	1998/08/28
WFAR	54 32.029	164 46.567	640	L-4	1998/08/28
WPOG	54 35.837	164 44.606	445	L-4	1998/10/17
WTUG	54 50.847	164 23.117	636	L-4	1998/10/17
Mount Wrangell subnet (4 stations - 6 components)					
WACK[3]	61 59.178	144 19.703	2280	L-22	2000/07/31
WANC	62 00.189	144 4.195	4190	L-4	2000/07/31
WASW	61 55.692	144 10.346	2196	L-4	2001/08/03
WAZA	62 04.506	144 9.132	2531	L-4	2001/08/03
Regional stations (14 stations - 14 components)					
ADAG	51 58.812	176 36.104	286	L-4	1999/09/15
BGM	59 23.56	155 13.76	625	L-4	1978/09/08
BGR	60 45.45	152 25.06	985	L-4	1991/07/01
CDD	58 55.771	153 38.558	622	S-13	1981/08/17
CNP	59 31.552	151 14.088	564	L-4	1983/07/01
ETKA	51 51.712	176 24.351	290	L-4	1999/09/15
HOM	59 39.50	151 38.60	198	L-4	1976/08/00
MMN	59 11.11	154 20.20	442	S-13	1981/08/22
NNL	60 02.66	151 17.30	381	L-4	1972/08/24
OPT	59 39.192	153 13.796	634	S-13	1974/00/00
PDB	59 47.27	154 11.55	305	S-13	1978/09/09
STLK	61 29.926	151 49.963	945	L-4	1997/09/01
SYI	58 36.60	152 23.45	149	S-13	1990/08/27
XLV	59 27.28	151 40.30	320	S-13	1987/09/16

Station Codes:
[3] Three-component short-period station
[B] Three-component broadband station
[S] Station also includes a single short-period vertical station
[*]REF also has a low-gain vertical component.

Seismometer Codes:
CMG-40T: Guralp CMG-40T 60 second natural period broadband seismometer
CMG-6TD: Guralp CMG-6TD 30 second natural period broadband seismometer
L-4: Mark Products L4 one second natural period seismometer
L-22: Mark Products L22 0.5 second natural period seismometer
S-13: Teledyne Geotech S-13 one second natural period seismometer

Appendix C: Figures showing the locations of the permanent AVO regional and volcano-specific seismograph stations. In all figures, closed triangles show volcanic centers and open squares show seismograph stations.

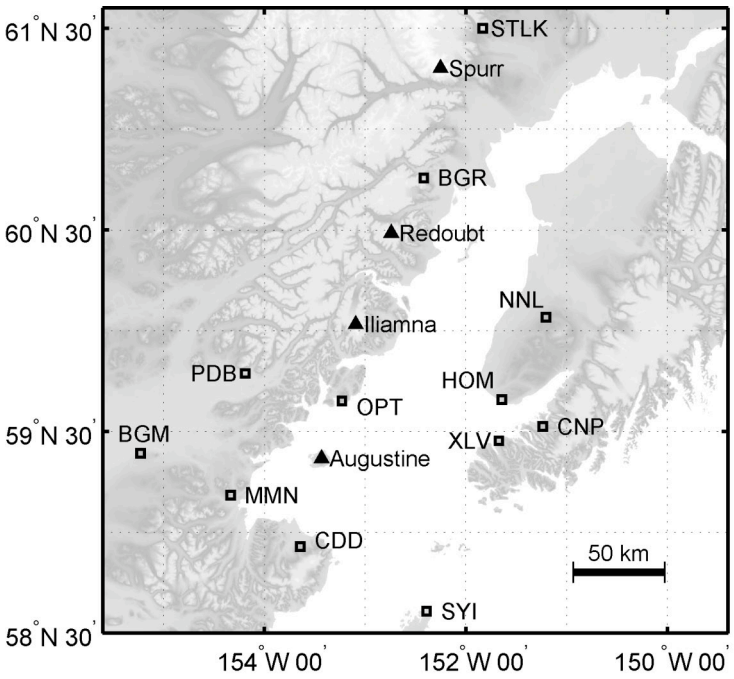

Figure C1. Regional AVO seismograph stations in Cook Inlet. Seismograph stations are shown by open squares. Closed triangles show volcanic centers.

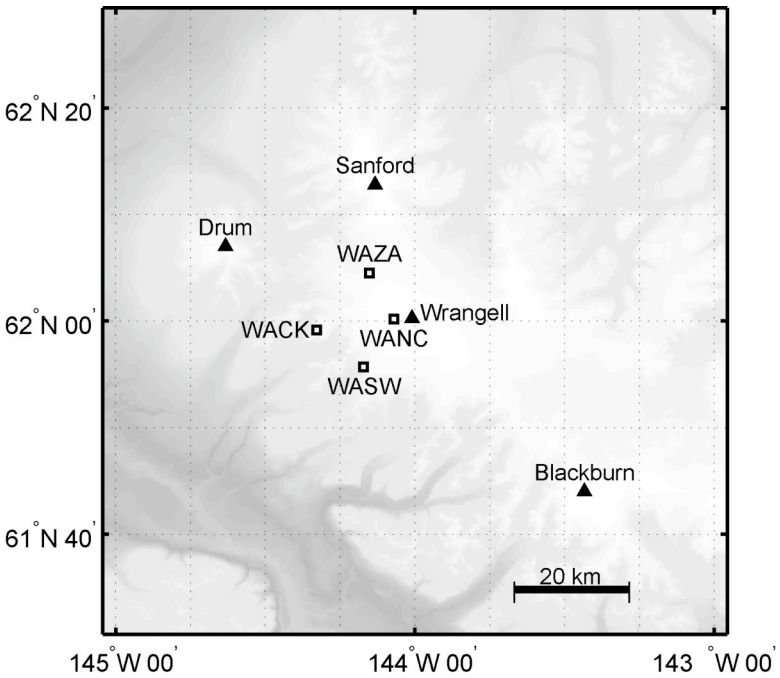

Figure C2. AVO seismograph stations near Mount Wrangell. Seismograph stations are shown by open squares. Closed triangles show volcanic centers.

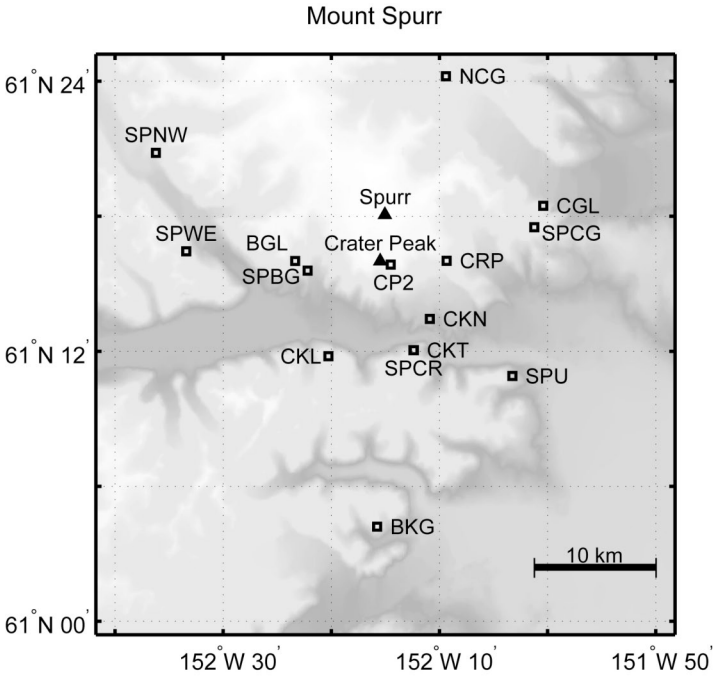

Figure C3. AVO seismograph stations near Mount Spurr. Seismograph stations are shown by open squares. Closed triangles show volcanic centers.

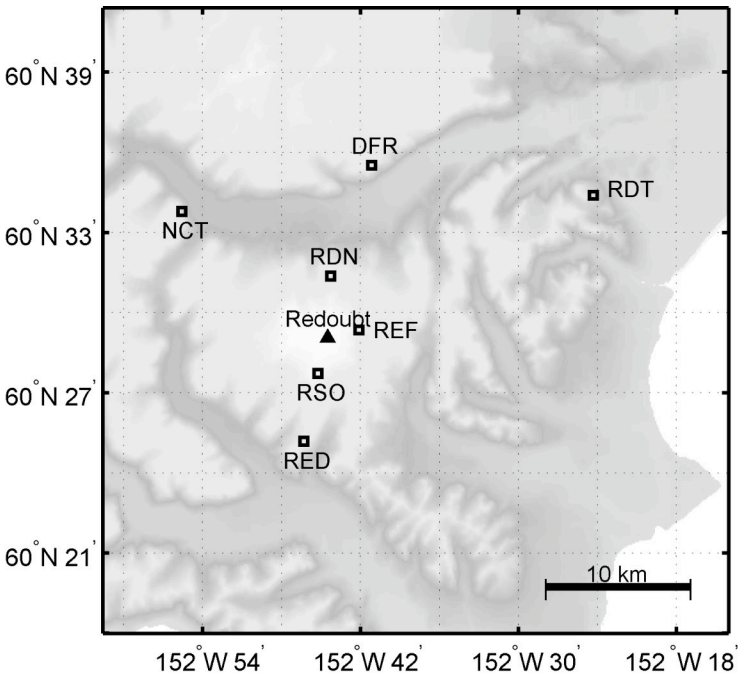

Figure C4. AVO seismograph stations near Redoubt Volcano. Seismograph stations are shown by open squares. Closed triangles show volcanic centers.

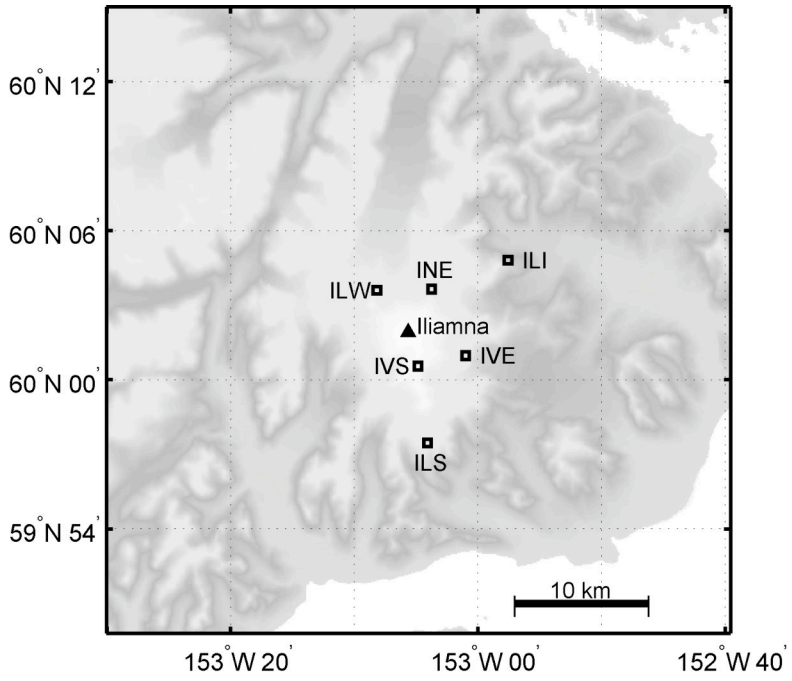

Figure C5. AVO seismograph stations near Iliamna Volcano. Seismograph stations are shown by open squares. Closed triangles show volcanic centers.

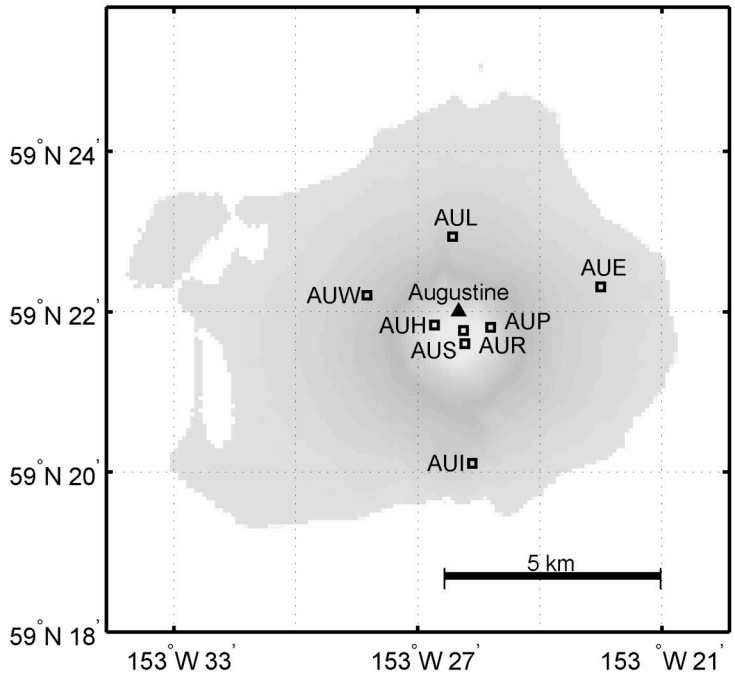

Figure C6. AVO seismograph stations near Augustine Volcano. Seismograph stations are shown by open squares. Closed triangles show volcanic centers.

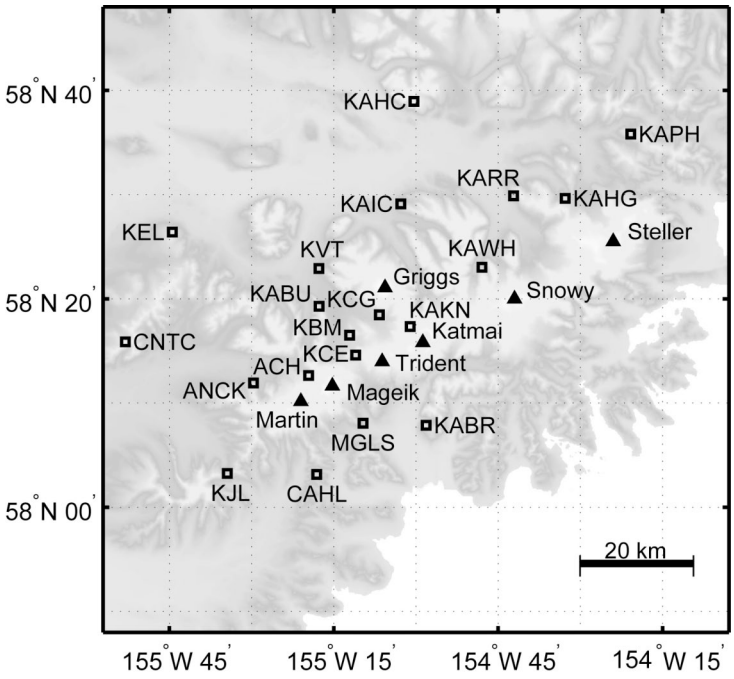

Figure C7. AVO seismograph stations near the Katmai volcanic cluster. Seismograph stations are shown by open squares. Closed triangles show volcanic centers.

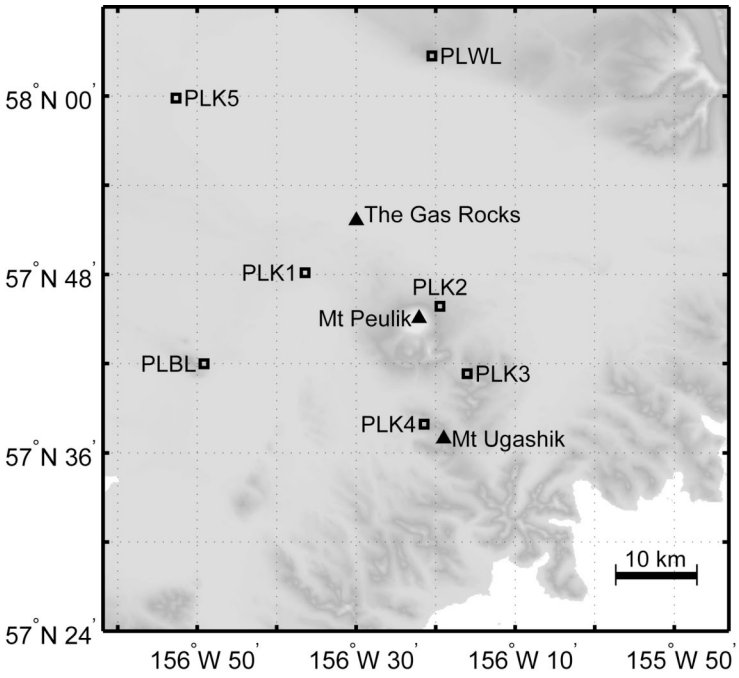

Figure C8. AVO seismograph stations near the Mount Peulik. Seismograph stations are shown by open squares. Closed triangles show volcanic centers.

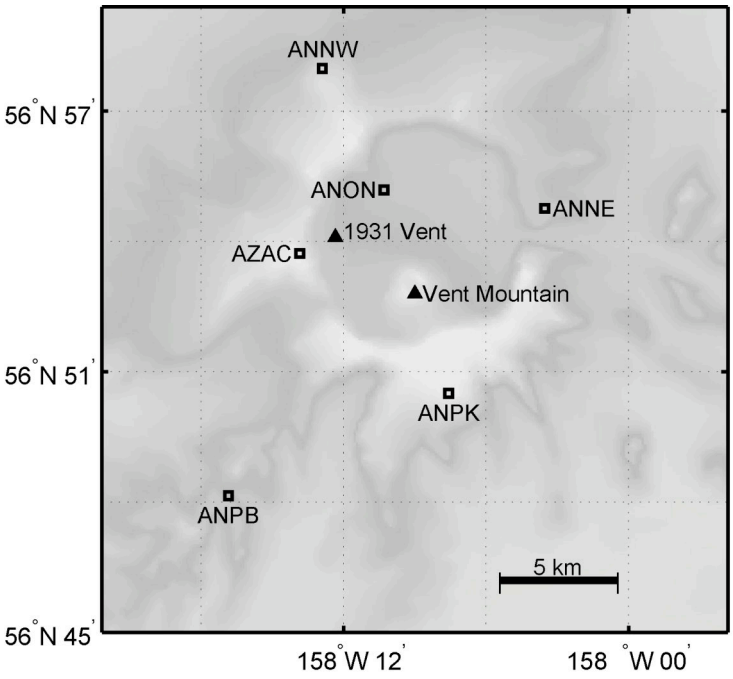

Figure C9. AVO seismograph stations near Aniakchak Crater. Seismograph stations are shown by open squares. Closed triangles show volcanic centers.

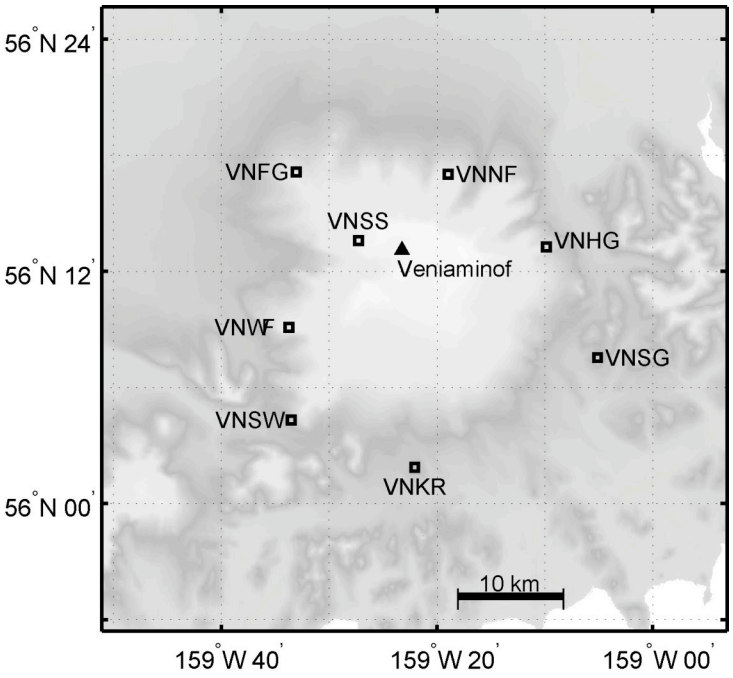

Figure C10. AVO seismograph stations near Mount Veniaminof. Seismograph station BPBC is not shown and is located 70 km northeast of Mount Veniaminof. Seismograph stations are shown by open squares. Closed triangles show volcanic centers.

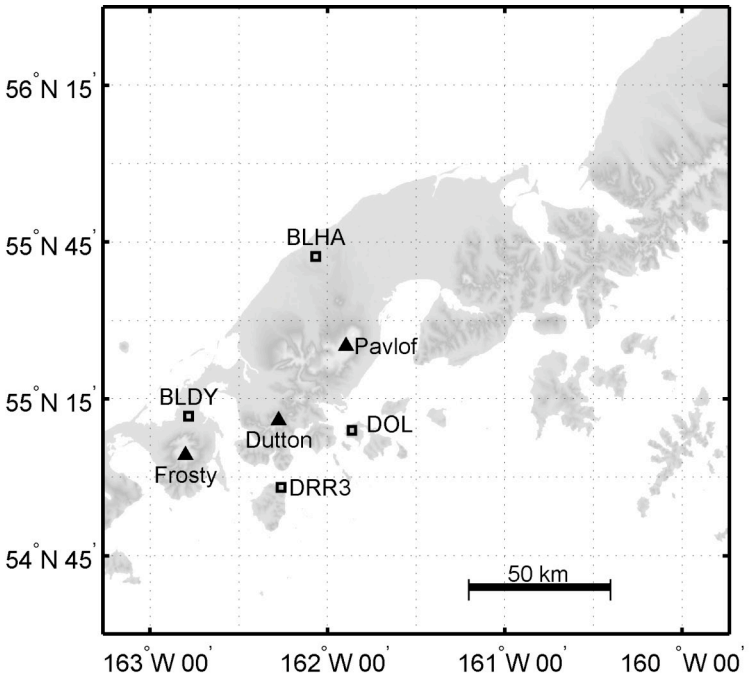

Figure C11. Regional AVO seismograph stations on the western end of the Alaska Peninsula. Seismograph stations are shown by open squares. Closed triangles show volcanic centers.

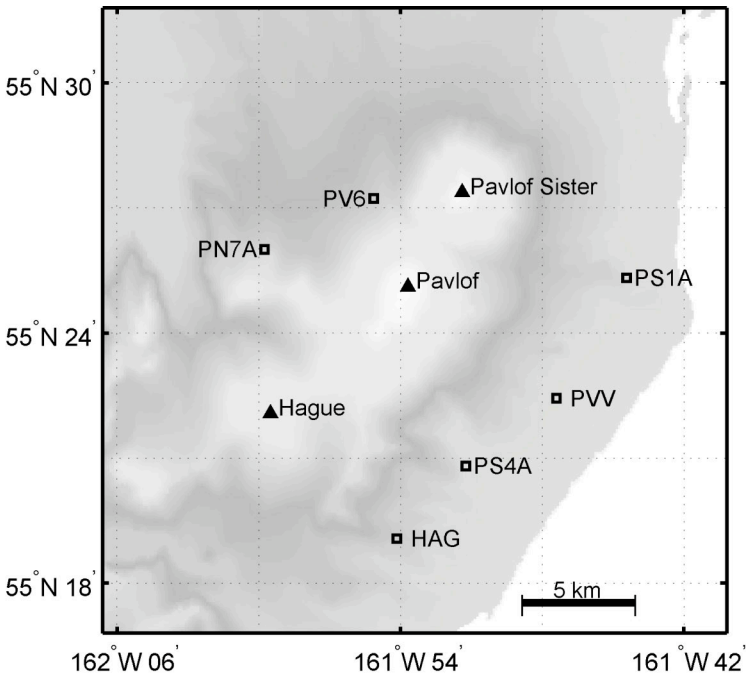

Figure C12. AVO seismograph stations near Pavlof Volcano. Seismograph stations are shown by open squares. Closed triangles show volcanic centers.

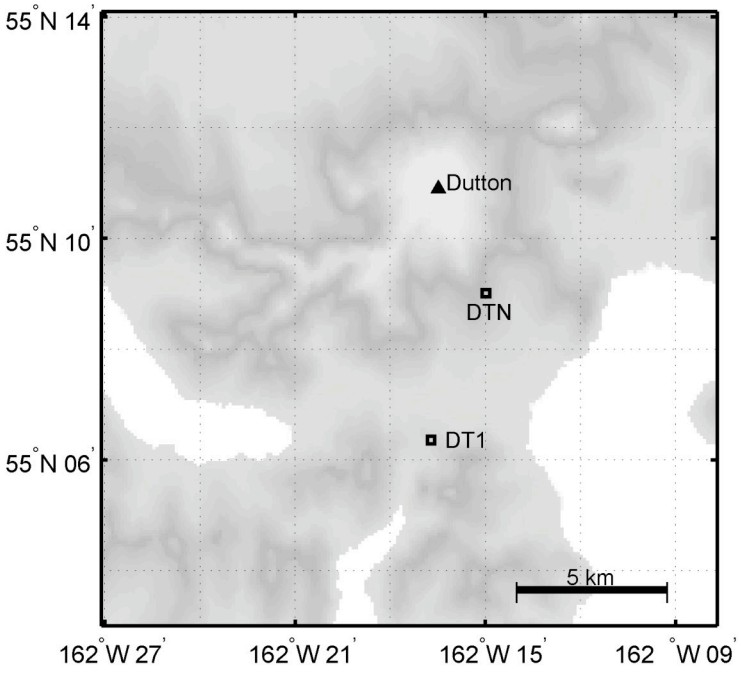

Figure C13. AVO seismograph stations near Mount Dutton. Seismograph stations are shown by open squares. Closed triangles show volcanic centers.

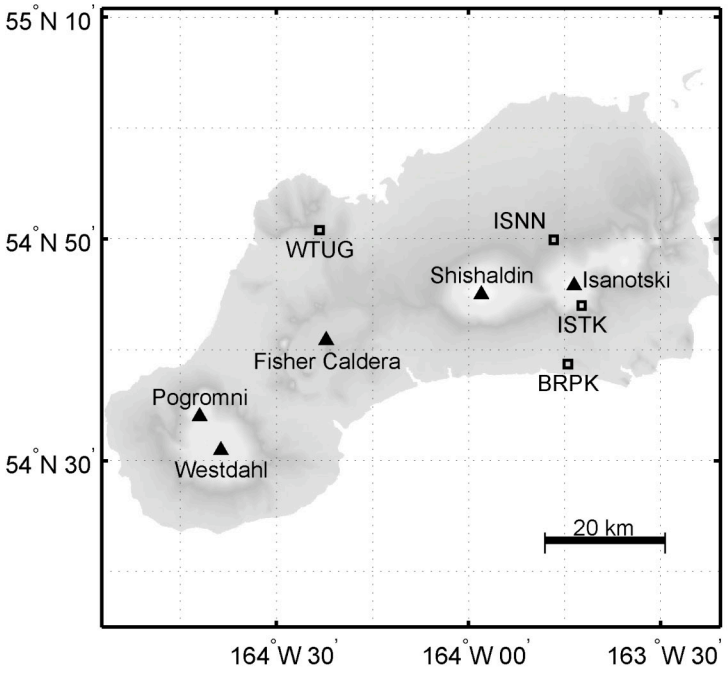

Figure C14. Regional AVO seismograph stations on Unimak Island. Seismograph stations are shown by open squares. Closed triangles show volcanic centers.

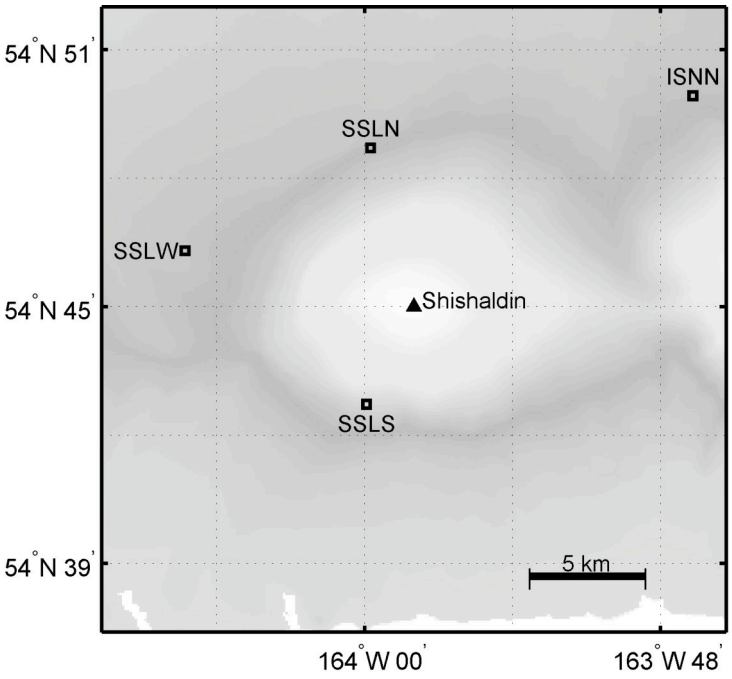

Figure C15. AVO seismograph stations near Shishaldin Volcano. Seismograph stations are shown by open squares. Closed triangles show volcanic centers.

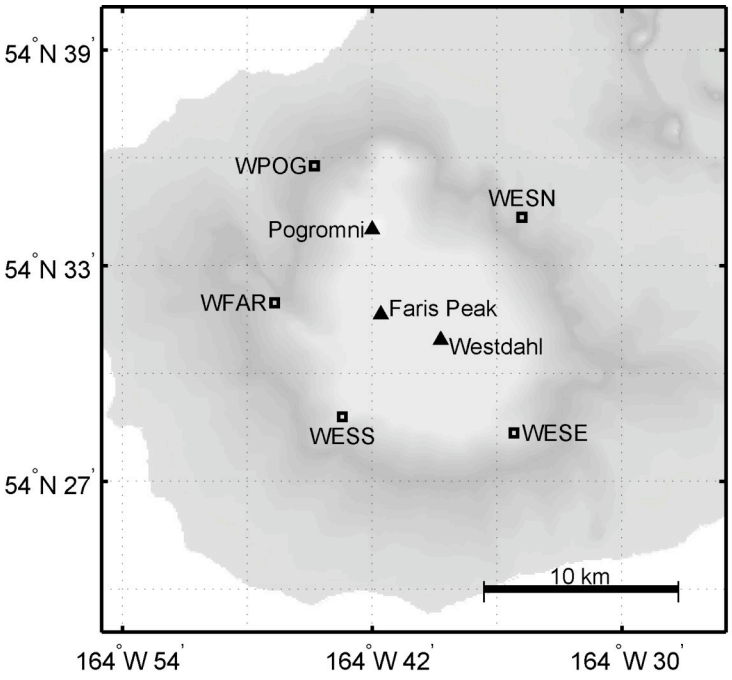

Figure C16. AVO seismograph stations near Westdahl Peak. Seismograph stations are shown by open squares. Closed triangles show volcanic centers.

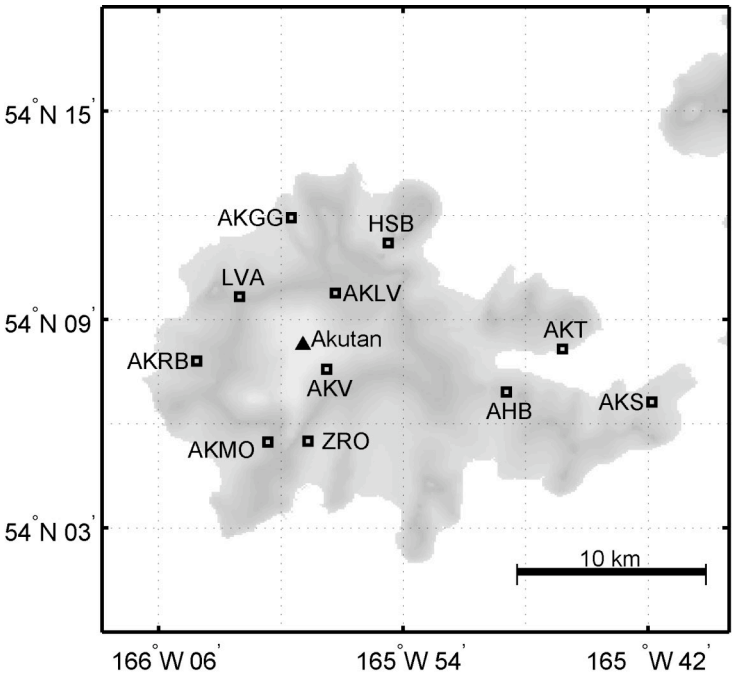

Figure C17. AVO seismograph stations near Akutan Peak. Seismograph stations are shown by open squares. Closed triangles show volcanic centers.

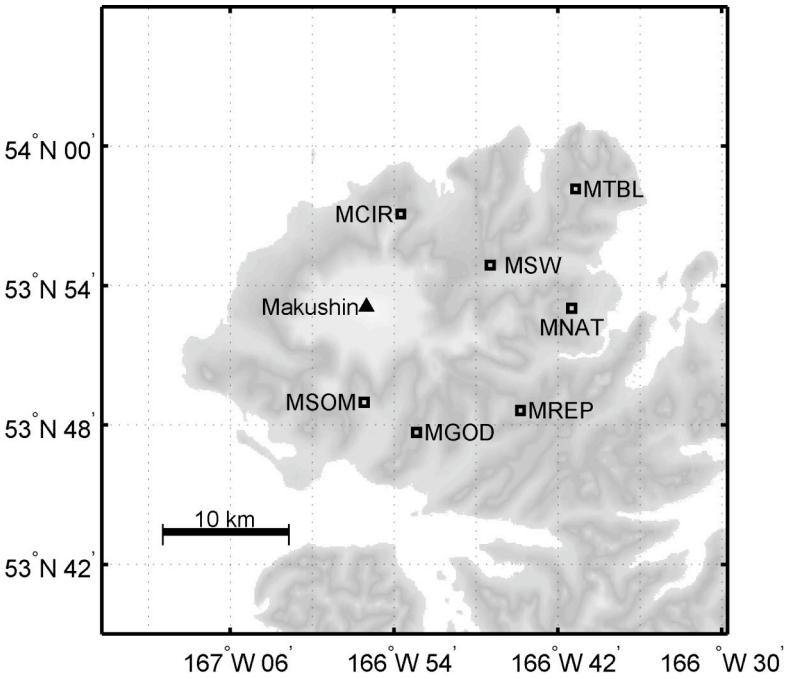

Figure C18. AVO seismograph stations near Makushin Volcano. Seismograph stations are shown by open squares. Closed triangles show volcanic centers.

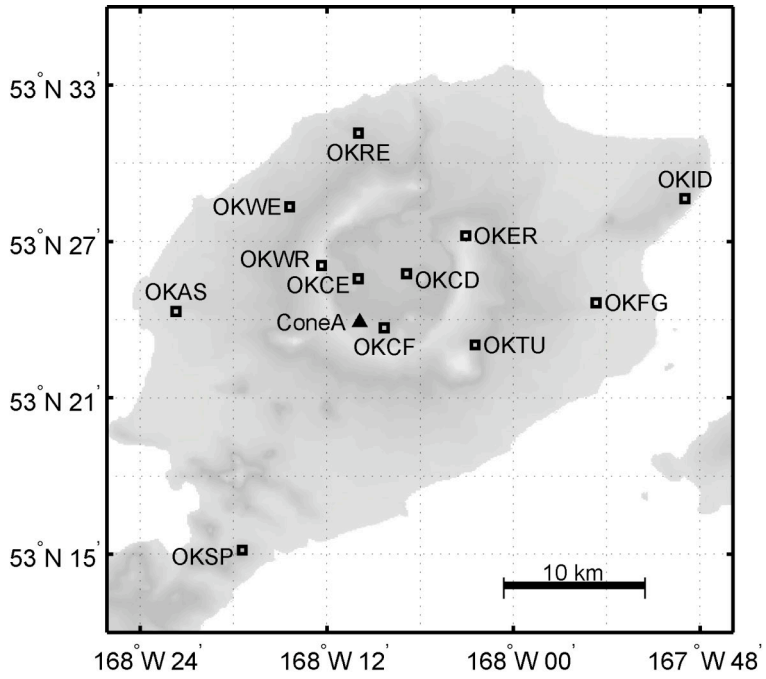

Figure C19. AVO seismograph stations near Okmok Volcano. Seismograph stations are shown by open squares. Closed triangles show volcanic centers.

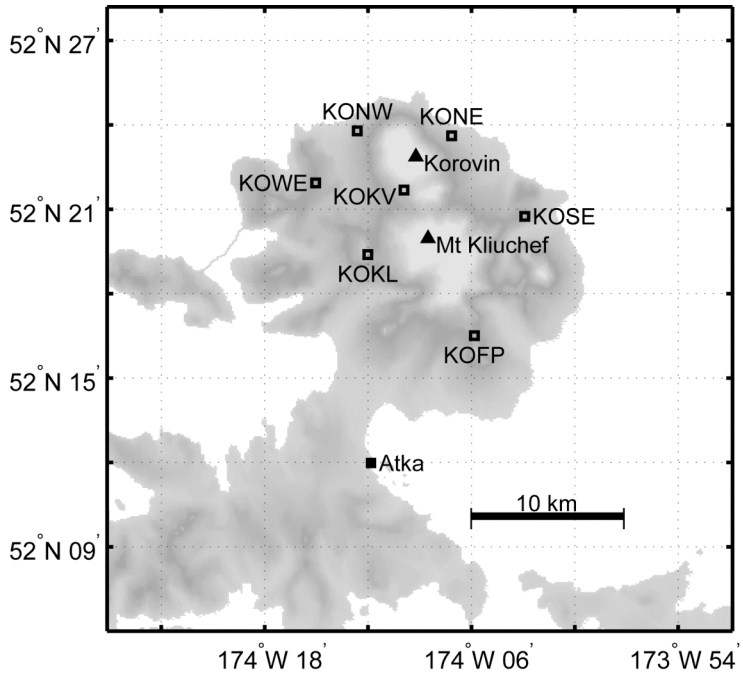

Figure C20. AVO seismograph stations near Korovin Volcano. Seismograph stations are shown by open squares. Closed triangles show volcanic centers.

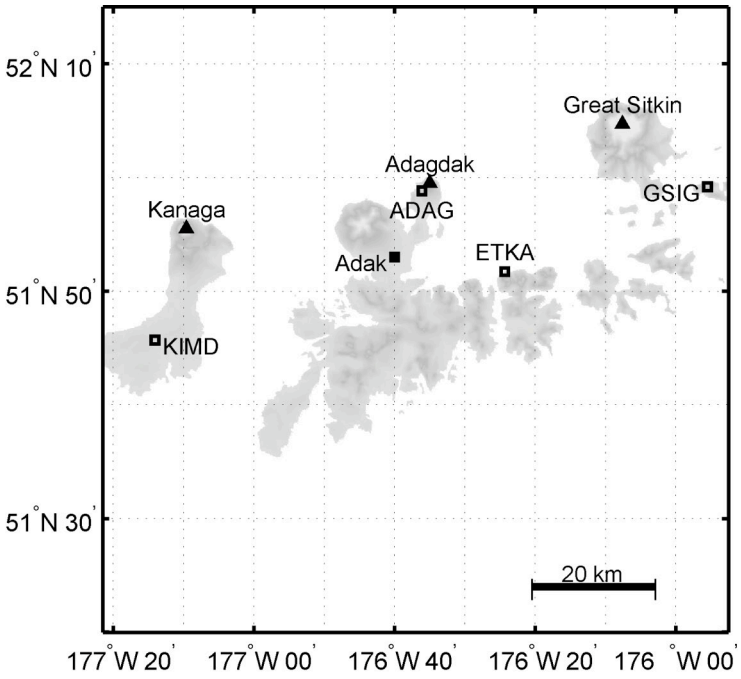

Figure C21. Regional AVO seismograph stations around Adak Island. Seismograph stations are shown by open squares. Closed triangles show volcanic centers.

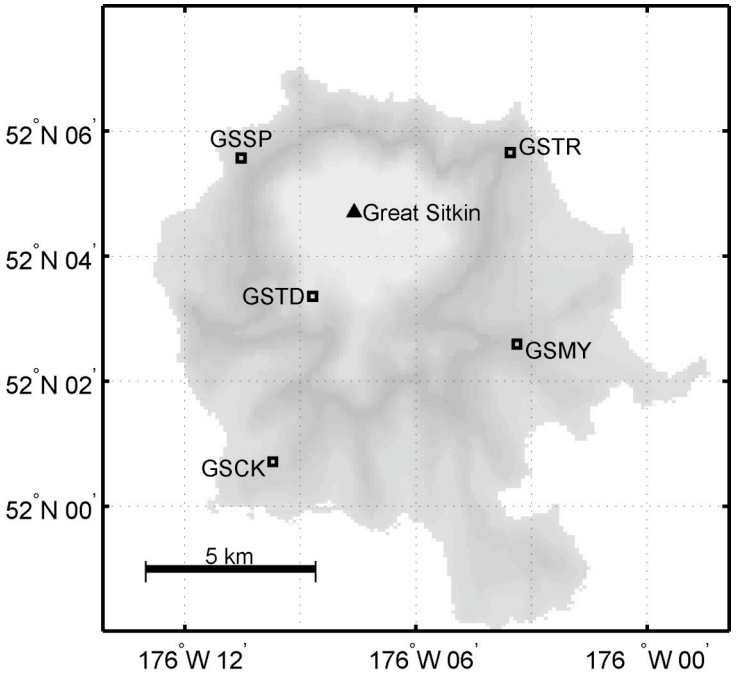

Figure C22. AVO seismograph stations near Great Sitkin Volcano. Seismograph stations are shown by open squares. Closed triangles show volcanic centers.

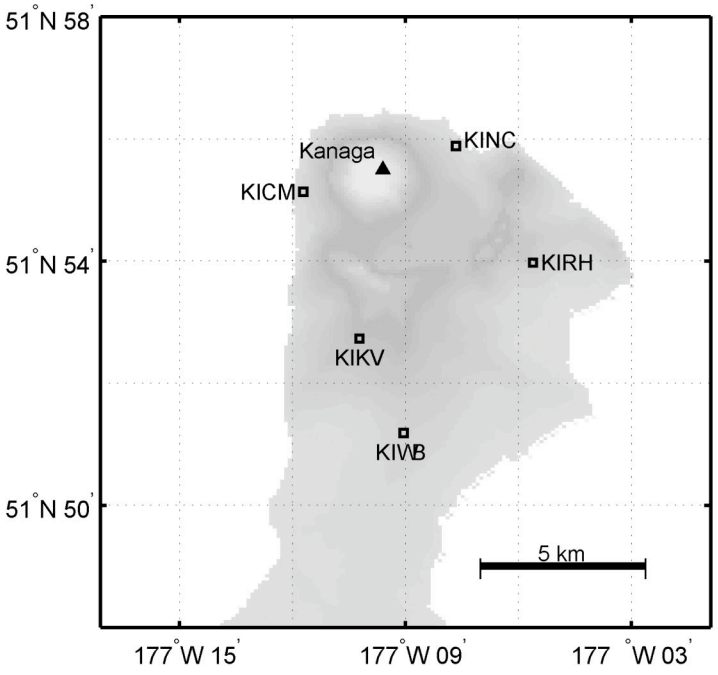

Figure C23. AVO seismograph stations near Kanaga Volcano. Seismograph stations are shown by open squares. Closed triangles show volcanic centers.

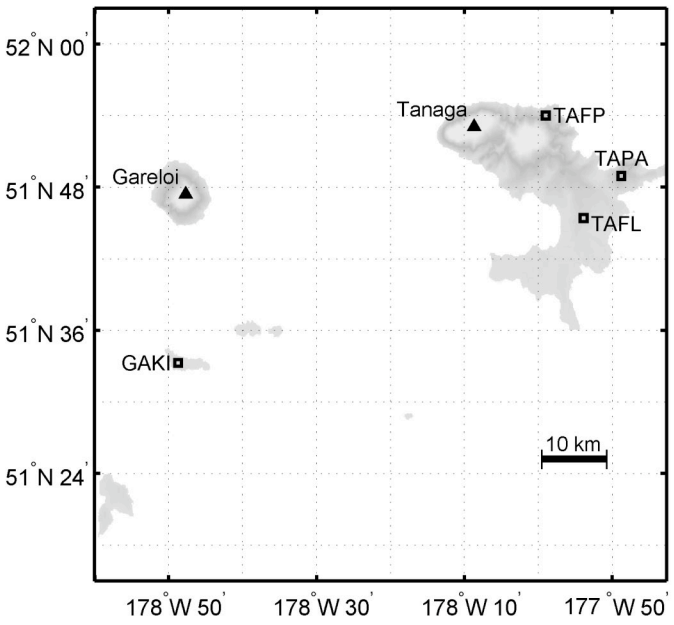

Figure C24. Regional AVO seismograph stations around Tanaga Volcano and Mount Gareloi. Seismograph stations are shown by open squares. Closed triangles show volcanic centers.

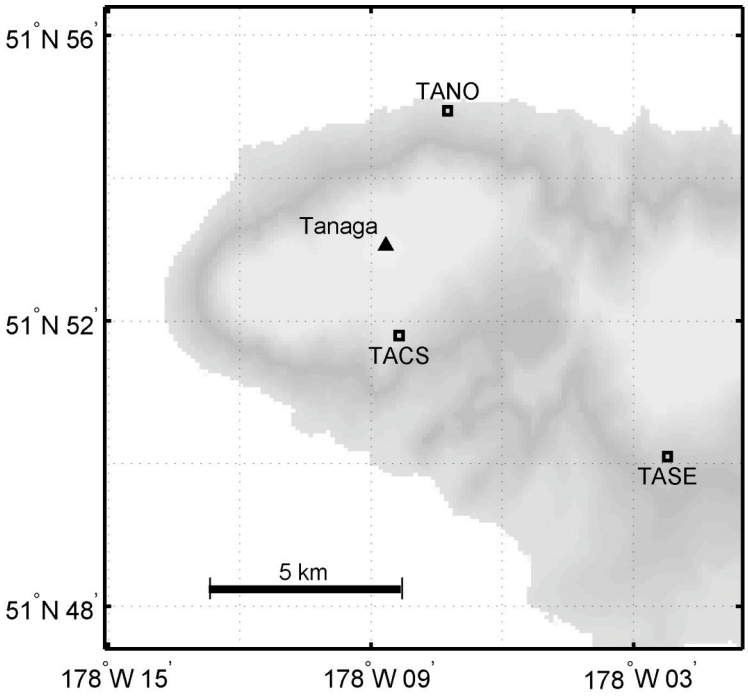

Figure C25. AVO seismograph stations near Tanaga Volcano. Seismograph stations are shown by open squares. Closed triangles show volcanic centers.

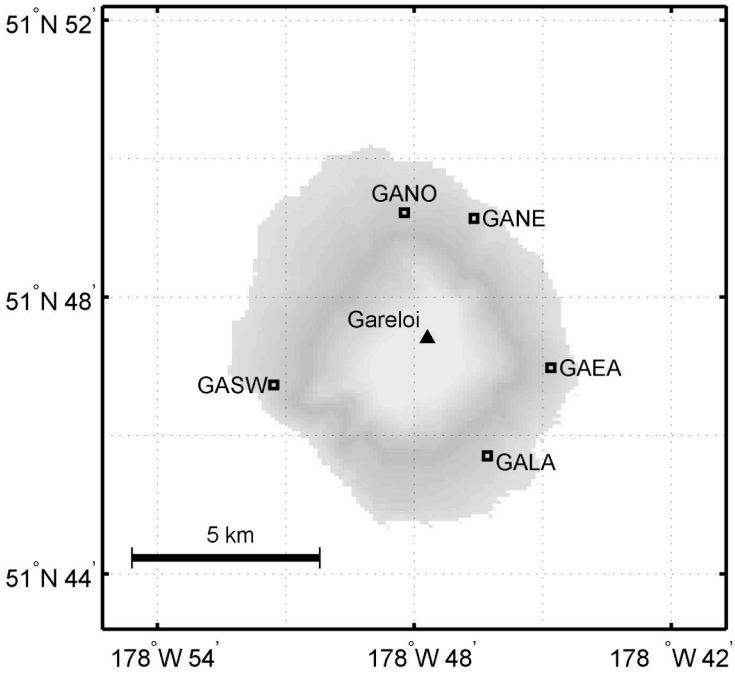

Figure C26. AVO seismograph stations near Mount Gareloi. Seismograph stations are shown by open squares. Closed triangles show volcanic centers.

Appendix D: Estimate of operational status for all AVO stations. A solid bar indicates periods of time a station was operational based on daily station use plots and weekly operational checks.

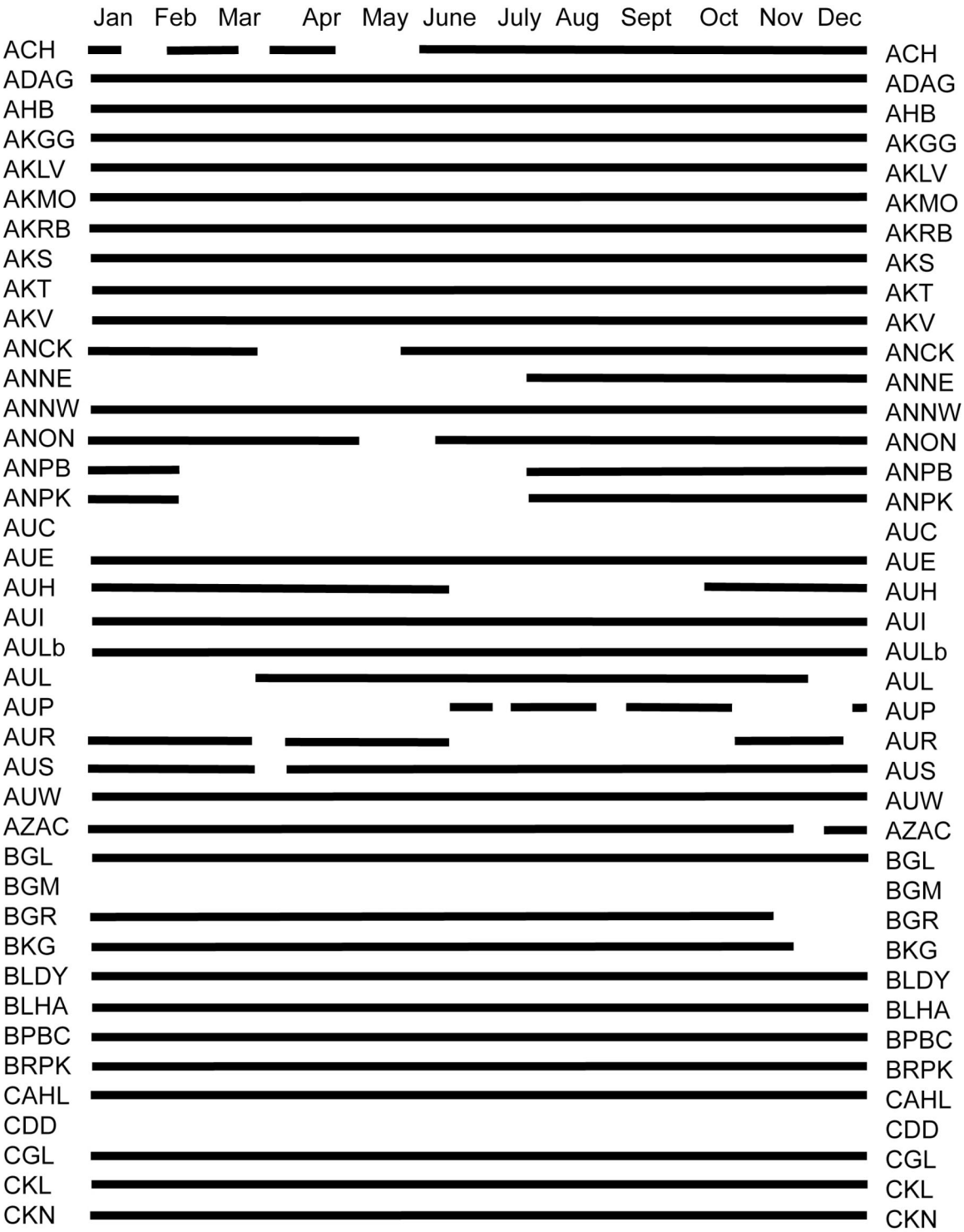

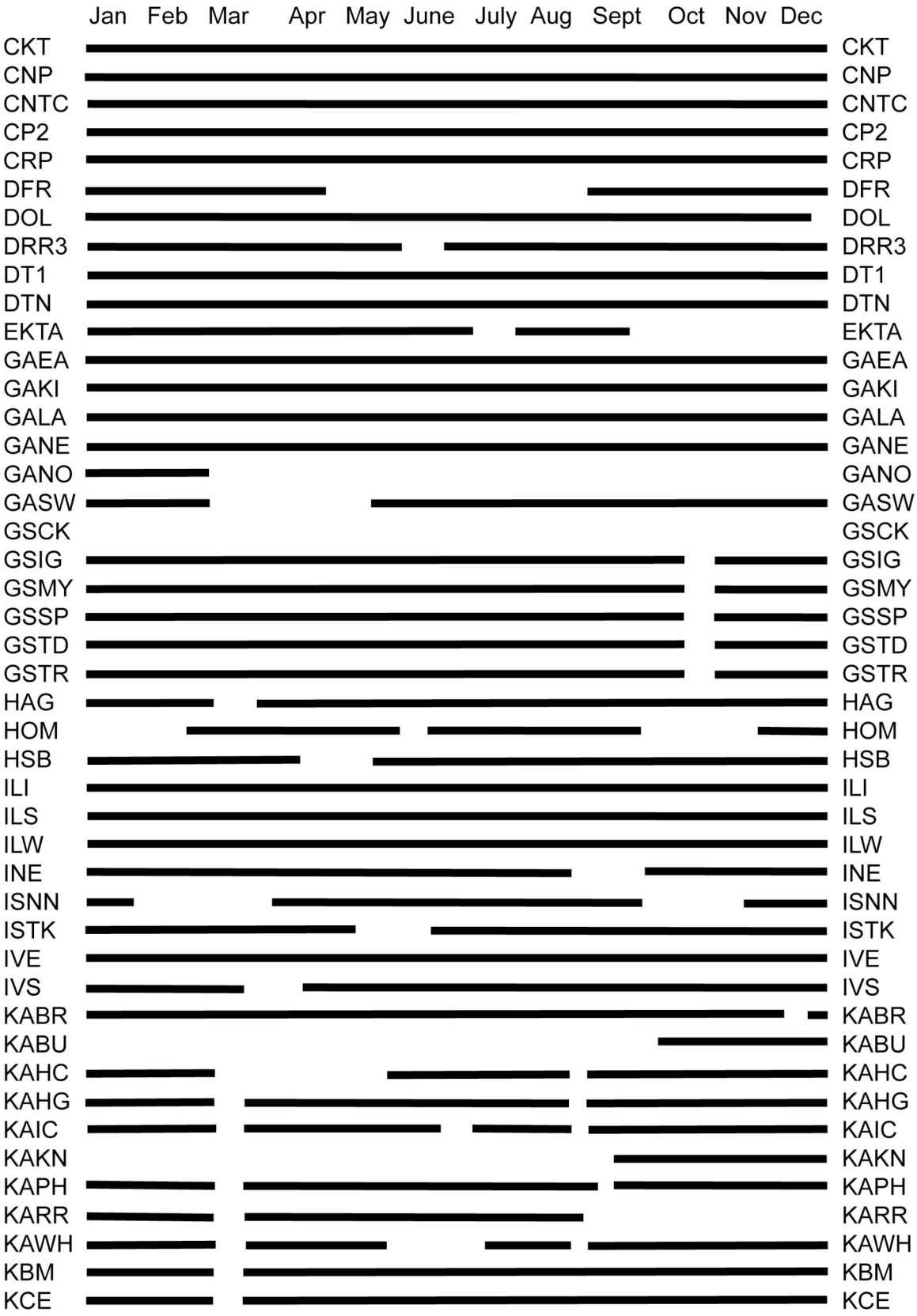
Jan
Feb
Mar
Apr
May
June
July
Aug
Sept
Oct
Nov
Dec
CKT
CNP
CNTC
CP2
CRP
DFR
DOL
DRR3
DT1
DTN
EKTA
GAEA
GAKI
GALA
GANE
GANO
GASW
GSCK
GSIG
GSMY
GSSP
GSTD
GSTR
HAG
HOM
HSB
ILI
ILS
ILW
INE
ISNN
ISTK
IVE
IVS
KABR
KABU
KAHC
KAHG
KAIC
KAKN
KAPH
KARR
KAWH
KBM
KCE

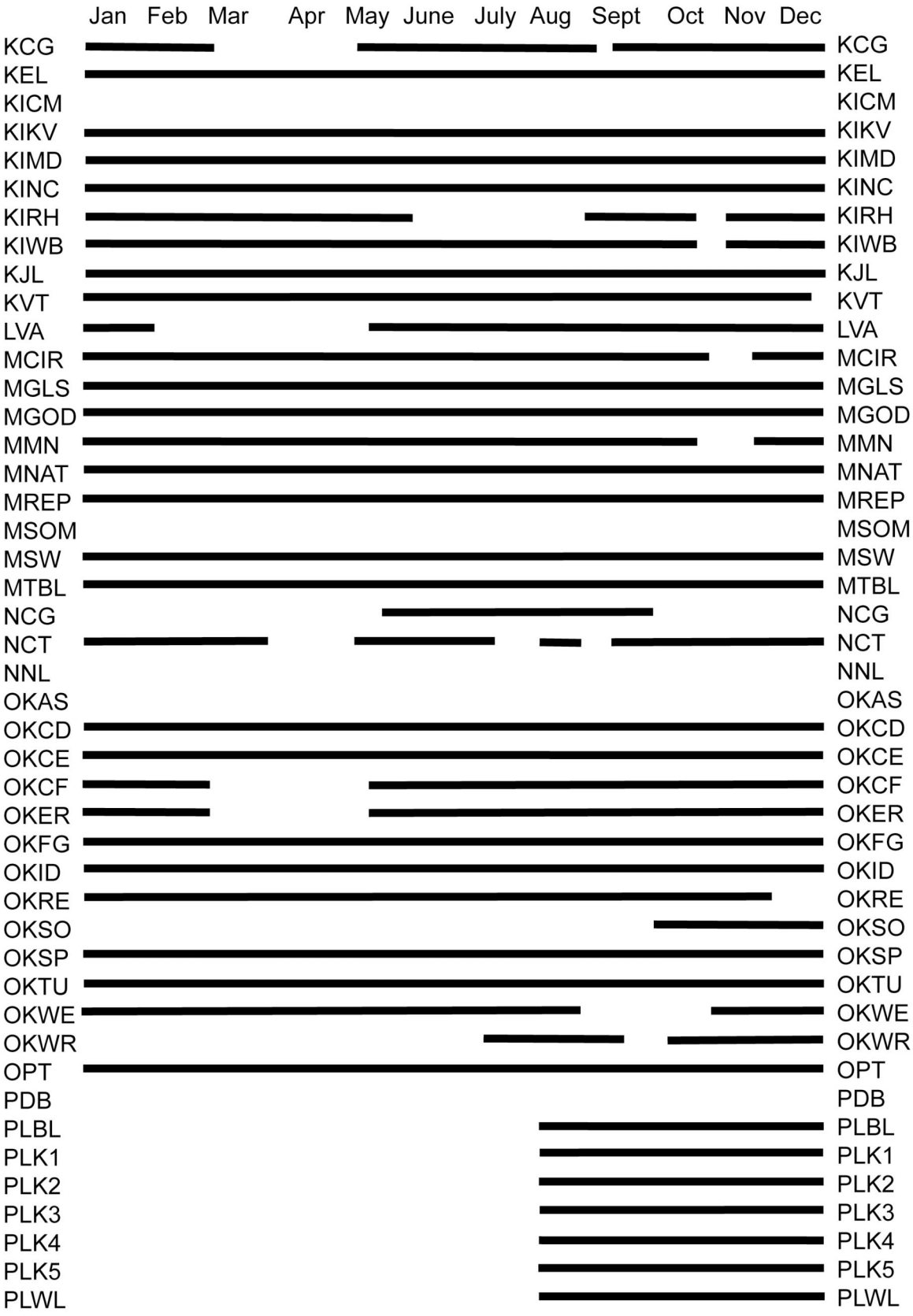
Jan
Feb
Mar
Apr
May
June
July
Aug
Sept
Oct
Nov
Dec
KCG
KEL
KICM
KIKV
KIMD
KINC
KIRH
KIWB
KJL
KVT
LVA
MCIR
MGLS
MGOD
MMN
MNAT
MREP
MSOM
MSW
MTBL
NCG
NCT
NNL
OKAS
OKCD
OKCE
OKCF
OKER
OKFG
OKID
OKRE
OKSO
OKSP
OKTU
OKWE
OKWR
OPT
PDB
PLBL
PLK1
PLK2
PLK3
PLK4
PLK5
PLWL

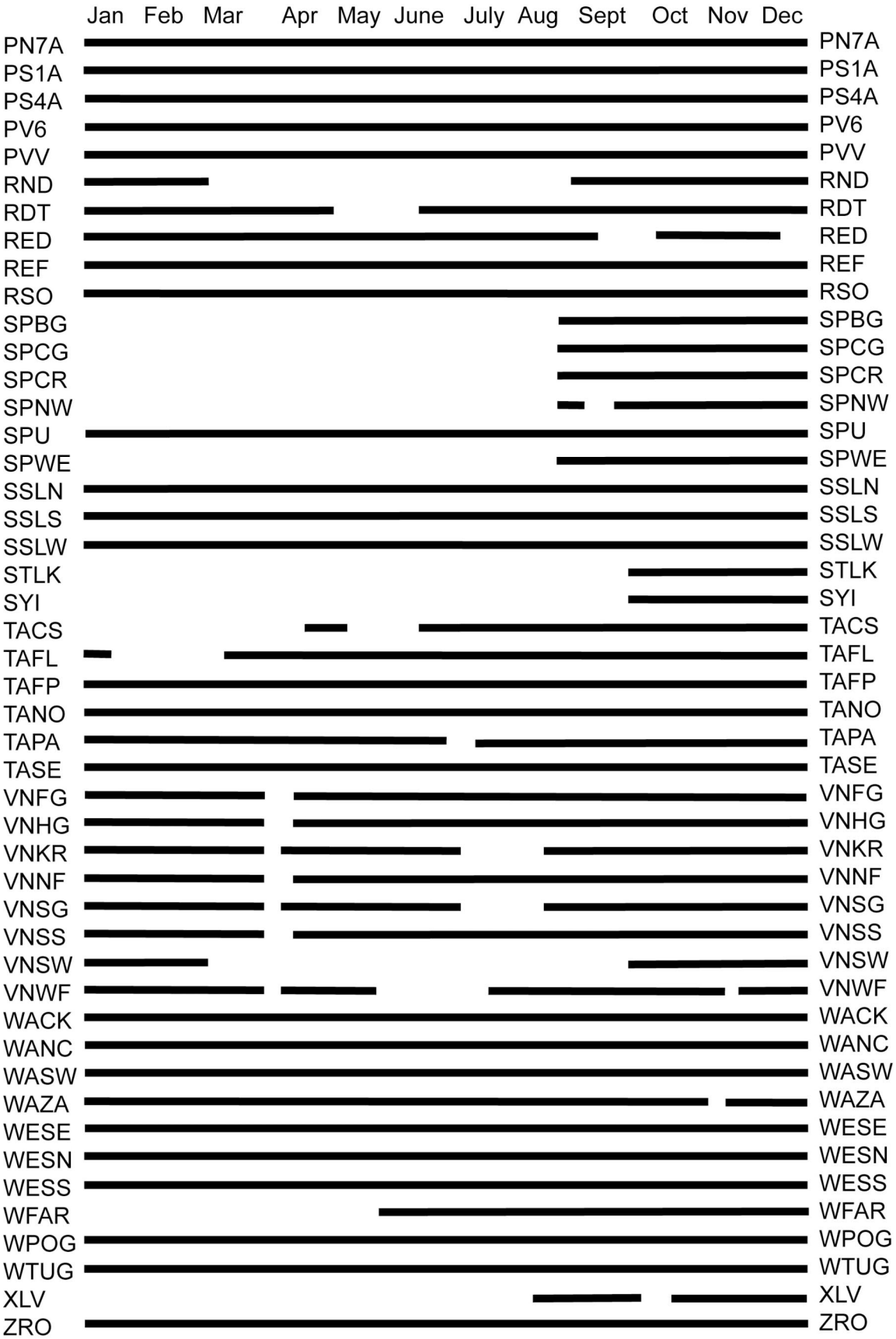
Jan
Feb
Mar
Apr
May
June
July
Aug
Sept
Oct
Nov
Dec
PN7A
PS1A
PS4A
PV6
PVV
RND
RDT
RED
REF
RSO
SPBG
SPCG
SPCR
SPNW
SPU
SPWE
SSLN
SSLS
SSLW
STLK
SYI
TACS
TAFL
TAFP
TANO
TAPA
TASE
VNFG
VNHG
VNKR
VNNF
VNSG
VNSS
VNSW
VNWF
WACK
WANC
WASW
WAZA
WESE
WESN
WESS
WFAR
WPOG
WTUG
XLV
ZRO

Appendix E: Velocity models used in locating the earthquakes described in this report. Following the name of each velocity model is a list of monitored volcanoes for which the model is used. Depths are referenced to sea level, with negative values reflecting height above sea level.

Cylindrical Model Parameters

Velocity Model	Latitude (°N)	Longitude (°W)	Radius (km)	Top (km)	Bottom (km)
Spurr	61.60	152.40	20	-3	50
Spurr	61.47	152.33	20	-3	50
Spurr	61.33	152.25	20	-3	50
Spurr	61.17	152.35	20	-3	50
Spurr	61.00	152.45	20	-3	50
Redoubt	60.83	152.55	20	-3	50
Redoubt	60.66	152.66	20	-3	50
Redoubt	60.49	152.75	20	-3	50
Redoubt	60.34	152.86	20	-3	50
Redoubt	60.19	152.98	20	-3	50
Redoubt	59.87	153.17	20	-3	50
Redoubt	59.70	153.25	20	-3	50
Redoubt	59.53	153.34	20	-3	50
Iliamna	60.03	153.09	20	-3	50
Augustine	59.36	153.42	20	-3	50
Katmai	58.17	155.35	20	-3	50
Katmai	58.29	154.86	20	-3	50
Katmai	58.35	155.09	20	-3	50
Katmai	58.43	154.38	20	-3	50
Cold Bay	55.42	161.89	20	-3	50
Cold Bay	55.18	162.27	20	-3	50
Cold Bay	54.76	163.97	30	-3	50
Cold Bay	54.52	164.65	20	-3	50
Akutan	54.15	165.97	20	-3	50
Andreanof	52.08	176.13	20	-3	50
Andreanof	51.93	176.75	20	-3	50
Andreanof	51.92	177.17	20	-3	50

Regional Velocity Model (for all areas south of 62.5°N not covered by a volcano specific model): Aniakchak Crater, Mount Gareloi, Korovin Volcano, Makushin Volcano, Okmok Volcano, Mount Peulik, Tanaga Volcano, Mount Veniaminof, and Mount Wrangell (Fogleman and others, 1993).

Layer number	Vp (km/sec)	Top of layer (km)	Vp/Vs
1	5.3	-3.0	1.78
2	5.6	4.0	1.78
3	6.2	10.0	1.78
4	6.9	15.0	1.78
5	7.4	20.0	1.78
6	7.7	25.0	1.78
7	7.9	33.0	1.78
8	8.1	47.0	1.78
9	8.3	65.0	1.78

Akutan Velocity Model: Akutan Peak (Power and others, 1996).

Layer number	Vp (km/sec)	Top of layer (km)	Vp/Vs
1	2.30 +0.37 km/sec for each km of depth	-3.0	1.80
2	6.30	7.0	1.80

Andreanof Velocity model: Great Sitkin Volcano, Kanaga Volcano (Toth and Kisslinger, 1984).

Layer number	Vp (km/sec)	Top of layer (km)	Vp/Vs
1	3.50	-3.0	1.73
2	3.88	-2.8	1.73
3	4.25	-2.6	1.73
4	4.62	-2.4	1.73
5	5.00	-2.2	1.73
6	5.50	-2.0	1.73
7	5.62	-1.0	1.73
8	5.74	0.0	1.73
9	5.86	1.0	1.73
10	5.98	2.0	1.73
11	6.10	3.0	1.73
12	6.60	4.0	1.73
13	6.68	5.0	1.73
14	6.80	8.0	1.73
15	6.92	11.0	1.73
16	7.04	14.0	1.73
17	7.16	17.0	1.73
18	7.28	20.0	1.73
19	7.85	23.0	1.73
20	8.05	37.0	1.73

Augustine Velocity Model: Augustine Volcano (Power, 1988).

Layer number	Vp (km/sec)	Top of layer (km)	Vp/Vs
1	2.3	-3.0	1.80
2	2.6	-0.7	1.80
3	3.4	0.0	1.80
4	5.1	1.0	1.80
5	6.3	9.0	1.78
6	8.0	44.0	1.78

Cold Bay Velocity Model: Mount Dutton, Fisher Caldera, Isanotski Peaks, Pavlof Volcano, Shishaldin Volcano and Westdahl Peak (McNutt and Jacob, 1986).

Layer number	Vp (km/sec)	Top of layer (km)	Vp/Vs
1	3.05	-3.00	1.78
2	3.44	0.00	1.78
3	5.56	1.79	1.78
4	6.06	3.65	1.78
5	6.72	10.18	1.78
6	7.61	22.63	1.78
7	7.90	38.51	1.78

Iliamna Velocity model: Iliamna Volcano (Roman and others, 2001) .

Layer number	Vp (km/sec)	Top of layer (km)	Vp/Vs
1	4.8	-3.0	1.78
2	6.1	-1.6	1.78
3	6.2	1.7	1.78
4	6.3	2.9	1.78
5	6.4	3.1	1.78
6	7.1	16.5	1.78

Katmai Velocity Model: Mount Griggs, Mount Katmai, Mount Mageik, Mount Martin, Novarupta, Snowy Mountain, and Trident Volcano (Searcy, 2003).

Layer number	Vp (km/sec)	Top of layer (km)	Vp/Vs
1	5.05	-3.0	1.78
2	5.10	1.0	1.78
3	5.41	2.0	1.78
4	5.49	3.0	1.78
5	5.65	4.0	1.78
6	5.67	5.0	1.78
7	5.69	6.0	1.78
8	5.76	7.0	1.78
9	5.80	8.0	1.78
10	6.00	9.0	1.78
11	6.04	10.0	1.78
12	6.08	12.0	1.78
13	6.30	15.0	1.78
14	6.73	20.0	1.78
15	7.54	25.0	1.78
16	7.78	33.0	1.78

Redoubt Velocity Model: Redoubt Volcano (Lahr and others, 1994) .

Layer number	Vp (km/sec)	Top of layer (km)	Vp/Vs
1	2.90	-3.0	1.80
2	5.10	-1.7	1.80
3	6.40	1.5	1.72
4	7.00	17.0	1.78

Spurr Velocity Model: Mount Spurr (Jolly and others, 1994).

Layer number	Vp (km/sec)	Top of layer (km)	Vp/Vs
1	5.1	-3.00	1.81
2	5.5	-2.00	1.81
3	6.3	5.25	1.74
4	7.2	27.25	1.78

Appendix F: Maps showing the location of the volcanic zones modeled using cylinders described in Appendix E.

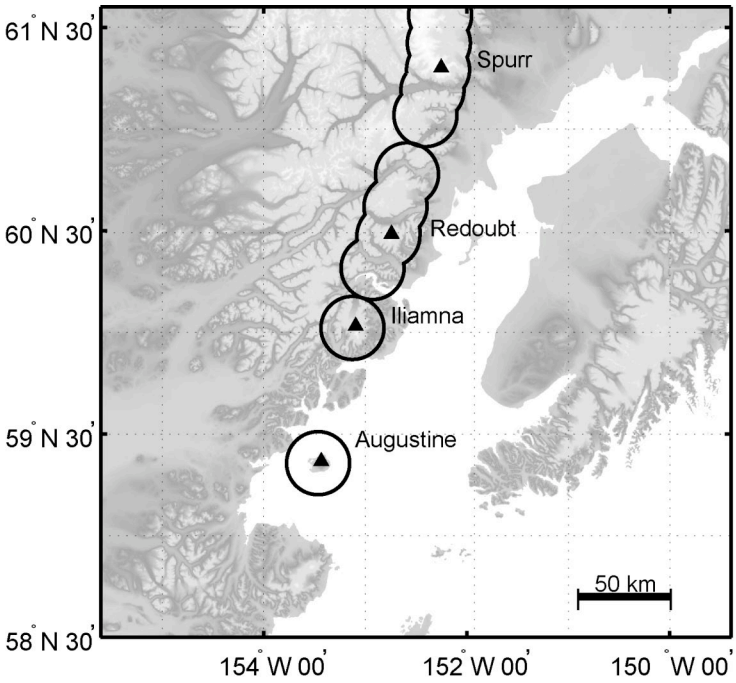

Figure F1. Volcanic zones for the Cook Inlet Volcanoes. Five overlapping cylinders model the Spurr volcanic zone. Four overlapping cylinders model the Redoubt volcanic zone. Single cylinders model the Iliamna and Augustine volcanic zones.

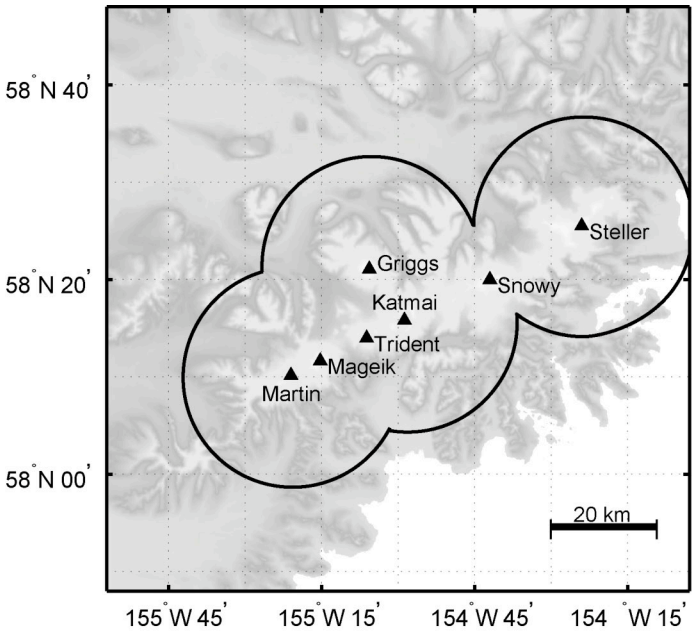

Figure F2. Volcanic zone for the Katmai volcanic cluster. The volcanic zone is modeled using four cylinders centered on Mount Martin, Mount Katmai, Mount Griggs and Mount Steller.

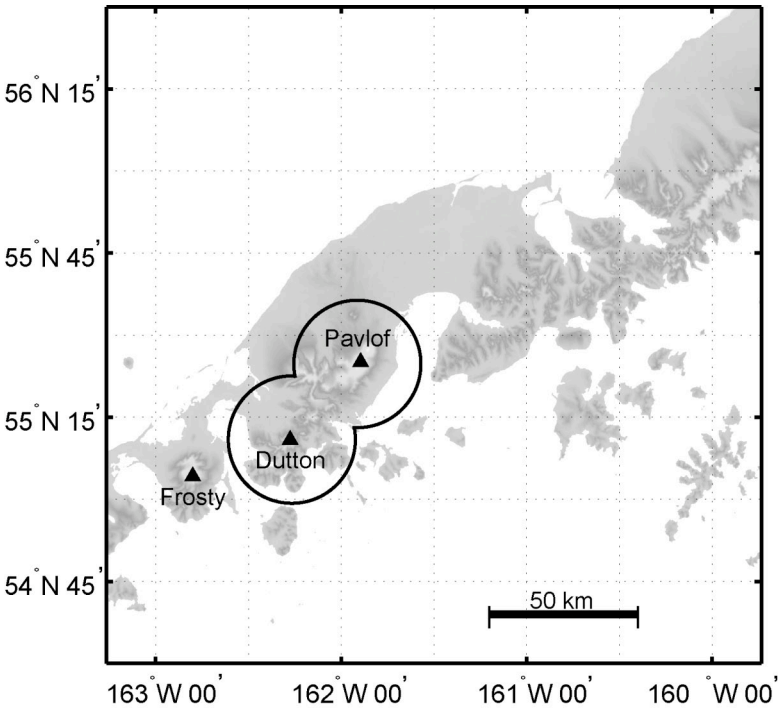

Figure F3. Volcanic zones for Pavlof Volcano and Mount Dutton. The volcanic zone is modeled using two cylinders centered on Mount Dutton and Pavlof Volcano.

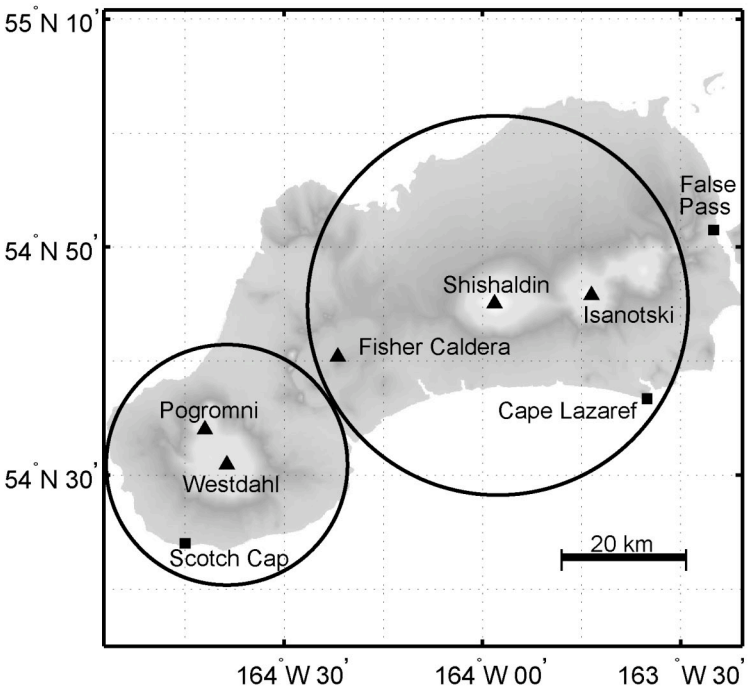

Figure F4. Volcanic zones on Unimak Island. The volcanic zones are modeled using a cylinder centered on Westdahl Peak and a cylinder centered on Shishaldin Volcano.

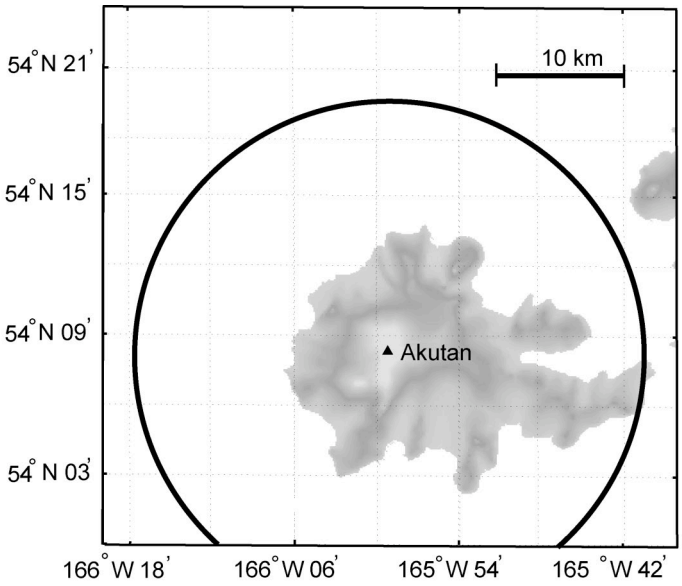

Figure F5. Volcanic zone for Akutan Volcano. The volcanic zone is modeled using a single cylinder.

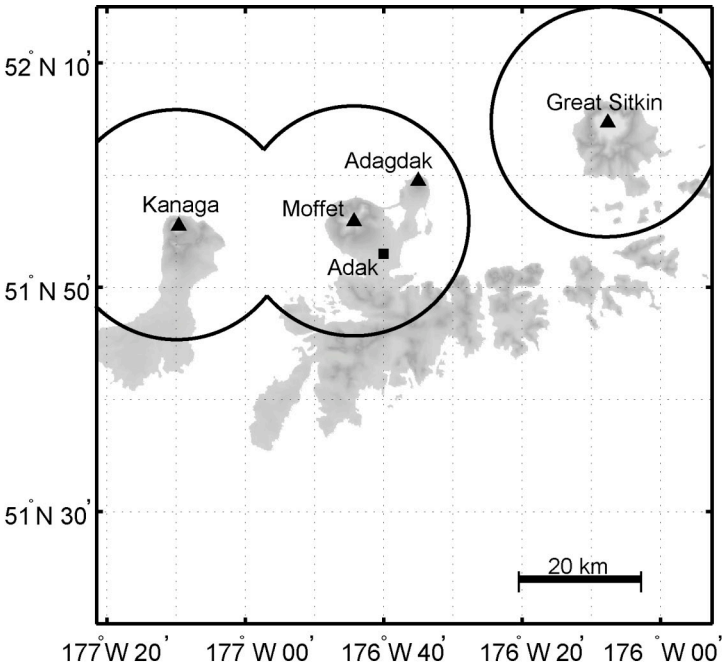

Figure F6. Volcanic zones in the Adak region. The volcanic zones are modeled using cylinders centered on Kanaga Volcano, Mount Moffet, and Great Sitkin Volcano.

Appendix G: Selected AVO papers published in 2004

Caplan-Auerbach, J., Moran, S.C., Tytgat, G., Plucinski, T.A., McNutt, S.R., and Paskievitch, J.F., 2004, Seismic Explorations in the Eastern Aleutians, Alaska, Seismological Research Letters, v.75, p. 8-21.

McNutt, S.R., and Marzocchi, W., 2004, Simultaneous earthquake swarms and eruption in Alaska, Fall 1996: Statistical Significance and Inference of a Large Aseismic Slip Event, Bulletin of the Seismological Society of America, v.94, p. 1831-1841.

Moran, S.C., Power, J.A., Stihler, S.D., Sánchez, J.J., and Caplan-Auerbach, J., 2004, Earthquake triggering at Alaskan volcanoes following the November3, 2002 Denali Fault Earthquake, Bulletin of the Seismological Society of America, v.94, p. 5300-5309.

Power, J.A., Stihler, S.D., White, R.A., Moran, S.C., 2004, Observations of deep long-period (DLP) seismic events beneath Aleutian arc volcanoes: 1989 – 2002, Journal of Volcanology and Geothermal Research, v. 138, p. 243 - 266.

Power, J.A., 2004, Renewed unrest at Mount Spurr Volcano, Alaska, EOS, v. 85, #43, p. 434.

Roman, D.C., Moran, S.C., Power, J.A., Cashman, K.V., 2004, Temporal and spatial variation of local stress fields during the 1992 eruption of Crater Peak vent, Mount Spurr, Alaska, Bulletin of Seismological Society of America, v. 94, p. 2366 - 2379.

Sánchez, J.J., Wyss, M., and McNutt, S.R., 2004, Temporal-spatial variations in stress at Redoubt volcano, Alaska, inferred from inversion of fault plane solutions. Journal of Volcanology and Geothermal Research, v. 130, p. 1-30.

Sánchez, J.J., McNutt, S.R., Power, J.A., and Wyss, M., 2004. Spatial variations in the frequency-magnitude distribution of earthquakes at Mount Pinatubo volcano. Bulletin of the Seismological Society of America, v. 94, p. 430-438.

Sánchez, J.J., and McNutt, S.R., 2004, Intermediate-term declines in seismicity at Mt. Wrangell and Mt. Veniaminof volcanoes, Alaska, following the 3 November 2002 Mw 7.9 Denali Fault Earthquake. Bulletin of the Seismological Society of America, v. 94, p. S370-S383.

Sánchez, J.J., and McNutt, S.R., 2004, Unexpected response of Mt. Wrangell Volcano, Alaska, to the shaking from a large regional earthquake: A puzzle for intermediate-term earthquake-volcanoes interactions. Earth Sciences Research Journal, v 8, p. 34-44.